

AD-A139 168

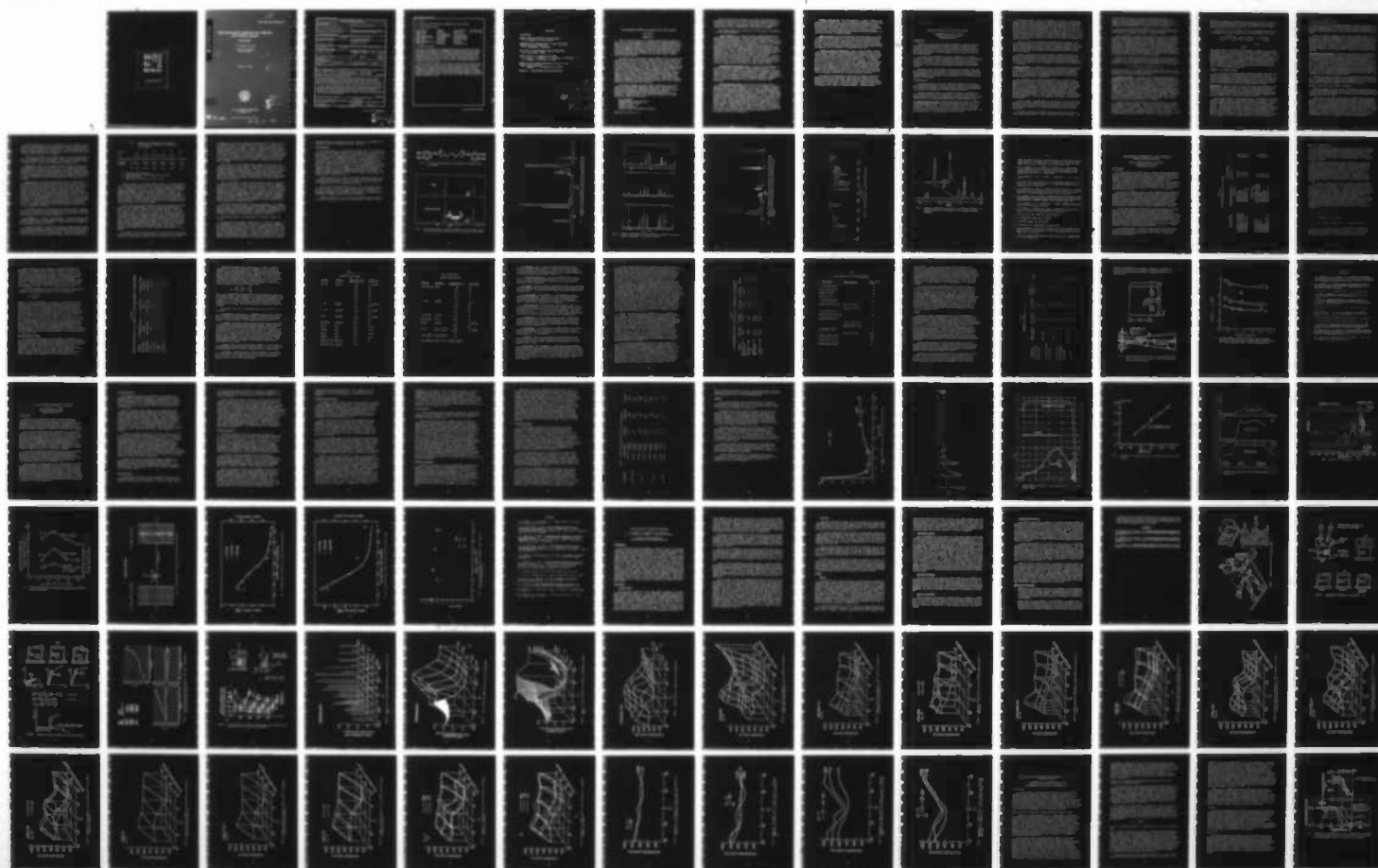
HIGH PERFORMANCE COMPOSITES AND ADHESIVES FOR V/STOL
AIRCRAFT(U) NAVAL RESEARCH LAB WASHINGTON DC
C F PORANSKI 22 FEB 84 NRL-MR-5231

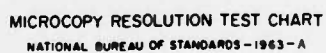
1/2

UNCLASSIFIED

F/G 11/4

NL





MICROCOPY RESOLUTION TEST CHART
NATIONAL BUREAU OF STANDARDS-1963-A

AD A139168

NRL Memorandum Report 5231

High Performance Composites and Adhesives for V/STOL Aircraft

Final Report

C. F. PORANSKI, JR., EDITOR

*Polymeric Materials Branch
Chemistry Division*

February 22, 1984



NAVAL RESEARCH LABORATORY
Washington, D.C.

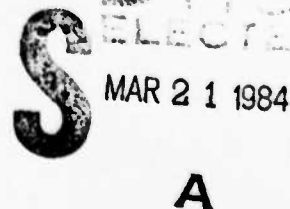
DTIC
ELECTRONIC
S MAR 21 1984
A

DTIC FILE COPY

Approved for public release; distribution unlimited.

84 03 21 073

REPORT DOCUMENTATION PAGE				
1a. REPORT SECURITY CLASSIFICATION UNCLASSIFIED		1b. RESTRICTIVE MARKINGS		
2a. SECURITY CLASSIFICATION AUTHORITY		3. DISTRIBUTION/AVAILABILITY OF REPORT		
2b. DECLASSIFICATION/DOWNGRADING SCHEDULE		Approved for public release; distribution unlimited.		
4. PERFORMING ORGANIZATION REPORT NUMBER(S) NRL Memorandum Report 5231		5. MONITORING ORGANIZATION REPORT NUMBER(S)		
6a. NAME OF PERFORMING ORGANIZATION Naval Research Laboratory	6b. OFFICE SYMBOL (If applicable)	7a. NAME OF MONITORING ORGANIZATION Naval Air Development Center		
6c. ADDRESS (City, State and ZIP Code) Washington, DC 20375		7b. ADDRESS (City, State and ZIP Code) Warminster, PA 18974		
8a. NAME OF FUNDING/SPONSORING ORGANIZATION Naval Air Systems Command	8b. OFFICE SYMBOL (If applicable)	9. PROCUREMENT INSTRUMENT IDENTIFICATION NUMBER		
8c. ADDRESS (City, State and ZIP Code) Washington, DC 20361		10. SOURCE OF FUNDING NOS.		
11. TITLE (Include Security Classification) (See page ii)		PROGRAM ELEMENT NO. 62761N	PROJECT NO. SF 54-502- 001	TASK NO. 61-C04-10; 61-0086; 63-1096
12. PERSONAL AUTHOR(S) C.F. Poranski, Jr., Editor				
13a. TYPE OF REPORT Final	13b. TIME COVERED FROM _____ TO _____	14. DATE OF REPORT (Yr., Mo., Day) February 22, 1984	15. PAGE COUNT 103	
16. SUPPLEMENTARY NOTATION				
17. COSATI CODES		18. SUBJECT TERMS (Continue on reverse if necessary and identify by block number)		
FIELD	GROUP	SUB. GR.		
			Chemical characterization Fracture toughness	
			Thermomechanical evaluation Composite testing	
			(Continues)	
19. ABSTRACT (Continue on reverse if necessary and identify by block number)				
<p>This is the final report of a NAVAIR sponsored program addressing aspects of the composite and adhesive materials requirements of V/STOL aircraft. The primary tasks were to develop and characterize high modulus, high toughness resins with use temperatures of 350°F to 450°F or higher; to develop graphite fiber reinforced composite fabrication technology for newly developed resin matrices; to develop failure criteria for composite design optimization; and to establish appropriate quality control parameters.</p> <p>During the course of the program a variety of matrix materials and adhesives were studied in the various tasks. Three matrix materials were picked for detailed study on the basis of performance and processing characteristics. They are NRL C10-diamide, Narmco 5208 epoxy and Hexcel F-178 bis-maleimide. Composites made from them with T-300 graphite fiber formed the key test set in the Failure Analysis Task. Detailed chemical and thermochemical characterization was carried out on these resins to provide a data base for developing quality assurance procedures.</p>				
(Continues)				
20. DISTRIBUTION/AVAILABILITY OF ABSTRACT		21. ABSTRACT SECURITY CLASSIFICATION		
UNCLASSIFIED/UNLIMITED <input checked="" type="checkbox"/> SAME AS RPT. <input type="checkbox"/> OTIC USERS <input type="checkbox"/>		UNCLASSIFIED		
22a. NAME OF RESPONSIBLE INDIVIDUAL C. F. Poranski, Jr.		22b. TELEPHONE NUMBER (Include Area Code) (202) 767-2488	22c. OFFICE SYMBOL Code 6120	



 S ELECTED

 MAR 21 1984

 A

11. TITLE

HIGH PERFORMANCE COMPOSITES AND ADHESIVES FOR V/STOL AIRCRAFT

18. SUBJECT TERMS (Continued)

Prepreg fabrication	Adhesives	T-300 Graphite fiber	Torlon 4000 (Amoco)
In-plane loader test	Thermosets	PMR-15 (NASA)	Ryton PPS (Phillips)
Radiation curing	Thermoplastics	T-600 (Gulf)	
V/STOL aircraft	(poly) phthalocyanines	NCNS (Ciba-Geigy)	
Nuclear magnetic resonance	(poly) phthalonitriles	Astrel (Carborundum)	
Dynamic dielectric analysis	C-10 Diamide	Radel (Union Carbide)	
Quality control	Narmco 5208	Udel (Union Carbide)	
Design optimization	Hexcel F178	P-300 (ICI)	
Differential scanning calorimetry	Epoxy resins	2080 (Upjohn)	
Failure analysis	Bis-maleimides	NR 150 B2 (Dupont)	

19. ABSTRACT (Continued)

This report covers the final phase of the program. Possible quality assurance tests, based on chemical characterization, are discussed for the C10-diamide, epoxy and bis-maleimide resins. Fracture toughness results and glass transition temperatures for neat resin are reported for six thermoset polymers (Narmco 5208, Hexcel F-178, NASA PMR-15, Gulf T-600, Ciba-Geigy NCNS and NRL C10 diamide), and eight thermoplastic polymers (Carborundum Astrel, Union Carbide Radel and Udel, ICI P300, Upjohn 2080, DuPont NR150B2, Amoco Torlon 4000 and Phillips Ryton PPS.) Adhesive fracture energies at room temperature and at 225°C are reported for a number of commercial and experimental thermosetting and thermoplastic adhesive systems. Composite fabrication procedures were developed for the NRL C10-diamide/T-300 graphite material system.

Composite test panels were fabricated from T-300 graphite with NRL C10-diamide, Narmco 5208 and Hexcel F-178 for fracture tests conducted on an in-plane loader developed at the Naval Research Laboratory. Tests were run at room temperature and at 232°C and various laminate layup angles. Critical loads and displacements and maximum loads supported by the samples were measured as functions of laminate orientation at the two temperatures and the data stored and analyzed with a computer. For the materials and loadings used in this study there is little difference in the in-plane fracture toughness. The laminate samples also retained significant strength at 232°C, a temperature considerably higher than the recommended maximum use temperature for the resins. This indicates that in-plane fracture toughness of fiber-reinforced composites is dominated by the fiber.

CONTENTS

Introduction	1
Chemical Characterization for Quality Control	5
C. F. Poranski, Jr. and W. B. Moniz	
Thermomechanical Characterization of High Performance Polymeric Resins and Adhesives.....	21
R. Y. Ting and R. L. Cottingham	
Fabrication of Phthalocyanine/Graphite Composites	39
R. Y. Ting and H. C. Nash	
Failure Criteria for Composite Structures	59
P. W. Mast, L. A. Beaubien, D. R. Mulville, S. A. Sutton, R. W. Thomas, J. Tirosh and I. Wolock	
Radiation Curing Studies Conducted as Follow-on to the V/STOL Program Initiative	91
F. J. Campbell, L. M. Johnson and J. S. Burr	
Appendix 1. Bibliography of Major Publications	97



Accession For	
NTIS GRA&I	<input checked="" type="checkbox"/>
DDP TAB	<input type="checkbox"/>
Unannounced	<input type="checkbox"/>
Justification	
Distribution/	
Availability Codes	
Dist	Avail and/or Special
A-1	

HIGH PERFORMANCE COMPOSITES AND ADHESIVES FOR V/STOL AIRCRAFT

Final Report

INTRODUCTION

This is the final report of a multidisciplinary program initiated in July 1975 to provide information on graphite fiber-reinforced composite materials and improved adhesives for potential use in Navy V/STOL aircraft. Today's military and civilian aircraft are making increasing use of fiber-reinforced composite materials as a substitute for metals because of the weight and performance advantage, and the cost effectiveness of these new structural materials. The weight saving is critical to the successful development and deployment of V/STOL aircraft which require a larger, heavier propulsion system.

The severe weight constraints on carrier-based aircraft in general and vertical/short take-off and landing (V/STOL) aircraft in particular, have caused the Navy to look to new design concepts utilizing easily fabricated, fiber-reinforced composites that combine superior stiffness with a high strength-to-weight ratio. At the time of initiation of this program it was felt that the temperature to be reached on portions of the V/STOL underbody would require a resin system that could withstand in excess of 260°C (500°F), far above the capability of state-of-the-art epoxies. With the passage of time, however, this temperature requirement has been relaxed somewhat while the effect of moisture absorption on the degradation of composite properties has drawn increased attention. Thus, there still remains a requirement for composite systems, with a significantly greater performance capability than is available from epoxies, for use in advanced V/STOL and other high performance aircraft.

This need to maximize structural weight savings led to an in-depth study at the Naval Research Laboratory (NRL) of the variables that influence the behavior of composites and adhesives. The overall effort was a blend of fundamental and applied research representing different scientific disciplines and organizational areas within the Laboratory. Administratively, the program was divided into six inter-related and interacting task areas:

- Resin Synthesis
- Thermomechanical Characterization
- Chemical Characterization
- Radiation Curing
- Composite Fabrication
- Failure Criteria for Composite Structures

Manuscript approved September 21, 1983.

The Resin Synthesis and Radiation Curing Tasks were completed and terminated at the end of FY78. This report gives a summary of the work of the other four Task Areas as well as a status report for the Radiation Curing task. Finally, a bibliography of published reports covering the various aspects of work associated with this program is included.

Some accomplishments of the Task Areas in this program are summarized in the following paragraphs.

Resin Synthesis: A new class of highly crosslinked polymers, was investigated in this program. Designated "polyphthalocyanines", these materials had been developed in an in-house basic research program. The C-10 diamide-linked phthalocyanine system chosen for evaluation was shown to be comparable in performance to the bis-maleimide, F-178, i.e. it could be readily processed by conventional techniques and had an upper use temperature of about 450° F (232° C). Although the phthalocyanine prepreg had poor drape and tack (disadvantages which could be removed by further development), it could be stored indefinitely at room temperature. Second generation resins of this class have evolved from the continuing basic research program. The new resins are based on diether-linked phthalonitrile precursors which may be readily synthesized in a one-step process from low-cost starting materials. Moreover, they have improved thermal stability, low moisture absorption, and reduced flammability with a high char yield. Further investigation of these new materials as matrix resins for composites is being carried out under another program.

Thermomechanical Characterization: A significant accomplishment of this task has been the acceptance, by the aerospace industry, of the concept of fracture toughness as an important material property of resins used as matrices for fiber-reinforced composites. Throughout this program emphasis has been placed on the evaluation of the toughness of candidate resins and how this parameter affects composite toughness. A study carried out with industry cooperation has clearly demonstrated that toughened matrix resins provide composites with improved interlaminar shear properties.

Chemical Characterization: Navy and DoD concern about quality control of composite matrix materials led to the incorporation of chemical characterization as a major component of this study. Aerospace industry fabricators of composites also have a stake in materials characterization. The NRL effort contributed significantly to the DoD-industry investigation of the characterization of epoxy components and thus led to a better understanding of composition-performance relationships. Further, the NRL effort provided information on the chemical characterization of bismaleimide and phthalocyanine precursors and detailed quality control procedures for the latter. It was clearly demonstrated that the exact composition of the single-component phthalocyanine precursor could be readily identified and that reasonable, simplified quality assurance technology was available for exploitation. The general effect of these efforts has been the acceptance by the producers of advanced resin systems of the necessity for cooperating with users in supplying information on product formulation and in maintaining stable product composition.

Composite Fabrication: This task prepared all composite samples used by the Failure Criteria Task. The two commercial prepregs were cured using manufacturer's standard recommendations, modified as necessary for the equipment available at NRL. The task demonstrated that NRL C10 diamide could be made into prepreg either by the hot melt method or by the solvent slurry method. Data from differential scanning calorimetry, dynamic dielectric analysis and thermogravimetric analysis were used to develop the cure cycles for NRL C10 diamide prepregs.

Radiation Curing: This task showed that radiation curing is a viable technique for curing adhesives. The process can often produce properties in adhesives which are better than those obtained through thermal cures because of the lack of heat induced strains. However, there must be more work in developing adhesive resins which can be cured through the radiation process. Such efforts would be rewarding because of the cost effectiveness of radiation curing as compared to conventional heat cures.

Failure Criteria for Composites: Using a novel automated in-plane loader testing instrument, this task extensively tested a series of three graphite fiber (T-300) reinforced composites, with different matrix resins (NRL C10 phthalocyanine, Hexcel F-178 and Narmco 5208). The complex data characterizing the failure behavior can be displayed by a 3-d graphical method using an analysis algorithm developed by the task. The results showed that there is little difference in the in-plane fracture toughness for the three composites at room temperature and at elevated temperature. There was significant in-plane fracture toughness at temperatures higher than the "use" temperatures of the resins. The conclusion is that in-plane fracture toughness is dominated by the fiber. The group also found that the analytical technique could be used to predict failure loads and location and they verified this by fracture tests on a box beam.

This task also investigated the application of fracture mechanics to adhesive joints. They found that a single fracture parameter may not characterize adhesive joints under complex loading. Classical fracture mechanics can be applied to joints under tensile loading and under tensile loading with a small degree of shear and bending. Combined tension, shear and bending usually leads to non-linear behavior of adhesive joints.

Chemical Characterization for Quality Control

C. F. Poranski, Jr. and W. B. Moniz
Polymer Diagnostics Section
Chemistry Division

INTRODUCTION

Programs to develop or select organic polymers for aerospace applications must include development of quality assurance procedures. These procedures should include tests to verify not only the processability and physical properties but also the chemical composition of the prepolymer. This threefold approach to quality assurance was an integral part of the NRL V/STOL program.

The Chemical Characterization Task was responsible for developing analytical procedures to monitor the chemical composition of polymer systems studied in the program. These procedures can now be coupled with those developed by the other Tasks for monitoring thermochemical and physical properties to form a complete quality assurance scheme for these polymer systems.

The final report of this task is divided into three parts. The first part covers the work of the past year. The second part outlines the major accomplishments of the whole period. The final part is an evaluation which contains suggestions for quality control procedures for the major materials studied in the program.

WORK DURING FY79

The primary effort in this Task during FY79 concerned N,N'-bis(3,4-dicyanophenyl)decanediamide, Figure 1, hereafter referred to as C₁₀-diamide. This compound was selected for development from a series of polyphthalocyanine precursors synthesized at the Naval Research Laboratory.

Chemical characterization of C₁₀-diamide by proton and carbon-13 nmr was completed earlier in this program (1a). The present work concerns characterization of fresh and aged prepreg made from C₁₀-diamide and graphite fiber and of the B-staged system formed from C₁₀-diamide and SnCl₂·H₂O.

C₁₀-diamide/Graphite Prepreg: Contracts had been placed with two companies to develop procedures for fabricating prepreg using C₁₀-diamide and Thornel-300 graphite fiber. One contractor employed a hot melt procedure resulting in a black prepreg with a 30% C₁₀-diamide content. The other contractor used a solvent slurry method to produce a green prepreg with a 40% C₁₀-diamide content. Both prepregs were dry and boardy.

The depth of color of the prepreg indicates the degree of heating (or B-staging) involved in each procedure. Initially, C_{10} -diamide is a near-white material. Upon melting, thermally-activated curing begins and the material quickly darkens. If heating is stopped soon after melting, the curing reactions stop, and the resulting material is green. If the heating is continued the material darkens, appearing black in reflected light. It appears, therefore, that the hot melt procedure, requiring the C_{10} -diamide to be fluid for a considerable time, results in a fairly advanced state of cure. In the solvent slurry method the prepreg is evidently heated enough to drive off the solvent and melt the C_{10} -diamide onto the fibers, then cooled to prevent further cure reaction.

Samples of these two prepregs were extracted with hot ethanol. The black prepreg gave a clear, colorless solution which on evaporation left a trace of white residue too small to analyze. The green prepreg gave a bright yellow solution which on evaporation left a considerable amount of light yellow precipitate. The precipitate was identified as C_{10} -diamide by its proton nmr spectrum.

Because it contained the desired 40% resin content, the prepreg prepared by the solvent slurry method was selected for further study. This prepreg was found, however, to contain volatiles which caused problems in producing cured composite. The volatiles were identified by nmr analysis to be a mixture of water and dimethyl formamide, the solvent used in manufacture of the prepreg.

Prepreg Aging Tests: The mechanism proposed for the cure of the C_{10} -diamide is condensation of its nitrile groups to give a phthalocyanine structure. Since this reaction occurs only above the melting point of C_{10} -diamide, around 200°C , it was felt that C_{10} -diamide prepreg would be stable indefinitely at room temperature. An aging study was carried out on the C_{10} -diamide prepreg to verify this hypothesis.

For this study, kits consisting of seventeen 6" x 6" pieces of C_{10} -diamide prepreg were aged at room temperature in chambers held at relative humidities of 16% and 95%. Every four weeks a kit was removed from each chamber. One piece from each kit was set aside for the chemical characterization work. The remaining 16 pieces from each kit were heated at 100°C under a vacuum of 30" Hg for 3-1/2 hours to remove volatiles. After the heat/vacuum treatment each set of "dried" prepreg was used to prepare a sixteen-ply composite panel. Flexural and shear properties of the cured composite panels are reported in the chapter, "Fabrication of Phthalocyanine/Graphite Composites". The plies set aside for the chemical tests were not vacuum dried.

For these tests a one-gram sample of each piece of the aged prepreg was extracted in a Soxhlet apparatus with 20 ml of ethanol for 3-1/2 hrs. The ethanol was evaporated and the extracted residue was air dried overnight. The samples were weighed, their melting points measured and proton nmr spectra run.

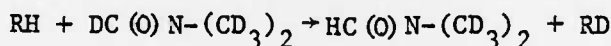
The amount of material recovered through the ethanol extraction of these samples ranged from 14% to 90% of the theoretical resin loading. There

was no dependence of amount of material extracted on either age or humidity. This variability may arise from non-uniform melting of the C_{10} -diamide during the prepreg manufacture. Thus there are "islands" of unmelted C_{10} -diamide distributed across the surface of prepreg. This was reflected in the non-uniformity of the green color of the prepreg.

Each of the extracted samples melted within a 2-4 degree range and all melting points were between 174 and 182°. These melting points are lower than that of the C_{10} -diamide from which the prepreg was made.

Proton nmr spectra of the air dried extracts were run in two solvents, dimethyl formamide- d_7 and dimethyl sulfoxide- d_6 . The first is an excellent solvent for C_{10} -diamide and thus offers a higher probability of detecting impurities. The spectra were also run in dimethyl sulfoxide- d_6 to monitor the presence of dimethyl formamide remaining from the manufacturing process. Basically the spectra are quite similar to those obtained with unheated C_{10} -diamide, as illustrated in Figure 2. In the spectra of the material extracted from the prepreg there are some features for which we have not yet been able to account. These features (Figure 2) are the broad resonance at 4.4 ppm and the multiplet at 7 ppm. There is a possibility that these peaks come from UC-309, the finish on the Thornel 300 fiber.

There is a new peak at 8 ppm which in this sample is a shoulder spike on the main band. This peak may be due to some of the solvent, dimethyl formamide- d_7 , which has exchanged the formyl deuteron for a proton. We have some evidence that the proton source is the amide group in the C_{10} -diamide



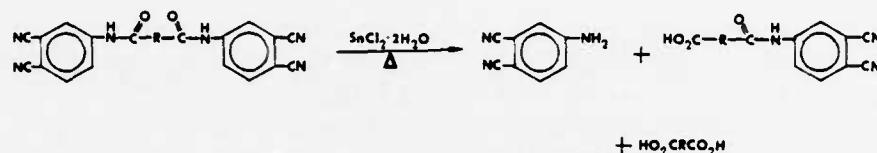
which has been heated. No exchange has been observed in the spectra of C_{10} -diamide which has not been heated. This peak does not occur in the dimethyl sulfoxide- d_6 solutions of the prepreg extracts.

C_{10} -diamide/ $SnCl_2$ System: C_{10} -diamide cures to form polyphthalocyanine at temperatures above 200°C. The reaction can be accelerated by addition of powdered metals or metallic salts. The metals or salts can also affect other properties. Thus, a mixture of C_{10} -diamide with a stoichiometric amount of $SnCl_2 \cdot 2H_2O$ not only cures faster, but also forms a polymer which has higher flammability resistance than cured C_{10} -diamide alone. It was reported, however, that the long term high temperature mechanical properties of this polymer were not as good as those of polymer prepared from C_{10} -diamide alone. We attempted to determine the cause of the change in mechanical properties by studying the C_{10} -diamide/ $SnCl_2$ prepolymer. This prepolymer is prepared by heating a thoroughly mixed charge of C_{10} -diamide and $SnCl_2 \cdot 2H_2O$ at 175°C until all of the water is eliminated, about 15-20 minutes. The resulting amber-colored solid is soluble in dimethyl formamide.

Figure 3 shows the proton nmr spectrum of this prepolymer. The peaks arise primarily from C_{10} -diamide. (Note that $SnCl_2$ has no protons and will not be detected by this technique.) There are, however, two features not attributable to C_{10} -diamide. First, the band at 2.0 ppm, normally a triplet arising from the protons of the methylene group adjacent to the amide carbonyl, appears to be an unsymmetrical quartet. Second, there are a number of additional lines between 6.5 and 7.0 ppm due to aromatic protons.

Comparison with spectra of authentic materials showed that the aromatic lines were due to 4-aminophthalonitrile and that the distortion of the band at 2 ppm is caused by overlap with a signal from methylene protons adjacent to the carbonyl group of sebacic acid.

The presence of these compounds in the C_{10} -diamide/ $SnCl_2$ mixture can be explained by assuming that hydrolysis of the C_{10} -diamide has occurred.



Scheme 1

This could easily occur during the early stages of heating the C_{10} -diamide/ $SnCl_2 \cdot 2H_2O$ mixture. The $SnCl_2$ could catalyze the hydrolytic attack at the amide group. The extent of hydrolysis will depend on the composition of the C_{10} -diamide/ $SnCl_2 \cdot 2H_2O$ mixture and the rate at which the mixture is heated to the B-staging temperature. By careful adjustment of these two parameters it would be possible to control the amount of 4-aminophthalonitrile and the C_{10} -monoamide present in the B-staged material. Both of these compounds can react as end-caps with the phthalonitrile groups of the growing polymer. Thus the degree of cross-linking in the final polymer could be altered to affect the final mechanical properties.

SUMMARY OF THE OVERALL PROGRAM

It is fitting in this final report to review in summary form the highlights of the efforts of the Chemical Characterization Task during the course of this program. One convenient way of doing this is to look at the classes of materials studied and the techniques used. This will include general observations and conclusions generated not only from this program, but also from interactions with other characterization programs.

Epoxy Resins: Initial activity in the area of epoxy resin analysis was the assembly of a catalog of carbon-13 and proton nmr spectra of a variety of epoxy resins and curing agents (2). This data base demonstrated that carbon-13 nmr could be used to identify different classes of epoxy resins (3) and how quantitative carbon-13 nmr could be applied to measurements of average oligomer content of DGEBA type epoxy resins (4).

Efforts then focused on epoxy systems based on tetraglycidyl methylene-dianiline, TGMDA, since this resin appeared headed for a primary role as a matrix for high performance composites in aerospace applications. Figure 4 gives an example of the usefulness of carbon-13 nmr for studying these systems. The figure shows carbon-13 nmr spectra of the matrix material extracted from graphite/epoxy prepregs obtained from three different commercial sources. Each formulation is based on TGMDA with diaminodiphenylsulfone (DDS) as the curing agent. Each system contains additional components, however, which are different in each formulation. The carbon-13 nmr spectra clearly reveal the presence of these additives, without the necessity of

separating the complex mixtures.

Further work on TGMDA/DDS systems resulted in a proton nmr method for quantitative analysis (5). While the procedure at present takes account only of the two primary components, it could be easily adapted to accommodate the presence of the additives found in the sophisticated prepreg matrix formulations.

Some of the greatest progress in the analysis of these systems has come in the field of liquid chromatography (LC). The cooperative efforts of government and industry have demonstrated the practicality of quality control procedures based in part on LC analysis. Most encouraging are the results obtained in a recent round-robin test for an LC procedure for a typical commercial formulation. The results of this round-robin test (6) showed that, by working together, a supplier and customer could develop reproducible and meaningful methods for monitoring chemical composition of proprietary formulations.

Polyimides and Other Materials: During the early stages of this program, a wide variety of materials was surveyed, with carbon-13 and proton nmr, including polyimide precursors, polysulfones, epoxy novolacs and Xyloks. Two of these materials were studied in detail; Hughes HR-600 and Hexcel F-178. The proposed structure of the prepolymer of HR-600 was confirmed by carbon-13 nmr (7). We determined that F-178 was predominantly a mixture of two components, the bismaleimide of methylene dianiline and triallyl isocyanurate. This latter compound is a high-boiling liquid which can react with the maleimide. This mixture resulted in a prepreg with tack and drape which could be laid up and cured following procedures developed for epoxy resin prepreps. In essence it is a 100% reactive system which avoids the solvent removal step required with dry polyimide precursor systems.

However, like the epoxy prepreg, the F-178 prepreg has a limited shelf-life. We postulated that this was due to the progression of cure via a free radical mechanism initiated during prepreg manufacture. We were not able to confirm this, however, in an aging study on F-178 prepreg (8).

CHEMICAL COMPOSITION QUALITY CONTROL PROCEDURES

The establishment of quality control procedures is an important step in any material procurement program. The tests to be used should be appropriate to assure consistency of material both in composition and performance without unnecessarily increasing costs.

During the past few years a great amount of attention has been given to the area of chemical characterization of matrix resins in high performance composites (9-11). This came about because of the need of the aerospace industry to reduce costs and assure product performance. Moral and financial support from DOD and NASA resulted in programs to develop and refine analytical tools and determine meaningful limits for concentration variations. This last point has indeed been the most difficult to assess because of the large investment in time and materials required, and it still is unresolved. Nonetheless, the concept of chemical characterization has gained acceptance and eventually should be incorporated into material specifications.

From the work done so far, it is clear that, for most systems, no one technique can accomplish the whole characterization task. The work required for each system will depend on the complexity of the system and the degree to which the various components are found to affect the final performance. And chemical characterization must be coupled with tests of processing variables to form a complete quality control program.

The materials studied in the composite matrix area of this program fall into three categories, epoxy resins (Narmco 5208), polyimide (Hexcel F-178), and polyphthalocyanine (NRL C₁₀-diamide). Each requires a different characterization scheme. Some possible approaches are described below.

Narmco 5208: Narmco has shown great interest in developing characterization methods for their resin systems (6,12). The company has indicated willingness to cooperate with their customers in developing quality control programs which will assure compositional consistency while nominally protecting the proprietary nature of formulations (6). The primary technique could be liquid chromatography, comparing chromatograms of shipped lots of prepreg to those of previously agreed upon standard solutions, supplied with the shipments.

Hexcel F-178: The chemical characterization of this system has not received as much attention as has been given the epoxies. Analysis of its carbon-13 and proton nmr spectra showed its major components to be methylene dianiline bis-maleimide and triallyl isocyanurate in a ratio close to 1:1. The proton nmr spectrum (Figure 5) offers a convenient, rapid analytical approach, because the peaks from the major components are well separated. There are two problems to overcome in the analysis of F-178 resin. The first is that the resin deteriorates rapidly when dissolved in acetone. Any analysis of acetone solutions must be carried out promptly. It is not known at present if the deterioration is due to the acetone, or if it will occur in any solvent. The second problem is that acetone is not a strong enough solvent to extract semi-cured products formed during aging of the resin (8). More work is needed to develop a solution-based analytical procedure (nmr, liquid chromatography, infrared).

The status of chemical characterization and quality control procedures for F-178 is similar to that in the epoxy field a few years ago. A good deal is known about the system, but much remains to be done if and when F-178 pre-pregs achieve high use in aerospace applications.

C₁₀-Diamide: In contrast to the complexity of the epoxy resin and F-178 systems, C₁₀-diamide is a single component system. As such, its analysis at the raw material stage is much simpler. It appears however that analysis of B-stage prepreg will be more difficult.

Much of the C₁₀-diamide used in this program was obtained under contract from a commercial vendor. Acceptance specifications included melting points, infrared spectra and elemental analyses. Other initial tests run at NRL included proton and carbon-13 nmr, and curability. Table 1 gives delivered batch size, melting point and elemental analyses of the five commercial lots.

Table 1. Comparison of Melting Points and Elemental Analyses for Five Commercially Produced Lots of C₁₀-diamide.

Lot No.	A7	B7	C7	D7	E7	Std ^a
Size	2.8 lbs.	6.6 lbs.	24.6 lbs.	44 lbs.	16 lbs.	---
Melting Point ^b	185°-187°	186°-188°	183°-187°	187°-190°	185°-187° ^c	190°-192°
Elemental ^d	C% 68.76	68.58	68.68	68.96	68.56	69.34
Analyses	H% 5.55	5.68	5.37	5.48	5.53	5.56
	N% 17.98	18.37	18.95	17.99	18.34	18.71

a. High purity NRL preparation.

b. Specification was 3 degree range within 185°-192°.

c. After oven drying.

d. Theoretical: C, 69.1%; H, 5.35%; N, 18.57%.

Since C₁₀-diamide is a distinct organic molecule, its melting point can be a valuable quality control parameter. Two points have to be amplified. First, a standard procedure must be established for melting point determinations for comparisons to be valid. Such a procedure, based on differential scanning calorimetry, has previously been proposed (13). Second, it is economically unsound to require commercial C₁₀-diamide to have the same melting point as the standard. Just how close to the standard and over how narrow a range a commercial lot must melt is still not fully determined. There is a variety of melting behavior among the five lots (Table 1) but all cured "properly." As yet, we have no complete set of thermomechanical test results for these lots to compare behavior.

Figure 6 shows the infrared spectrum obtained from a sample synthesized at NRL. We have assigned some of the more prominent bands as follows: 3330 cm⁻¹ (N-H), 3100 cm⁻¹ (aromatic C-H), 2940 and 2860 cm⁻¹ (aliphatic C-H), 2240 cm⁻¹ (C≡N), 1710 cm⁻¹ (C=O), 1590, 1520, 1490 cm⁻¹ (C=C), 1340 cm⁻¹ (PhN-H), 1255 cm⁻¹ (amide III). Inspection of the infrared spectra of the various batches of C₁₀-diamide showed that all of them were similar to the spectrum in Figure 6. However, variations occurred in some bands which could not be correlated with melting point or method of purification of the batch. The two major variations were changes in the width and shape of the carbonyl band, and the occasional appearance of a moderately strong band at 1410 cm⁻¹ which overwhelmed the three small bands in that region. Clearly, much work is required before infrared spectroscopy could function as a quality control vehicle in any way other than gross identification of C₁₀-diamide.

The quality control role of carbon-13 nmr is much the same as for infrared spectroscopy, but for a different reason. It is sensitivity, rather than precision or reproducibility, which limits the potential of carbon-13 nmr.

For example, the carbon-13 chemical shifts measured from the spectra of over 16 separate batches (NRL and commercial) were constant to $\pm .3$ ppm over a chemical shift range of 200 ppm. There are no obvious problems due to the previous histories of the samples. However, carbon-13 nmr is hard pressed to detect impurities at low levels, say below 5%, without resorting to time-consuming data accumulations impractical for routine use. The primary reason for this low sensitivity is the 1% natural abundance of the carbon-13 isotope. In the case of C_{10} -diamide, the problem is compounded by its low solubility: this results in lowering the effective sensitivity towards impurities and leads to dynamic range problems in the detection system due to the large solvent signals.

Proton nmr, on the other hand, does not suffer from low sensitivity. It provides, therefore, a quick method of identification as well as for determining impurities at the 1-5% level. In spite of the low solubility of C_{10} -diamide in dimethyl sulfoxide ($DMSO-d_6$) (~ 9 mg/ml) we were able to detect in one sample $\sim 2\%$ dimethyl formamide (DMF), a solvent used in the commercial preparation (Figure 7). In more concentrated solutions in $DMF-d_7$ (~ 160 mg/ml) we have observed in the proton nmr spectrum of several samples, traces ($\sim 1\%$) of acetone or ethyl alcohol, solvents which may be used to wash the material after synthesis.

Future C_{10} -diamide procurement contracts should include the following chemical acceptance tests: proton nmr spectra in both dimethyl formamide- d_7 and dimethyl sulfoxide- d_6 , infrared spectrum, melting point, and elemental analysis. The procedures and test limits are given below. They are aimed at assuring that received material is, in fact, C_{10} -diamide and does not contain unacceptable levels of contaminants, such as inorganic fillers, unreacted starting materials (4-aminophthalonitrile and sebacyl chloride), reaction by-products, and manufacturing solvents. The practical limits for contaminant levels are not known at present. Those given below (see Test Procedures) should assure receipt of C_{10} -diamide equivalent in quality to material previously received from commercial sources.

Additional tests are advisable to assure processability. For example, a curing test can be developed based on specified sample configuration, temperature, and time to reach a given hardness. The texture of the material is an important processing variable and should be specified in some manner such as particle size, grind or a flow property. Finally, some physical test to determine the strength of the cured polymer should be specified.

A written test report, including copies of the spectra, should be required.

The validity of the elemental analysis rests on the type of impurity, if any, contained by the C_{10} -diamide. If present at a 1% level an inorganic filler material which does not contribute to the measured carbon would lower the carbon elemental analysis result enough to disqualify the material. But the presence of an organic impurity, such as dimethyl formamide, does contribute to the measured carbon content. A sample of C_{10} -diamide containing 2% dimethyl formamide would still give an acceptable elemental analysis. A contaminant such as dimethyl formamide or acetone quite possibly could evaporate during a melting point determination, and thus escape detection in both the

elemental analysis and melting point tests. However, such contaminants are detectable using the recommended proton nmr procedures.

Test Procedures

Proton nmr spectra: a. The proton nmr spectrum of a 0.05 to 0.08% (by weight) solution in dimethylformamide- d_7 shall match that of a supplied standard material. The ratio of the area of the aliphatic proton peak (0.7-1.9 ppm) to the area of the aromatic proton peaks (7.5 to 8.5 ppm) shall be 2 ± 0.15 when measured by standard quantitative proton nmr techniques (14). (The error limit of ± 0.15 is tentative and subject to change based on future statistical studies of the errors in this analysis.) The intensities of extraneous solvent peaks (acetone, water, etc.) shall be measured, by reference to a calibration curve, to assure that their concentration is below some acceptable level, yet to be determined. b. The proton nmr spectrum of a 0.008% (by weight) solution in dimethylsulfoxide- d_6 shall be examined for presence of residual dimethyl formamide peaks between 2.8 and 3.0 ppm. The dimethyl formamide content shall be 2% or less by weight as determined from comparison with a calibration curve.

Infrared spectrum: The spectrum (1% in KBr pellet) shall match that of a supplied standard material. This test serves to confirm the presence of the phthalonitrile $C \equiv N$ groups through the presence of a band at 2240 cm^{-1} . At the present time this is a qualitative test only.

Melting point: Melting shall occur over a 3°C or less range, between the limits of 185°C and 194°C . Note any sign of solvent evaporation, pre-melting or sintering. The measurement shall be made on a Fisher-Johns melting point apparatus in the standard configuration. A procedure based on differential scanning calorimetry may be an alternative.

Elemental analysis for C, H, N: The results shall agree with theoretical values for $C_{26}H_{24}N_6O_2$ within $\pm 0.5\%$ (C, 69.0%; H, 5.3%; N, 18.6%).

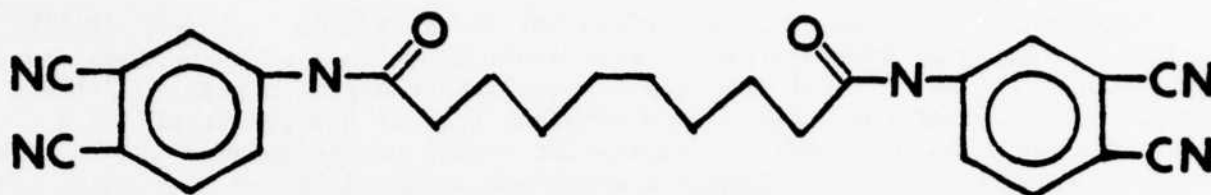


Fig. 1 - N,N'-bis(3,4-dicyanophenyl) decanediamide, commonly known as C_{10} -diamide.

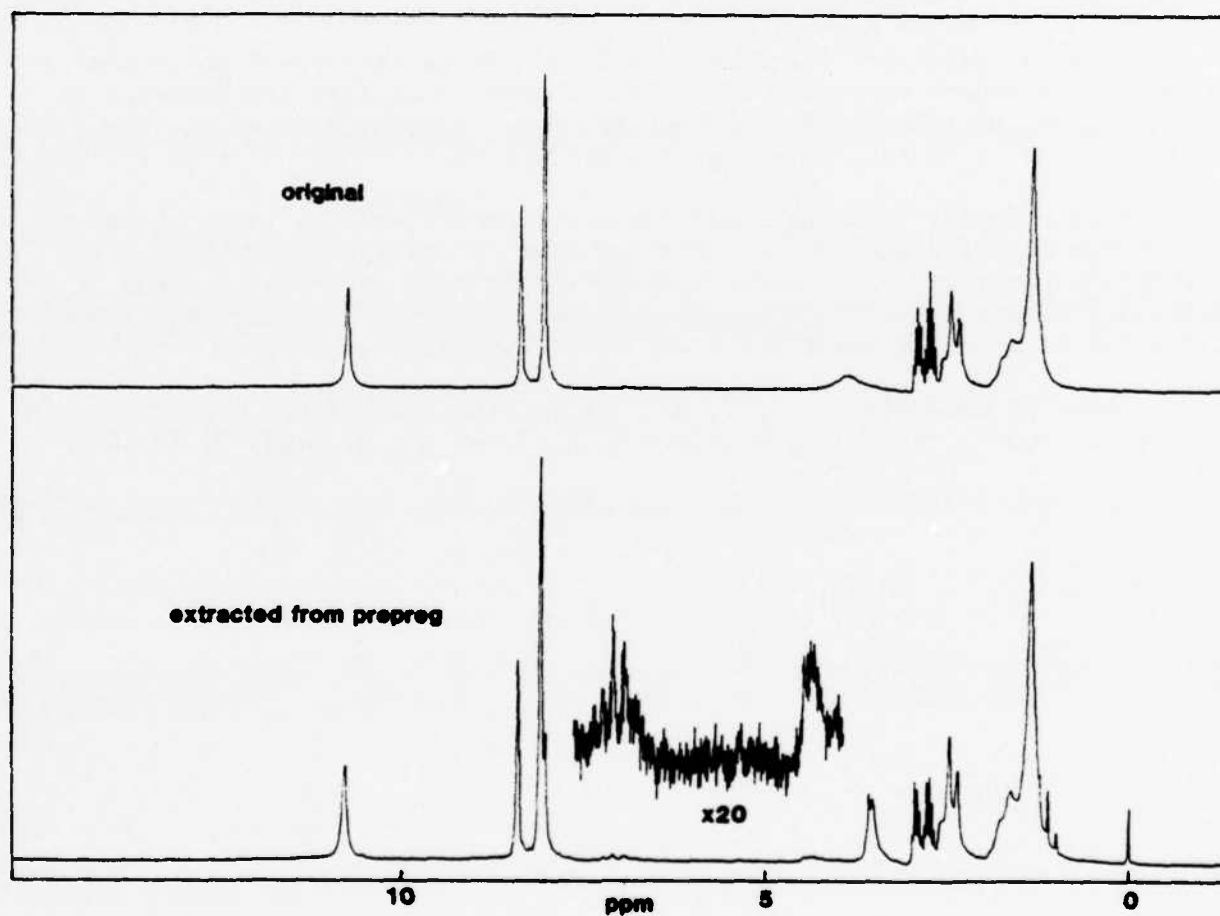


Fig. 2 - Proton nmr spectra, in dimethyl formamide- d_7 , of C_{10} -diamide (upper spectrum) and material extracted from a C_{10} -diamide/T-300 prepreg.

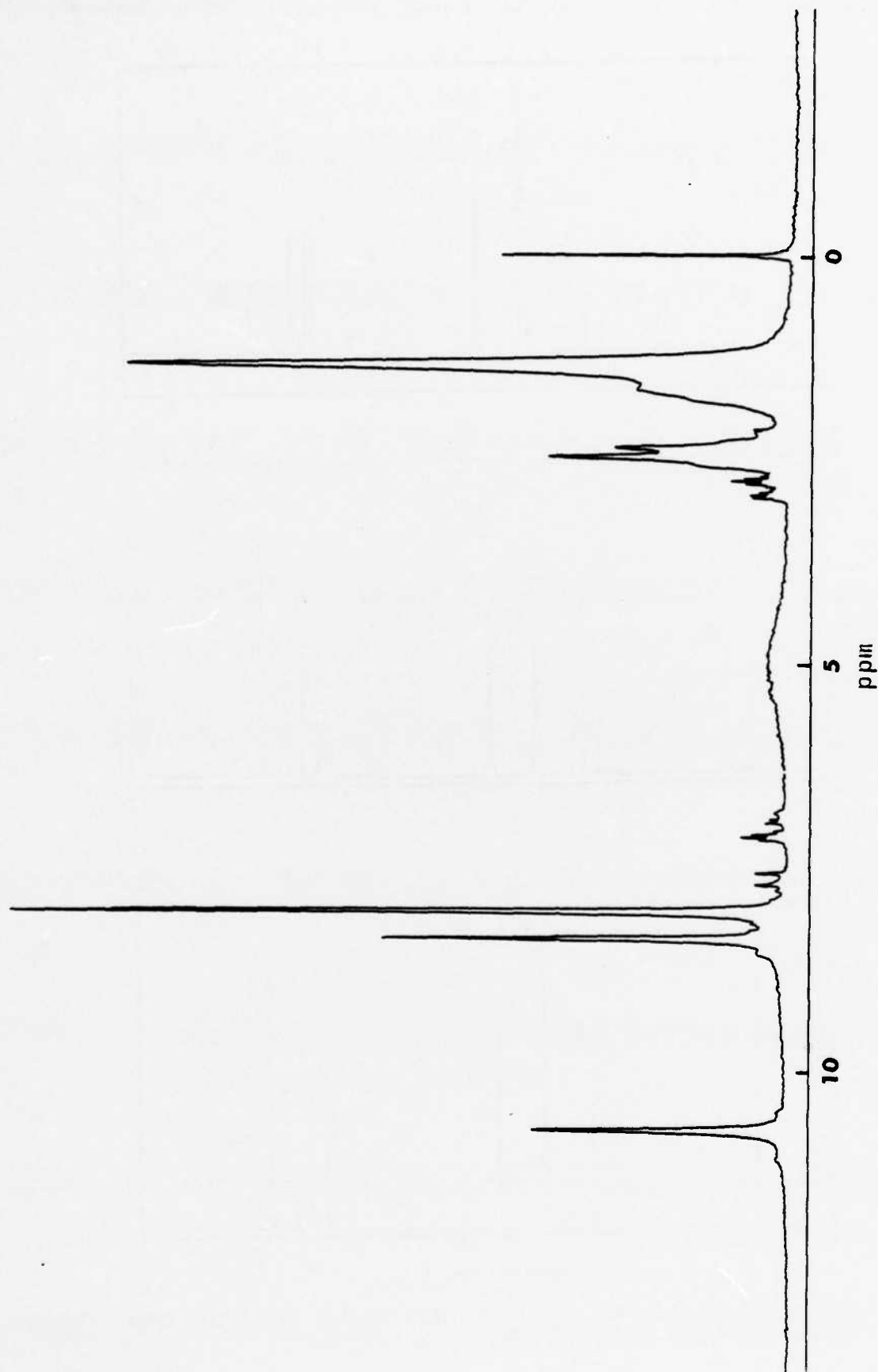


Fig. 3 - Proton nmr spectrum (60 MHz) of the material resulting from the B-staging of a stoichiometric mixture of C_{10} -diamide and $SnCl_2 \cdot 2H_2O$.

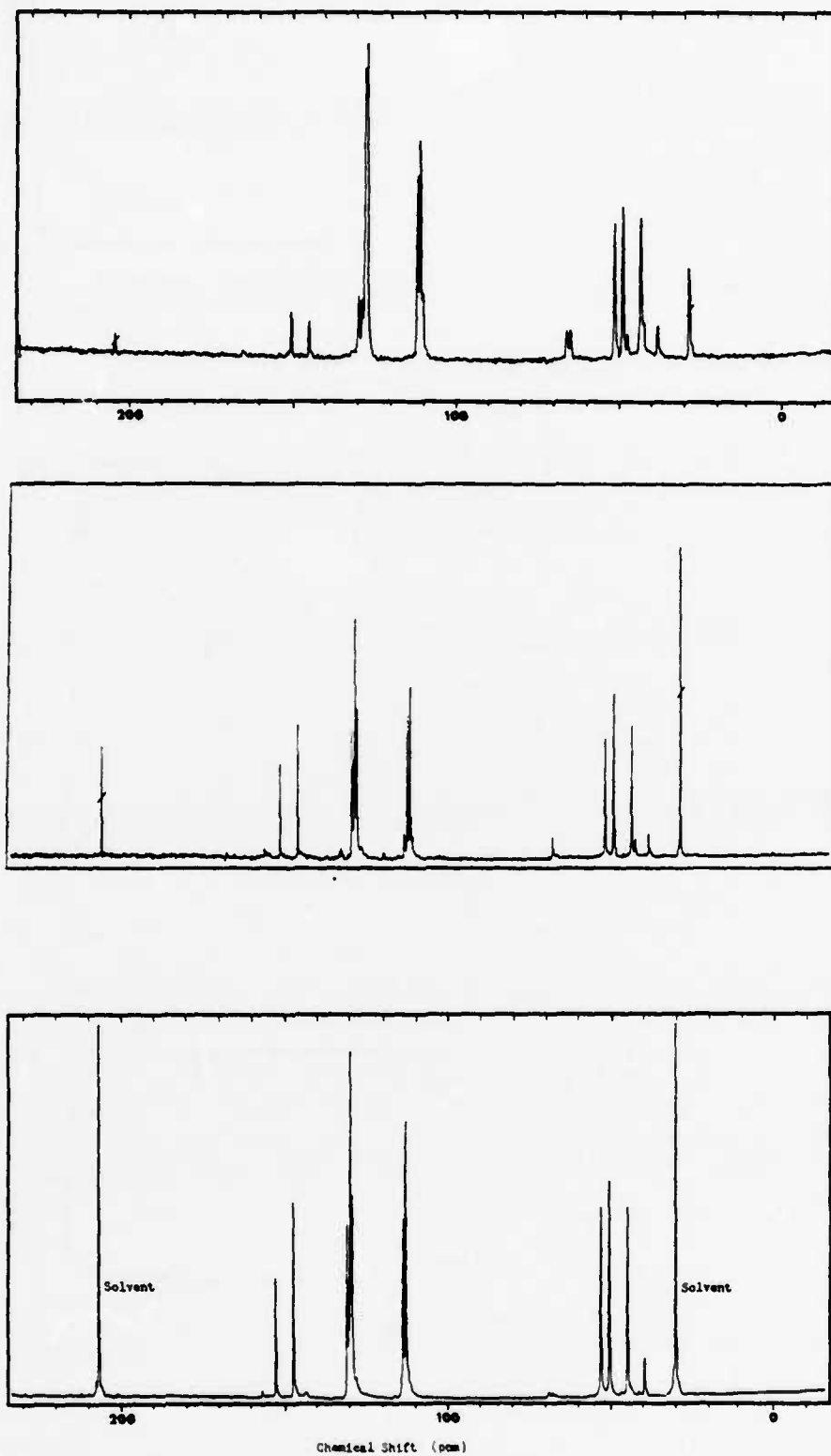


Fig. 4 - Carbon-13 nmr spectra of three commercially available resin systems based on TGMDA/DDS. The solvent is acetone.

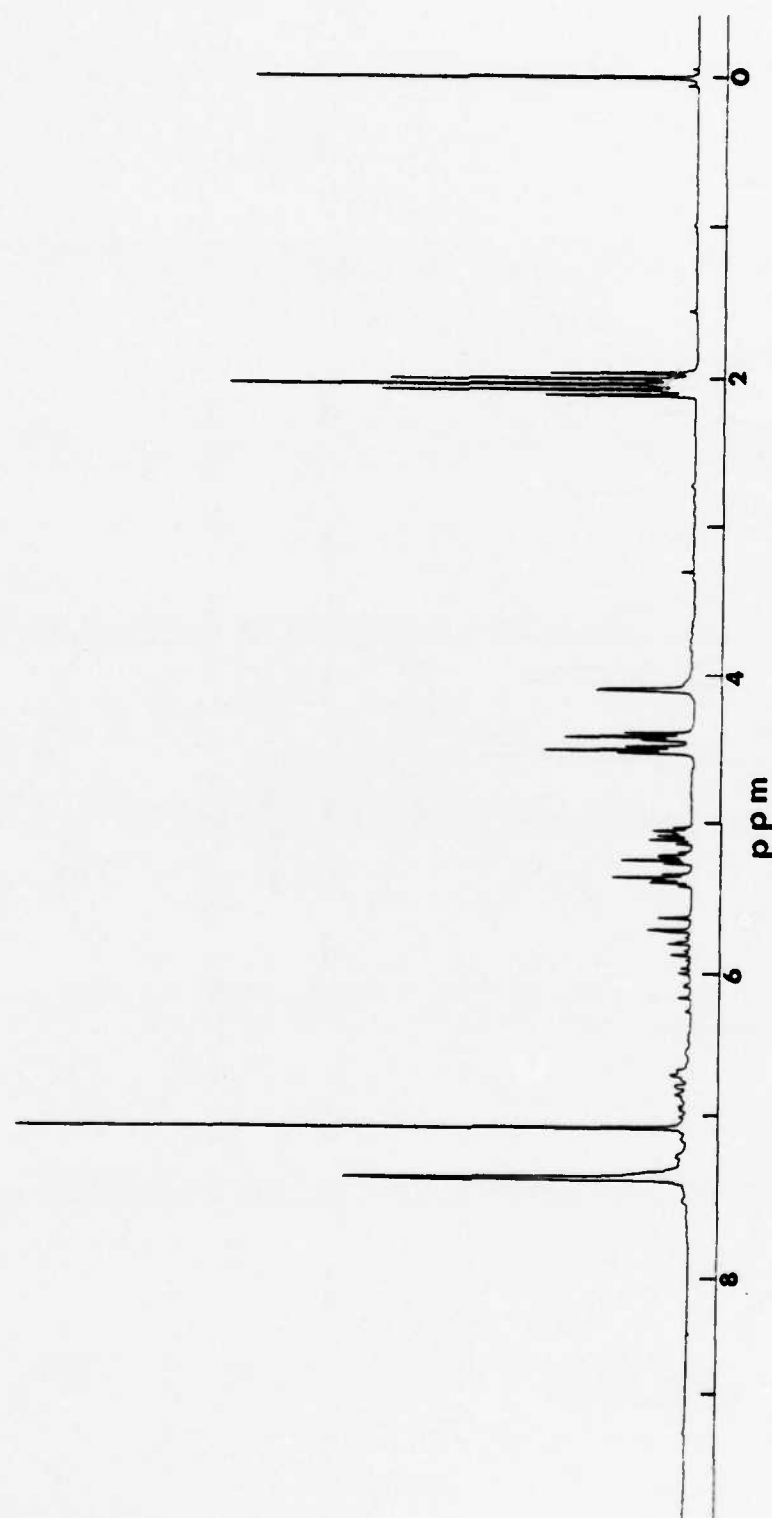


Fig. 5 - Proton nmr spectrum of material extracted from a Hexcel F-178/T-300 prepreg. The peaks at 0 and 2 ppm are due, respectively, to tetramethylsilane (the chemical shift reference) and acetone- d_6 (the solvent).

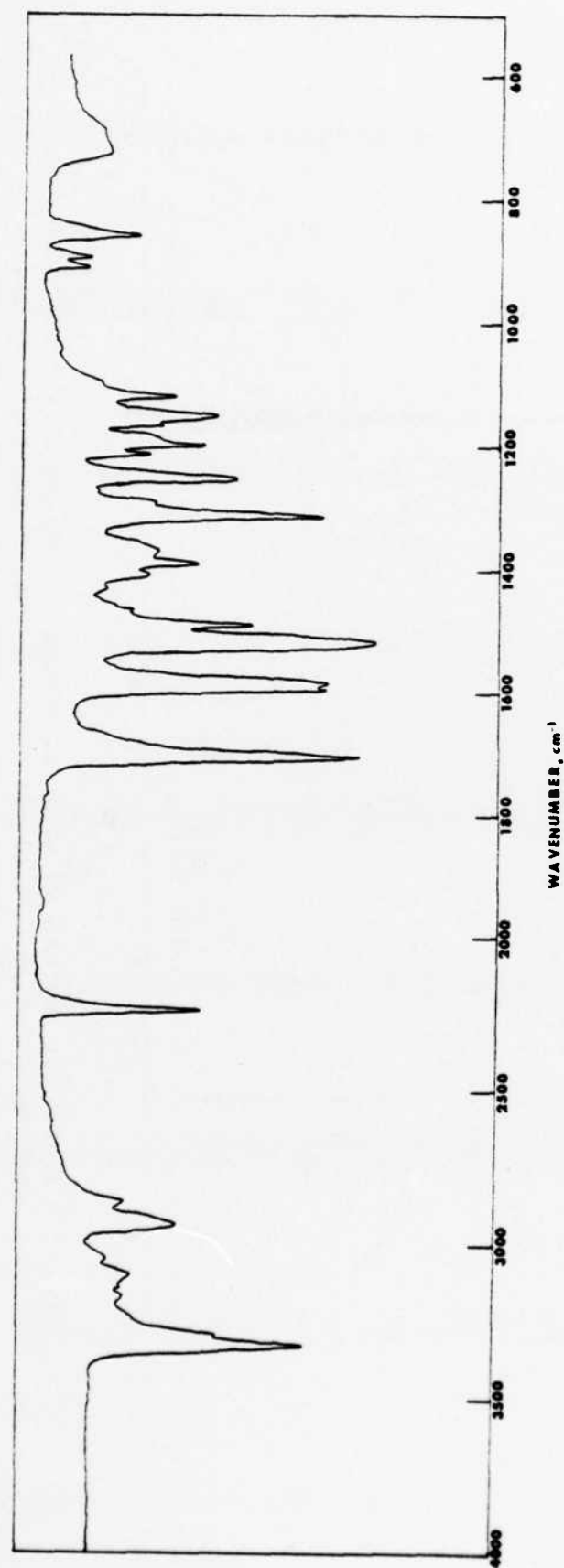


Fig. 6 - Infrared spectrum of C_{10} -diamide (KBr pellet).

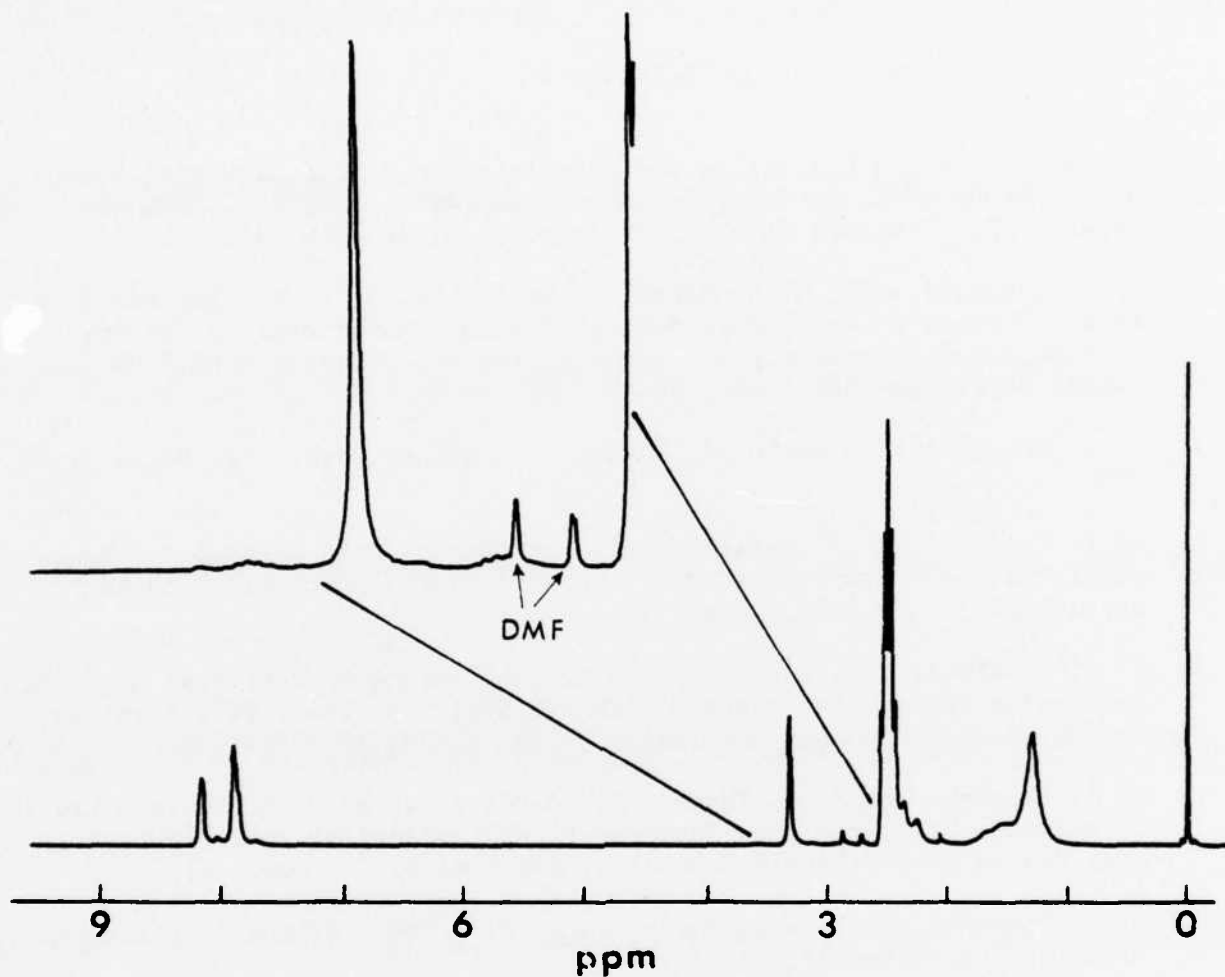


Fig. 7 - Proton nmr spectrum of C_{10} -diamide in dimethyl sulfoxide- d_6 . The expanded region shows the two peaks due to residual dimethyl formamide.

References

1. "High Performance Composites and Adhesives for V/STOL Aircraft; Second Annual Report", W. D. Bascom and L. B. Lockhart, Jr., Eds., NRL Memo Report 3721, February 1978, a) p 63; b) p 18. AD A054 637.
2. C. F. Poranski, Jr., W. B. Moniz, D. L. Birkle, J. T. Kopfle, and S. A. Sojka, "Carbon-13 and Proton NMR Spectra for Characterizing Thermo-setting Polymer Systems. I: Epoxy Resins and Curing Agents," NRL Report 8092, June 20, 1977. AD A044 214
3. C. F. Poranski, Jr. and W. B. Moniz, J. Coatings Tech., 49, No. 632, 57 (1977).
4. W. B. Moniz and C. F. Poranski, Jr., in "Epoxy Resin Chemistry," R. S. Bauer, Ed., ACS Symposium Series, No. 114, American Chemical Society, Washington, D.C., 1979, Chap. 7.
5. C. F. Poranski, Jr., and W. B. Moniz, in "Composite Materials: Testing and Design (Fifth Conference)" ASTM STP 674, S.W. Tsai, Ed., American Society for Testing and Materials, Phila., 1979, pp 553-565.
6. R. J. Hinrichs and J. M. Thuen, "Standardization of High Pressure Liquid Chromatographic Techniques (Reverse Phase) to Achieve Intra-Laboratory Data Equivalency," Narmco Materials, Costa Mesa, CA, Aug. 1979.
7. C. F. Poranski, Jr., W. B. Moniz and T. W. Giants, Organic Coatings and Plastics Preprints, 38, 605 (1978).
8. H. C. Nash, C. F. Poranski, Jr., and R. Y. Ting, in "Resins for Aerospace," C. May, Ed. ACS Symposium Series, 132, 1980.
9. C.A. May, Proc. Nat. SAMPE Sym., 24, 390 (1979).
10. J. F. Carpenter, ibid., 24, 446 (1979).
11. H. Borstell, ibid., 24, 422 (1979).
12. R. Hinrichs and J. Thuen, ibid., 24, 404 (1979).
13. "High Performance Composites and Adhesives for V/STOL Aircraft," Third Annual Report," L. B. Lockhart, Jr., Ed., NRL Memo Report 4005, May 23, 1979, p 68. AD A069 611
14. F. Kasler, "Quantitative Analysis by NMR Spectroscopy," Academic Press, N. Y., 1973, Chaps. 4-6.

THERMOMECHANICAL CHARACTERIZATION OF HIGH PERFORMANCE POLYMERIC RESINS AND ADHESIVES

Robert Y. Ting and Robert L. Cottingham
Polymeric Materials Branch
Chemistry Division

INTRODUCTION

For application as the matrix resin of fiber-reinforced composites for advanced V/STOL aircraft, the more important mechanical properties required of a polymer include stiffness (high modulus) and toughness (high fracture energy). The objective of this task has been to determine the effect of temperature, moisture and thermal aging on these properties for a variety of candidate resins. One fundamental criterion for resin selection was that the candidate be a potential matrix material that offered temperature capabilities in excess of 200°C (approximately 400°F). An experimental determination of the fracture toughness of available high-temperature adhesives was also made.

The modulus and fracture energy of various commercial high performance polymers and the C-10 phthalocyanine polymer have been determined and the results reported (1,2). By using a freely oscillating torsion pendulum operating at ca. 1 Hz, the dynamic shear modulus and the damping factor of polymers were evaluated over the temperature range of -200°C to +350°C. The glass transition temperature was defined as the temperature where a rapid decrease in shear modulus and increase in damping factor took place. Polymer fracture energy was measured by using compact tension specimens.

For the wide variety of resins studied, an important trend is clearly seen from the results reported in Table 1; namely, the thermoplastic polymers exhibit much higher fracture energies than the thermosetting materials. This striking difference is attributed to the high free volume available in thermoplastics for molecular flow and energy dissipation. While the values of resin fracture energies were calculated by assuming that the plane-strain conditions prevailed, the actual fracture tests were carried out using specimens with thicknesses varying from 0.3 cm to 1.3 cm. In order to assess the validity of the plane-strain assumption the effect of specimen thickness on polymer fracture energy was studied.

In the second portion of this task report, work on the evaluation of high performance adhesives is described. The adhesive fracture energy, measured at both room temperature and at 225°C (435°F), is given for various resin candidates.

Table 1
FRACTURE ENERGIES OF MATRIX POLYMERS

<u>Chemical Type</u>	<u>Commercial Designation</u>	<u>Fracture Energy, G_{Ic} kJ/m²</u>	<u>T_g, °C</u>
THERMOSETS			
tetrafunctional epoxy	NARMCO 5208	0.076	260
polyimide (addition)	Hexcel F-178	0.12	360
polyimide (addition)	PMR-15 (NASA)	0.20	350
polyimide (acetylenic)	Gulf T-600	0.19	330
polytriazine	Ciba-Geigy NCNS	0.075	250
polyphthalocyanine	NRL/Eastman, C ₁₀	0.19	360
THERMOPLASTICS			
polyarylsulfone	Carborundum, ASTREL	3.0	350
polyarylsulfone	Union Carbide, RADEL	5.5	-
polysulfone	Union Carbide, UDEL	3.1	174
polyethersulfone	ICI, P300	2.6	230
polyimide	Upjohn 2080	0.81	326
polyimide	DuPont NR150B2	2.1	365
polyamide-imide	Amoco 4000	3.4	275
polyphenylene sulfide	Phillips RYTON PPS	0.21	-

Specimen Thickness Effect

As indicated above, the reported polymer fracture energies (2) were obtained by using standard compact tension specimens of various thicknesses. It is possible that in many cases the plane-stress contribution at the crack tip was important relative to the plane-strain contribution. It is well known (3) that the contribution of plane-stress to fracture failure, relative to plane-strain contribution, increases with decreasing specimen thickness.

This issue of plane-stress vs. plane-strain effects for fracture failure is important to engineering design. The fracture energy based on the plane-stress condition is higher than that of the plane-strain condition by a factor of $(1 - \nu^2)$, where ν is the material Poisson's ratio (4). By using the plane-stress value, therefore, one could be overestimating the toughness of the material. In fact, in many structural components fracture tends to initiate from flaws such as surface scratches or from internal cracks, which, under stress, are subjected to essentially pure-strain conditions. Therefore, the appropriate design criterion should be based on the plane-strain fracture energy.

The effect of specimen thickness on the fracture energy was examined for three thermoplastic polymers: RADEL polyphenylsulfone, UDEL polysulfone (both from Union Carbide Co.) and VICTREX polyethersulfone (from ICI America Inc.). The materials were received as extruded or injection molded plates of various thicknesses. Standard compact tension specimens, schematically shown in Fig. 1, were cut from the plates and annealed in an air-circulating oven following annealing cycles recommended by the manufacturers. Since, for thick specimens, precracks could not be successfully formed by tapping the edge of the dovetail with a razor blade, the dovetail was eliminated and a precrack was introduced by using a blade at the end of the saw cut. Specimens were then fractured in an INSTRON with the cross-head speed of 0.125 cm/min. Polymer fracture energy (opening mode) was calculated from the following equation (5).

$$G_{Ic} = Y^2 P_c^2 a/E W^2 b^2 \quad (1)$$

where Y is a geometrical factor given as

$$Y = 29.6 - 186 (a/W) + 656 (a/W)^2 - 1017 (a/W)^3 + 639 (a/W)^4$$

P_c is the critical fracture load, a the crack length, W the specimen width, and b the specimen thickness. The modulus of the sample, E , was determined by performing a four-point bending test for each polymer and the result used in Eq. (1) for evaluating the fracture energy G_{Ic} .

Fig. 2 shows the fracture energies of the sulfone polymers as a function of the compact-tension specimen thickness. Each data point represents the average result of 6-8 tests. The data show that the G_{Ic} values indeed decrease gradually as sample thickness increases, except for the 1.25 cm polyphenylsulfone specimens. This abnormality may be due to the specific sample plate received from the manufacturer. The fracture energies level off to constant values for specimens thicker than 1 cm. These constant values may therefore be taken as the plane-strain G_{Ic} . In the case of polysulfone, the value of 3.1 kJ/m^2 is in good agreement with that of 3.2 kJ/m^2 reported by Gales and Mills (6).

It has been suggested (7) that for satisfactory plane-strain fracture toughness testing the specimen thickness should be greater than

$$b \geq \frac{2.5 G_{Ic} E}{\sigma_o^2} \quad (2)$$

where σ_o is the yield strength of the material. The minimum thickness required for each polymer sample, calculated based on this criterion, is given in Table 2. These results agree very well with the experimental observation in Fig. 2. It can therefore be concluded that, for the sulfone polymers, one would readily satisfy the requirement for plane-strain testing if 1 cm thick specimens were used. For the thermosetting polymers shown in Table 1, the minimum thickness required is much less than that required for thermoplastics because the G_{Ic} values for the thermosets are only 0.2 kJ/m^2 or less. Based on the criterion of Eq. (2), this thickness is only about 0.04 cm for $G_{Ic} = 0.2 \text{ kJ/m}^2$ and $\sigma_o = 70 \text{ MPa}$. The tensile strengths for the Upjohn 2080 and DuPont NR150B2 polyimides are as high as 120 MPa. Even at this stress level the materials usually fail by fracture before yielding, so 120 MPa underestimates the yield strength, σ_o . In view of these considerations, the requirement of 1 cm minimum thickness derived from the sulfone polymer test results is actually an overestimate of the minimum specimen thickness for plane-strain testing of these polyimides.

Adhesive Fracture Energy

Joining composite structural elements, either to themselves or to metals, can be most effectively done by adhesive bonding. However, there are many design problems associated with the adhesive bonding of composites and there is a need to establish failure criteria based on the onset of crack growth. Part of the efforts in the Failure Criteria Task, described in a later section of this report, is concerned with the development of such information. In the present study the adhesive fracture energy, or the opening-mode strain energy release rate, of an adhesive layer has been determined for various candidate adhesives.

Table 2
MINIMUM SPECIMEN THICKNESS, b_{min} , REQUIRED FOR PLANE-STRAIN TESTING OF SULFONE POLYMERS

Polymer	Polyphenylsulfone	Polysulfone	Polyethersulfone
Trade Name	RADEL	UDEL	VICTREX
Manufacturer	Union Carbide	Union Carbide	ICI America
E (GPa)	2.49	3.15	3.4
G_{Ic} (kJ/m ²)	5.5	3.1	2.6
σ_o (MPa)	71.7	70.4	84.2
b_{min} (cm)	0.64	0.49	0.26

A tapered double-cantilever beam specimen as devised by Mostovoy and Ripling (8) was used for adhesive evaluations. Fig. 1 gives the schematic of the specimen geometry. The adherends were 5086 aluminum alloy, cleaned by acid-chromate etching. After the adhesive was applied, the two aluminum half beams were clamped together with 0.025 cm Teflon spacers, which established the bond-line thickness. The complete beam assembly was then placed in an air-circulating oven for cure. Specimens were tested in an INSTRON with the crosshead moving at 0.125 cm/min until fracture in order to determine the failure load P_c . The adhesive fracture energy was calculated by using Eq. (3).

$$G_{Ic} = \frac{4P_c^2}{b^2 E} \left[\frac{3a^2}{h^3} + \frac{1}{h} \right] \quad [3]$$

Here h is the beam height corresponding to the crack length, a , and b is the sample thickness. The advantage of the tapered double-cantilever beam is that the specimen may be tapered in such a way that the quantity in the bracket of Eq. (3) becomes a constant. The fracture energy therefore is independent of the crack length, and can be easily calculated once the failure load P_c is known. The Young's modulus E in this case is that for aluminum.

The materials that have been evaluated are briefly described in the following:

(a) Hexcel 976: This resin is a condensation-type polyimide supplied as a 70% paste in N-methyl-pyrrolidone (NMP). The manufacturer claimed that this adhesive had high strength retention at 500°F for continuous service. The curing process is quite complicated (see Table 3).

(b) HR 602: The commercially available polyimide called Thermid 600 (formerly HR 600 developed by Hughes Aircraft Research, marketed by Gulf Oil Chemicals) has been chemically modified by Hughes into this new thermosetting resin HR 602. This new polymer was reported as having good flow-characteristics and superior lap shear strength (9). Samples were provided by the Hughes Research Group in both powder and adhesive prepreg forms. Previous study (2) showed that the acetylene-terminated polyimide (Thermid 600), although low in fracture energy as typical of all thermosetting polymers, seemed to exhibit very good thermal stability. After heat-soaking at 350°C for 240 hours, the G_{Ic} value for this material practically did not change.

(c) FM 73: This is the so-called PABST adhesive of the Air Force, an epoxy-base material manufactured by American Cyanamid. It was supplied as a yellow adhesive film to be used in conjunction with a primer, BR-127.

(d) FM 300K: Also manufactured by American Cyanamid, this adhesive was claimed to have 300°F capability and was considered for application in F-18 aircraft. The material was supplied as a dark green adhesive prepreg with a polyester woven reinforcement.

Table 3

ADHESIVE CURE SCHEDULES

<u>Polymer</u>	<u>Supplier</u>	<u>Temperature (°C)</u>	<u>Time (min)</u>
HX 976	Hexcel	135	60 (degas)
		185	75
		204	60
		232	60
		260	60
		258	60
		316	60
HR 602	Hughes	177	5 (primer)
		316	240
FM 300K	Cyanamid	121	30 (primer)
		177	60
FM 73	Cyanamid	121	60 (primer)
		121	60
FM-34B-18	Cyanamid	285	90
C-6PC	NRL	220	48 hrs
C-10PC	NRL	220	48 hrs
C-22PC	NRL	200	24 hrs
C-36PC	NRL	220	72 hrs
Plastilock 655	Goodrich	177	85
Plastilock 650	Goodrich	260	45

Table 3 (Continued)
ADHESIVE CURE SCHEDULES

<u>Polymer</u>	<u>Supplier</u>	<u>Temperature (°C)</u>	<u>Time (min)</u>
LARC-13/AATR	NASA	70	30
		125	60
		175	30
		200	15
		235	15
SR-5208	NARMCO	93	20 hrs
		121	180
		149	120
		177	120
		204	240
Upjohn 2080	Upjohn	340	20
Torlon 4000	Amoco	188	30
NR056X	DuPont	82	10 (degas)
		316	120
P-1700	Union Carbide	260	10 (degas)
		260	5
P-1700 (melt)	Union Carbide	371	5

* All adhesives cured at ca. 0.35 MPa pressure.

(e) FM-34B-18: This is a polyimide adhesive system from the American Cyanamid Company, claimed to retain high lap-shear strength for long exposure to temperatures up to 700°F (360°C). NASA-Langley is studying this material for possible applications in the CASTS (Composites for Advanced Space Transport System) Program (10).

(f) Plastilock 650 and 655: Two nitrile-rubber phenolic resins from B. F. Goodrich Company were provided in the form of thin sheets of pure resin with no reinforcements. Both adhesives were supposed to offer 500°F (260°C) capability.

(g) SR 5208: This epoxy resin is essentially tetraglycidyl methylenedianiline (TGMDA) cured with diaminodiphenyl sulfone (DDS) along with some minor constituents. The material was obtained from Narmco Materials Inc. in powder form.

(h) LARC-13/AATR: This adhesive is a high temperature resin developed by NASA-Langley. Basically it is a polyimide modified with 15% in-chain butadiene-acrylonitrile elastomer. The samples were supplied by NASA both as a 50% solution in DMF and in an adhesive film form. A rather complex B-staging cycle is required.

(i) Phthalocyanines: Four amide type phthalocyanine resins (11), containing 6, 10, 22 and 36 carbon units in the aliphatic chains linking the stable phthalocyanine nuclei, were tested as adhesives. They were designated as the C-6, C-10, C-22 and C-36 phthalocyanines. The resins were applied by melting to coat the adherend surfaces, and specimens cured in an oven according to the specified cure cycles for each resin.

(j) Torlon 4000 T: This is a poly (amide - imide) thermoplastic compound developed by the Amoco Chemicals Corporation. It has a glass transition temperature $T_g = 274^\circ\text{C}$ as determined by torsion pendulum analysis. Resin fracture toughness was exceedingly high, a G_{Ic} value of 3.9 kJ/m² being reported (2).

(k) Upjohn 2080: This thermoplastic polyimide material was supplied by the Upjohn Company as a 55% solution in dimethylformamide (DMF). Characterization of the bulk polymer shows it to have a $T_g = 326^\circ\text{C}$ and a fracture energy $G_{Ic} = 0.92 \text{ kJ/m}^2$ (2).

(l) NR 056 X: This is a DuPont polyimide adhesive derived from NR-150 solutions to give a linear amorphous polymer structure free of crystallinity and cross linking. The material was supplied as a concentrated solution in DMF.

(m) Udel Pl700: This thermoplastic polysulfone was manufactured by Union Carbide Corp., and was supplied as molding pellets and as extruded sheets of various thicknesses. For the pellets, DMF was used as a solvent to prepare a polysulfone solution (~10%) for coating the adherends. A hot melt method was employed in order to use the extruded sheet. A thin strip of Udel material was cut to size and clamped between aluminum beams. The specimen was then placed in an oven to melt the thermoplastic strip for bond formation.

The cure cycles required for the adhesives are listed in Table 3. Manufacturers' recommended processing procedures were generally followed. In some cases, the cure cycle was adjusted to available laboratory equipment capabilities until satisfactory adhesive bonding was achieved. This usually included a visual inspection of the bond before fracture test and a microscopic examination of the fractured adhesive surface after the test to ensure that the presence of blisters or voids was minimized, and that failure was of a cohesive type instead of an interfacial fracture. For the thermoplastic polymers, when applied as a solution coating, the solvent was not completely released within the 0.025 cm thick bond-line. Numerous trapped gas bubbles caused voids in the adhesive layer. This phenomenon consistently occurred even when the coated beam surfaces were degassed before being clamped together. In order to alleviate this gas entrapment, adhesive tapes were prepared for each thermoplastic polymer. A low concentration solution (10-35% solid content) was first prepared by using either DMF or NMP as the solvent. Atomized #400 aluminum powder (Reynolds, 90% particles < 13 μ , and 50% < 7 μ) was added to the solution, which was warmed to ca. 85°C. The mixture was brushed onto a piece of #112 glass cloth with A1100 (siloxane) finish. Finally, the cloth was placed in an oven and subjected to the time-temperature cycles shown in Table 4 to remove some of the solvent. The end product was a dry adhesive film about 0.018 - 0.025 cm thick. The presence of the glass cloth provided a path for the release of volatiles during the fabrication of the adhesive bond and minimized the formation of small gas bubbles within the bond-line.

Adhesive fracture tests were performed both at room temperature and at 225°C. For the high temperature tests, the specimen was mounted in the INSTRON with an environmental chamber, and heated from room temperature to 225°C at a rate of 3°C/min. The temperature was held at 225°C for five minutes to ensure thermal equilibrium before the specimen was fractured. The room temperature test results are given in Table 5. Materials are listed from top to bottom in the order of increasing adhesive fracture energy. It can be seen that both the Plastilock adhesives and the PABST FM-73 epoxy adhesive exhibited very high toughness ($G_{Ic-RT} > 1 \text{ kJ/m}^2$). For the acetylene-terminated polyimide (HR 602) a G_{Ic} value of 815 J/m² was measured, but the other thermosetting materials tested showed G_{Ic} values less than 400 J/m². For the FM 300K adhesive system, the fracture performance is so poor that one would wonder about its application in F-18 aircraft for bonding graphite composites to titanium.

The thermoplastic polyimides (Upjohn 2080, DuPont NR-056X) and Amoco Torlon 4000 amide-imide polymer showed a toughness similar to that of the thermosetting LARC-13 adhesive. A polysulfone resin (Union Carbide Udel P1700) gave the highest fracture energy, ca. 1 kJ/m². However, the adhesive fracture energies measured here are considerably lower than those reported for bulk thermoplastic polymers (see Table 1). One reason may be related to the bond fabrication technique used for these adhesives. The optimum processing conditions for these thermoplastic adhesives have not been established. Manufacturer-recommended conditions for the extrusion or molding process require 200-300 psi pressure applied over very narrow temperature "windows" as high as

Table 4

TIME-TEMPERATURE CYCLES FOR THE PREPARATION OF THERMOPLASTIC ADHESIVE FILMS

<u>Polymer</u>	<u>(°C)/(min)</u>	<u>(°C)/(min)</u>	<u>(°C)/(min)</u>	<u>(°C)/(min)</u>	<u>(°C)/(min)</u>
20% Upjohn 2080 in DMF + 22% Al	82/60	100/20	120/20	140/20	
10% Pl700 in DMF + 20% Al	80/120	110/45	120/30	130/35	140/45
35% TORLON 4000 in NMP + 21% Al	90/20 180/30	105/20 200/35	115/20	140/30	160/30
35% NR056X in DMF + 35% Al	85/40	100/20	120/20		

Table 5

ROOM TEMPERATURE ADHESIVE FRACTURE ENERGY

<u>Thermosets</u>	<u>Thermoplastics</u>	<u>$G_{Ic-RT} (J/m^2)$</u>
C-6 phthalocyanine		56
C-36 phthalocyanine		63
NARMCO SR 5208		82
Hexcel HX 976		94
C-10 phthalocyanine		124
Cyanamid FM-300K (film)	Udel P1700 (melt)	306
	Upjohn 2080 (film)	310
C-22 phthalocyanine		373
Cyanamid FM-34B-18 (film)		385
LARC-13/AATR (film)		387
	Torlon 4000T (film)	480
	DuPont NR056X (film)	620
Hughes HR602 (film)		815
	Udel P1700 (film)	1026
Plastilock 650 (film)		1037
Plastilock 655 (film)		1513
Cyanamid FM-73 (film)		2107

~700°F (385°C). These temperature and pressure requirements are essential for achieving sufficient melt flow, which has been difficult to obtain when preparing an adhesive bond in the laboratory. Furthermore, since polymer solutions were used to prime the specimen beams and for impregnating glass fabric to prepare an adhesive film, some volatiles released during bonding still produced voids within the adhesive layer. Furthermore, the presence of a thin bond-line may severely limit the extent of plastic deformation at the crack tip (12). This could also contribute to the poor adhesive fracture performance of thermoplastic polymers.

The results from tests performed at 225°C are shown in Table 6, in which both the adhesive fracture energy G_{Ic-225} and the retention ratio of toughness, G_{Ic-225}/G_{Ic-RT} , are listed. The glass-to-rubber transition temperature, T_g , for each resin system is also tabulated. For thermosetting materials, since T_g depends on the degree of cure, the listed values indicate only the approximate limiting use temperature of the resin. For materials such as epoxies and phenolics (which have T_g lower than the test temperature), it is clear that their toughness was lost rapidly at temperatures higher than T_g . In those cases, the test results show that the retention ratios range from 0.01 to 0.32. On the other hand, the high temperature polyimide resins remained effective, retaining ~90% or more of their room temperature toughness values when tested at 225°C.

SUMMARY

During the course of this program, work in the Thermomechanical Characterization Task has emphasized the evaluation of the modulus and fracture energy of various candidate resins suitable for applications in advanced V/STOL aircraft. Dynamic mechanical analysis using a torsion pendulum led to the determination of polymer glass transition temperatures and to the conclusion that the dynamic shear moduli of most resins are at about the 10^{10} N/m² level except when the temperature is near the glass transition temperature. Results of fracture characterization using standard compact tension specimens showed that the thermoplastic polymers have fracture energies 10 to 40 times greater than those of the thermosetting materials. Fracture studies carried out using an epoxy/graphite and a polysulfone/graphite composite system also showed that resin fracture energy greatly affected the interlaminar toughness of composites.

Thermal aging experiments revealed that prolonged heat-soak of polymers advanced the state of cure and reduced polymer fracture energy. Thermal aging was also shown to increase the initial rate of moisture uptake in polymers and, for thermosetting polyimides, to cause an increase in their equilibrium absorption of water.

Currently available high performance adhesives have been evaluated for their adhesive fracture energies both at room temperature and at 225°C. The results indicate that high resin toughness does not necessarily translate into high adhesive toughness and that adhesive fracture energy is greatly reduced at temperatures above the glass

Table 6

ADHESIVE FRACTURE ENERGY AT 225°C

Thermosets	Thermoplastics	$G_{Ic-225} (J/m^2)$	$G_{Ic-RT} (J/m^2)$	$\frac{G_{Ic-225}}{G_{Ic-RT}} \times 100\%$	$T_g (°C)$
Cyanamid FM-300K		23	191	12	
Cyanamid FM-73		27	2107	01	
	Udel PI700	40	1026	05	174
C-10 phthalocyanine		59	124	48	360
Plastilock 655		131	1513	09	
	Torlon 4000T	185	480	39	275
Plastilock 650		322	1037	32	
Cyanamid FM34B-18		342	385	89	
LARC-13/AATR		399	387	100	~280
	DuPont NR056X	515	620	83	365
Hughes HR 602		749	815	92	330

transition temperature of the polymer. These results indicate the need for formulating new high temperature adhesives containing a dispersed second phase that can impart a toughening effect to the brittle resin.

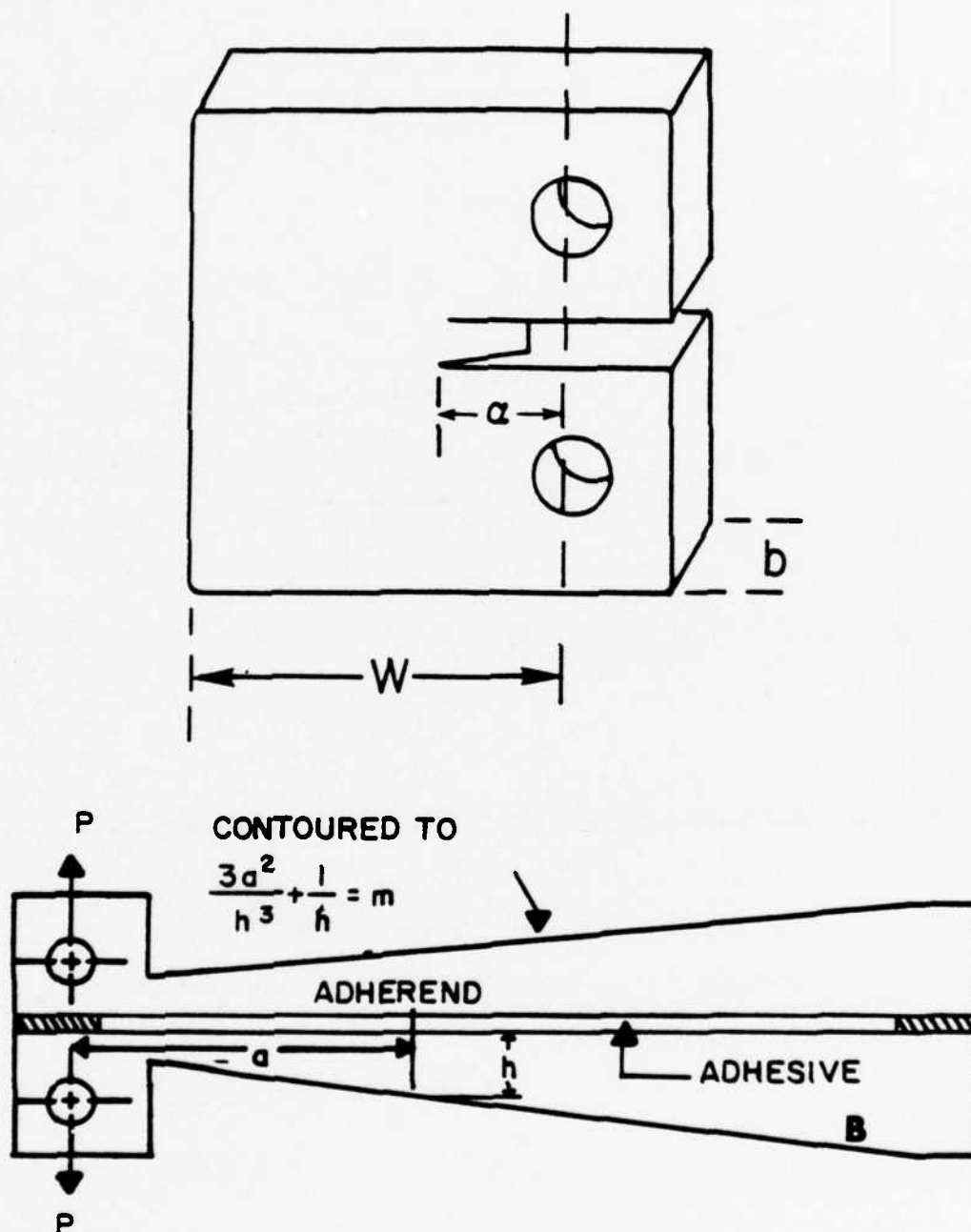


Figure 1. Specimen geometries for fracture toughness measurements. Upper: Compact tension specimen. Lower: Tapered double-cantilever beam specimen.

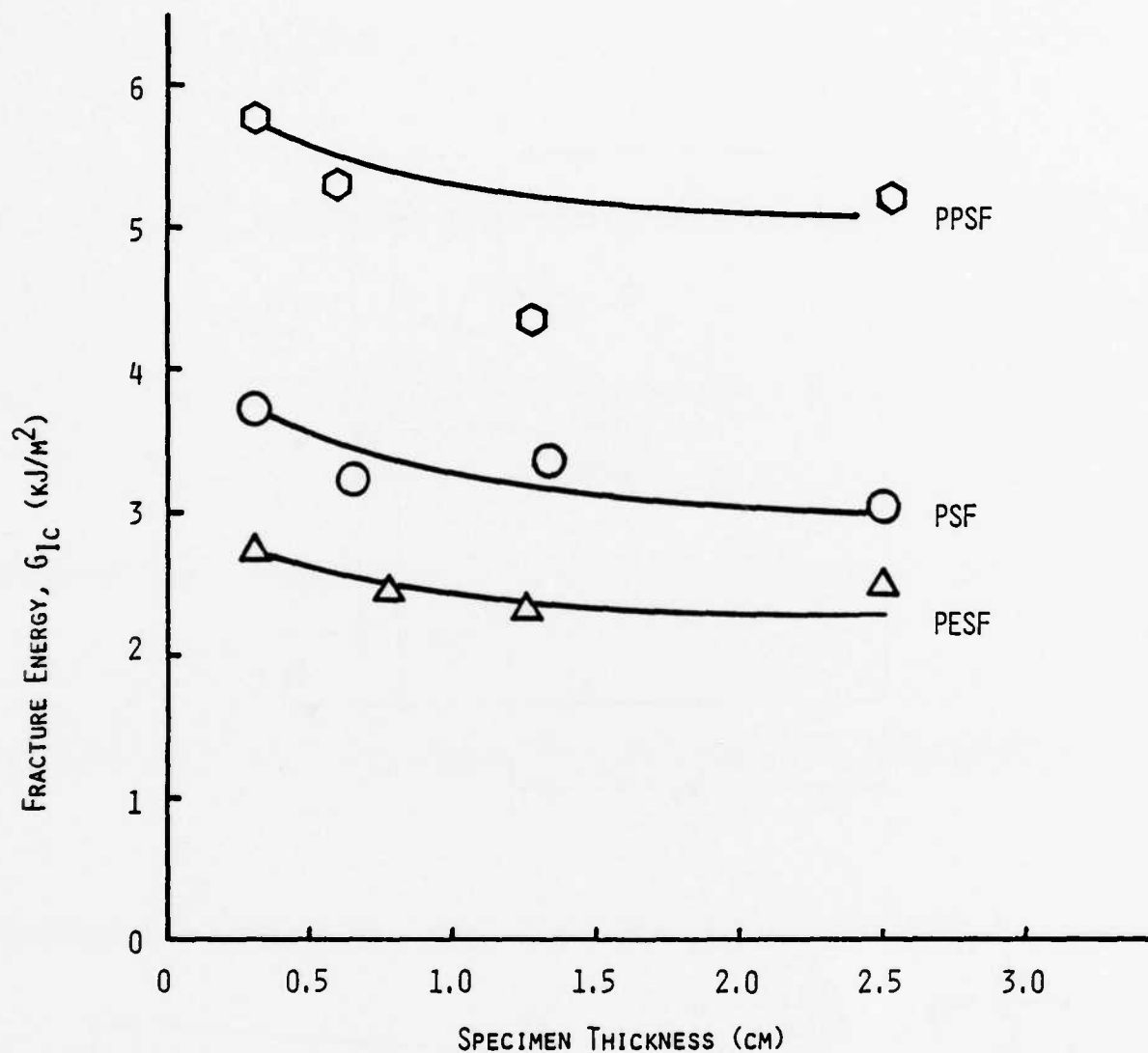


Figure 2. Fracture energy as a function of compact tension specimen thickness for three polysulfones: PPSF - Radel polyphenylsulfone; PSF - UDEL polysulfone; PESF - VICTREX polyethersulfone.

REFERENCES

1. W. D. Bascom and L. B. Lockhart, Jr., High Performance Composites and Adhesives for V/STOL Aircraft, NRL Memo Report 3721, Washington, D. C., February 1978, p. 23. AD A054-637
2. L. B. Lockhart, Jr., High Performance Composites and Adhesives for V/STOL Aircraft, NRL Memo Report 4005, Washington, D. C., May 1979, p. 13. AD A069-611
3. M. Parvin and J. G. Williams, J. Mater. Sci., 10, 1883 (1975).
4. J. F. Knott, Fundamentals of Fracture Mechanics, Butterworths, England, 1973.
5. W. Schultz, in Fracture Mechanics of Aircraft Structures, ed. H. Liebowitz, AGARDograph, AGARD Report AG-176, NTIS, Springfield, VA, 1974, p. 370. AD 777 641
6. R. D. R. Gales and N. J. Mills, J. Eng. Fracture Mech., 6, 93 (1974).
7. W. F. Brown and J. E. Srawley, Plain Strain Crack Toughness Testing, ASTM Spec. Tech. Pub. 410 (1966).
8. S. Mostovoy and E. J. Ripling, J. Appl. Polym. Sci., 15, 641 (1971).
9. N. Bilow, ACS Org. Coat. Plast. Chem. Preprint, 40, 597 (1979).
10. J. G. Davis, Jr., Composites for Advanced Space Transportation Systems, NASA-Langley TM-80038, March 1979. AD-D427 165
11. W. D. Bascom and L. B. Lockhart, Jr., High Performance Composites and Adhesives for V/STOL Aircraft, NRL Memo Report 3433, Washington, D. C., December 1976. AD-A035 928
12. W. D. Bascom, R. L. Cottingham and C. O. Timmons, J. Appl. Polym. Sci.: Appl. Polym. Symp., 32, 165 (1977).

FABRICATION OF PHTHALOCYANINE/GRAPHITE COMPOSITES

R. Y. Ting and H. C. Nash
Polymeric Materials Branch
Chemistry Division

INTRODUCTION

The objective of this task has been to develop fabrication conditions for the preparation of fiber-reinforced resin-matrix composites of interest to the V/STOL program. This involved first the identification of the critical steps and control parameters in the fabrication process, and then the fabrication and characterization of angle-ply laminates prepared for testing in the Failure Criteria Task.

Three composite systems have been fabricated in this task for a comparison study of their mechanical properties. The reinforcement selected was Thornel 300 graphite fiber (T-300, Union Carbide). Three different resin systems were selected for this study: a tetraglycidyl methylene dianiline (NARMCO 5208), a bismaleimide system (Hexcel F-178) and the C-10 phthalocyanine resin developed at NRL (1). The fabrication of the composites involves a complex combination of physical and chemical processes. Basically, it begins with the hand lay-up of prepreg plies, which is followed by a consolidation process, properly designed cure cycle, and a post-cure treatment.

In the case of commercially available prepreg systems, 5208/T-300 and F-178/T-300 prepreps were obtained from the manufacturers. Optimum cure cycles were developed by modifying the manufacturer's recommended fabrication conditions. Systematic variations from these conditions have led to successful processing of these materials using equipment available in our laboratory (2,3).

In this report, the development of fabrication procedures for the C-10 phthalocyanine/T-300 graphite composite is discussed. The bulk thermal properties and cure behavior of the C-10 resin were studied to determine its potential in composite applications. Dwell time, cure temperature, applied pressure, the type and amount of bleeder material and the design of dam and vacuum bag were varied in order to optimize the physical and mechanical properties of laminates produced. An aging study of C-10/T-300 prepreps was also carried out to examine the effect of humidity and out-time on the processing behavior and the mechanical properties of C-10/T-300 composites.

C-10/T-300 Prepreg

The chemistry involved in the synthesis of the phthalocyanine polymers has been discussed previously (4). Polymerization of C-10 phthalocyanine (N,N'-bis(3,4-dicyanophenyl)decanediamide) is initiated simply by heating the resin at temperatures above its melting temperature, i.e. above 200°C (5). The "B" stage and post-cure lead to the development of stable phthalocyanine nuclei linked through aliphatic diamide linkages.

Brief "B" staging, however, gives a liquid intermediate state, which can be utilized for fiber impregnation. Depending on the "B" staging temperature and the dwell time, the degree of crosslinking varies and the oligomers formed are different. The resin melting point at the same time is greatly depressed. Figure 1 shows the melting temperature variation of the C-10 resin heated at 220°C for different periods of time. At this temperature, the polymerization reaction proceeds rapidly and the resin melting temperature may be reduced to as low as 85°C in 20 minutes. At this stage, the material remains sufficiently fluid for proper prepregging. Further heating may increase the melt viscosity beyond the point at which fiber impregnation is possible.

Because the equipment necessary for large-scale prepreg production was not available at NRL, the prepregging of the C-10/T-300 system was developed in collaboration with two commercial sources: U. S. Polymeric and the Composite Division of the Ferro Corporation. Both the hot-melt prepregging technique and a resin/solvent slurry technique were demonstrated capable of successfully producing 12-inch wide prepreg tapes. In the latter technique, dimethylformamide was the solvent selected for prepreg preparation, and the final product contained about 6-8% volatiles. The cure of this material has been studied (6), and the results showed that the added DMF solvent was difficult to remove, even by extended staging under vacuum. The residual solvent was undesirable because it caused the formation of voids and/or blisters in the laminate samples when post-cured at high temperatures.

Prepregs produced by the conventional hot-melt technique had a resin content of ca. 32% with less than 1% residual volatiles. The material was shipped in rolls, but appeared dry and brittle. Sufficient tack, however, could be developed by heating the material briefly at 110°C. The detailed analysis of this material is discussed in the following sections.

Thermal Analysis

A Perkin-Elmer DSC-2 unit was used to perform DSC scans over the temperature range of 310°K (37°C) to 500°K (227°C) at a heating rate of 10°K/min under a dry nitrogen atmosphere. A DuPont 900 Series TGA unit

was used to analyze sample weight loss as a function of temperature over the temperature range of 20°C to 350°C. The sample was heated at a rate of 5°C/min and was continuously purged with dry nitrogen at a flow rate of 100 ml/min.

Figure 2 shows the results of a DSC scan of the C-10/T-300 prepreg prepared by the hot-melt method. The trace, when compared with the reference baseline, shows a multiple of endotherm peaks at 144°C, 156°C, 168°C and 190°C, respectively. The appearance of those peaks is believed to be related to the melting of resin oligomers formed during prepreg manufacture. This multiple melting behavior was also observed in a torsion braid analysis of this resin (7). The DSC trace shows no exotherm, implying that for practical purposes the cure of C-10/T-300 prepreps should be carried out at temperatures higher than 500°K (227°C). However, a TGA study of the same prepreg material indicated rapid weight loss takes place at temperatures higher than 275°C. Previous study also showed that the cured C-10 phthalocyanine polymer was stable for extended usage up to 245°C and for short-term exposure at 260°C (5). These results therefore suggest that the initial cure temperature for the C-10/T-300 prepreps should not exceed 260°C. For extended post-cure the temperature limit is set for 245°C.

Dielectric Analysis

A dynamic dielectric technique (8) was used to monitor the curing of prepreg materials by continuously measuring sample capacitance and dielectric dissipation factor ($\tan \delta_\epsilon$) as a function of cure time and temperature. The capacitance is directly proportional to the real part of the complex dielectric permmissivity, k' , whereas $\tan \delta_\epsilon$ is the ratio of the imaginary to the real part of k . This technique is analogous to a dynamic mechanical analysis in that the capacitance corresponds to the mechanical storage compliance and $\tan \delta_\epsilon$ to the mechanical loss tangent (9). Therefore, DDA results can be related to chemo-rheological changes during the curing of a thermosetting system.

An Audrey III Dielectric Analyzer was used for this work. Single-ply samples, 6.35 cm in diameter, were covered with Kapton insulating films and placed in the test cell of a Di/An 300 mini-press. The cell was then closed with a pressure of ca. 0.35 MN/m² (50 psi) and sample temperature brought up to the cure temperature for isothermal cure study. Dielectric dissipation factor ($\tan \delta_\epsilon$) was continuously monitored as a function of time at a fixed frequency of 10³ Hz.

Figure 3 shows the DDA result of the isothermal cure study for a single-ply prepreg sample. As the sample was heated, a small $\tan \delta_\epsilon$ peak first appeared at ca. 100°C, indicating the release of moisture. When the temperature exceeded 200°C, the material quickly melted and polymerization of phthalocyanine was thermally activated. This resulted in a rapid increase of the dielectric dissipation until a maximum was reached, which was believed to be the gelation point (10). The time to gelation was determined at various cure temperatures, and was plotted as a function of the inverse of temperature in Fig. 4. The result indicated that the gelation process followed an Arrhenius

relationship with an activation energy of 14.95 kcal/mole, a value comparable to that for the epoxies (11). This suggests that the processability of C-10 phthalocyanine is similar to that of the epoxies.

Monitoring the Press Cure

The dynamic dielectric analysis (DDA) technique may also be applied to perform in situ monitoring of the cure of large composite samples in a hydraulic press. Angle-ply laminates, 25.4 cm x 25.4 cm, were laid up by hand between two aluminum foil electrodes with a glass fabric dam around the sample. The whole lay-up was then placed in a Kapton vacuum bag for press cure. Connections were made from the foil electrodes to the Audrey III system, which measured both the sample capacitance and dissipation factor as a function of cure time and temperature at a fixed frequency of 10^3 Hz.

Figure 5 shows the DDA result when this technique was applied in situ to the fabrication of a 16-ply laminate sample in a press. The sample, subjected to the cure cycle of Fig. 5C, was cured at 260°C. When sample temperature was rapidly raised to this cure temperature, the dissipation curve showed initially a broad melting peak (Fig. 5A), followed by a rapid increase in $\tan \delta$ to reach the gel point. This information was used to determine the desired time for the application of pressure in order to fabricate laminates with very low void contents.

Since the prepregs produced by the conventional hot-melt method had only ca. 32% resin content, an attempt was made to increase laminate resin content by adding resin powder to the sample. Initially, a pre-measured amount of raw resin was distributed uniformly by sprinkling it between plies as part of the hand lay-up procedure. However, upon heating one observed an excessive amount of resin flow accompanying the melting, which could not be contained by the glass fabric dam. The corresponding dissipation record in Fig. 5B showed a very pronounced melting peak in this case. Proper control of resin flow is necessary.

Samples of raw resin were briefly "B" staged in an oven preheated to 195°C for different periods of time, and DSC scans performed on each sample. Figure 6 shows the DSC records for these samples performed at a heating rate of 10°K/min from 310°K (37°C) to 500°K (227°C). It can be seen that initially the resin had a single melting peak centered around 189°C (462°K), but as the sample was heated for over 10 minutes at 195°C, multiple melting peaks began to appear. Broad exotherms were also observed, indicating the presence of a meta-stable, crystallized phase formed as the sample was removed from the oven and rapidly "quenched" at room temperature. If the cooling rate was reduced, and repeated DSC scans were taken, those exotherms would disappear. As the dwell time at 195°C was increased to 55 minutes, the melting temperature was suppressed to ca. 57°C (330°K) with an additional, very weak endotherm at 177°C (450°K). From Fig. 4 it may be estimated that at 195°C the gelation time is over 4 1/2 hours. So, even after 55 minutes, the percent of gel is negligible. A suppression of the melting

temperature to as low as ca. 60°C could be very significant for future prepregging of this material. The DSC record of the 20-min. sample compared favorably with that of the C-10/T-300 prepreg. Therefore heating the raw resin to be added to a laminate at 195°C for 20 minutes, assured that the added resin had thermal characteristics similar to those in the prepreps. Adding this preheated resin to the base prepreg resulted in a press cure cycle which followed the dynamic dielectric record of Figure 5A. With this technique, laminate resin contents were successfully controlled over the range of 32-40%.

Post-Cure Study

In order to optimize laminate mechanical properties, a proper post-cure for the composite sample is required. Based on the thermal stability data for the C-10 resin (5), it was decided that the post-cure temperature should not exceed 245°C .

Unidirectional 16-ply composite laminates were fabricated and specimens cut from the laminate for mechanical testing. The short beam shear test (ASTM-D 2344) was chosen to determine the interlaminar shear strength (ILSS), a resin-dominated property. The flexure test (ASTM-D 790) was selected to measure the laminate flexural strength and modulus, which are fiber-dominated properties. Before testing, specimens were post-cured at 245°C for various length of time. Figure 7 shows the measured mechanical properties as a function of the post-cure time. It is clear that all three properties, the flexural strength and modulus and the ILSS, showed optimum values when post-cured at 245°C for 72 hours. Results of an earlier thermal aging study on the fracture energy of neat C-10 resins also showed that C-10 phthalocyanine exhibited maximum toughness when aged at 240°C for ca. 72 hours (12). As the post-cure time exceeded 72 hours, the mechanical properties decreased and eventually leveled off, indicating that the C-10/T-300 system is more than adequate for $400\text{--}450^{\circ}\text{F}$ ($204\text{--}232^{\circ}\text{C}$) applications. For practical purposes, laminates perhaps should be post-cured for 60 to 65 hours so that the maximum strength and modulus may develop in the field as the composite components continue to be exposed to the thermal flux from the environment. However, for laboratory evaluation all laminates were post-cured at 245°C for 72 hours in order to obtain optimized mechanical properties.

Mechanical Properties

Sixteen-ply angle plies and 16-ply quasi-isotropic laminates were prepared. Because the amount of prepreg material was limited, the angle plies consisted of only two orientations: $\pm 15^{\circ}$ and $\pm 45^{\circ}$. The quasi-isotropic laminates had the configuration of $(90^{\circ}, \pm 45^{\circ}, 0^{\circ})$. The stacking sequence is schematically shown in Fig. 8. The mechanical response of the laminates was evaluated by performing tensile tests using specimens $10\text{ cm} \times 1.25\text{ cm} \times 0.2\text{ cm}$ in size. The specimens were machined in such a way that the loading direction bisected the included angle between fiber orientations. All tests were carried out in an INSTRON with the cross-head moving at a speed of 0.125 cm/min . A three-point flexural test was also performed in accordance with ASTM-D 790.

Test results for the C-10/T-300 are given in Table 1, which also includes data for the NARMCO 5208/T-300 and Hexcel F-178/T-300 composites. The C-10/T-300 system and the F-178/T-300 material exhibited similar tensile and flexural moduli, but in all cases, the 5208/T-300 composite showed higher strength, particularly when the fiber orientation was $2\theta=30^\circ$. The tensile properties have been plotted as a function of the included angle in Figs. 9 and 10 to show the strong dependence of tensile properties on fiber orientation. For small θ , the tensile properties are dominated by the fiber strength. As the included angle increases, the role of the matrix becomes increasingly important in its contribution to the distribution of the load. In those cases, the data clearly show that all three systems are essentially equivalent. For the popular quasi-isotropic design of laminates, the C-10/T-300 composite also showed very excellent strength property, with higher tensile modulus than the other two systems. All laminate thicknesses were ca. 0.0125 cm/ply and resin contents ranged from ca. 30% for the 5208/T-300 laminates to ca. 38% for the C-10/T-300 and the F-178/T-300 laminates.

Prepreg Aging Study

As fiber-reinforced composite materials become increasingly important in aerospace applications, the storage, handling and processing of composite prepreg materials are receiving greater attention. A major difficulty in handling many prepregs is that the material must be stored at very low temperatures. The shelf life of these prepregs is generally only a few months at freezer temperatures, and very much less (ca. a few weeks) at room temperature. Presumably, continued B-staging occurs at room temperature while, at the same time, the resin may be affected chemically by absorbing moisture from the atmosphere. An aging study of the F-178/T-300 prepregs was carried out earlier, and the result indeed showed that room temperature aging greatly affected the processing properties and, consequently, the laminate mechanical properties of that material (6).

The C-10 phthalocyanine resin differs greatly from other thermosetting materials such as epoxy and polyimide in this respect. The material is practically inert at room temperature, and the polymerization is activated simply by staging the resin at a temperature higher than its melting temperature without any catalytic action. Therefore, the material, both in resin and in prepolymer form, should exhibit very good room-temperature stability. A 28-week prepreg aging study was thus carried out to demonstrate this point.

The C-10/T-300 prepreg material was cut into 15.2 cm x 15.2 cm sheets, and stored at room temperature in two separate environmental chambers, controlled at 16% and 95% relative humidity, respectively. At the end of every four-week period, material was removed and a 16-ply laminate fabricated on the same day. Test specimens were cut from the laminate and their flexural and shear properties evaluated according to ASTM-D 790 and ASTM-D 2344, as described earlier. Fig. 11 shows the short-beam shear strength (SBSS) of unidirectional C-10/T-300 composites, a resin-dominated property, as a function of the aging period in weeks. It is clear that over the 28-week period laminate

Table 1: Laminate Mechanical Properties at Room Temperature

<u>Orientation</u>	<u>Property (GPa)</u>	<u>5208/T-300</u>	<u>F-178/T-300</u>	<u>C10/T-300</u>
Quasi-isotropic	Strength: tensile	0.48	0.39	0.47
	flexural	-	0.52	0.46
	Modulus: tensile	48.3	62.8	75.2
	flexural	-	37.3	33.8
$2\theta = 30^\circ$	Strength: tensile	0.75	0.61	0.56
	flexural	1.03	0.81	0.66
	Modulus: tensile	104.9	97.3	93.2
	flexural	107.0	91.1	75.2
$2\theta = 90^\circ$	Strength: tensile	0.16	0.13	0.11
	flexural	-	0.28	0.18
	Modulus: tensile	26.9	40.7	37.3
	flexural	-	17.3	9.7
$2\theta = 150^\circ$	Strength: tensile	0.041	0.035	0.031
	Modulus: tensile	10.4	26.2	22.8

shear strength showed almost no change, confirming that room temperature aging up to 28-weeks had not caused any chemical degradation or affected the processability of the C-10/T-300 prepreg system.

Summary

The C-10 phthalocyanine resin has been shown to be a potential matrix material for advanced composites. This polymer exhibits long-term stability at temperatures up to 245°C (5), and its moisture uptake is less than that of epoxies or polyimides (6).

The phthalocyanine reaction can be induced to proceed under less severe thermal and catalytic conditions than those required for the acetylene reaction (4). Upon melting, the resin flows readily and successful prepregging has been demonstrated using the conventional hot-melt technique and the solvent/slurry method. The resin monomer represents a chemically simple and pure system for easy quality control when compared with the complex formulations of other systems such as epoxies (See Chemical Characterization Task).

Instrumental techniques including DSC, TGA and DDA have been developed for identifying necessary processing parameters for the development of fabrication procedures for the C-10 resin system. The processability of C-10 phthalocyanine is shown to be similar to that of conventional epoxies. The combined application of DSC data and in situ DDA during a press cure has proved to be a useful technique in controlling laminate resin content when additional resin needs to be added to the sample lay-up.

Mechanical properties have been determined in both tensile and flexural tests for the C-10/T-300 system, which are comparable with those of the 5208/T-300 and the F-178/T-300 composites. With the quasi-isotropic design for the laminates, the C-10/T-300 samples even showed better properties than the others.

A 28-week prepreg aging study at room temperatures confirmed that exposures to either a high or a low humidity environment at room temperatures caused no chemical degradation or changes in the processability of C-10/T-300 prepreg.

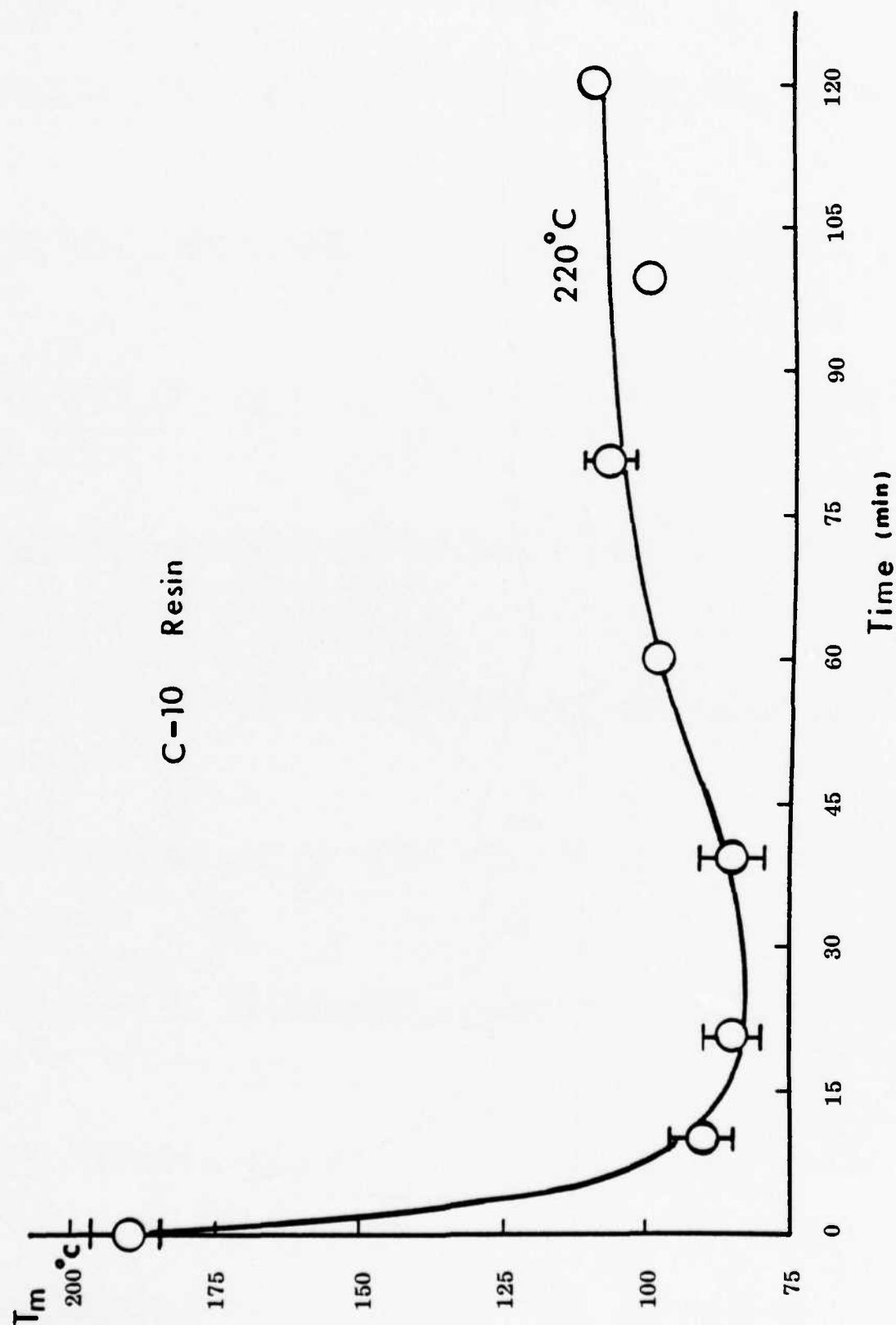


Fig. 1 - Melting temperature of C-10 resin as a function of dwell time at 220°C.

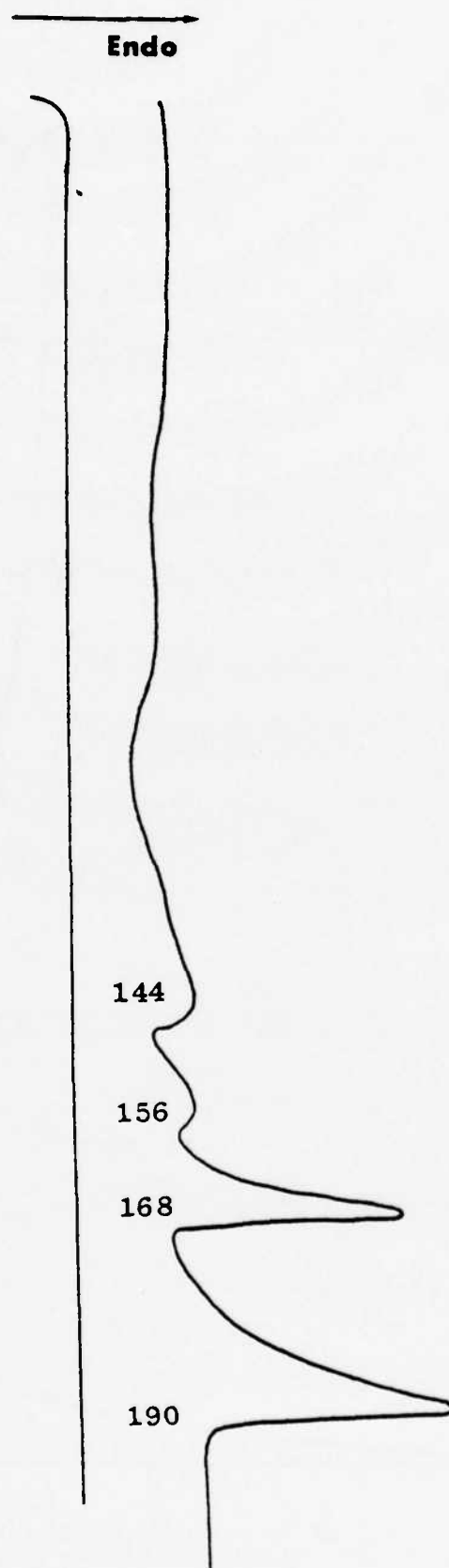


Fig. 2 - DSC record of C-10/T-300 prepreg.

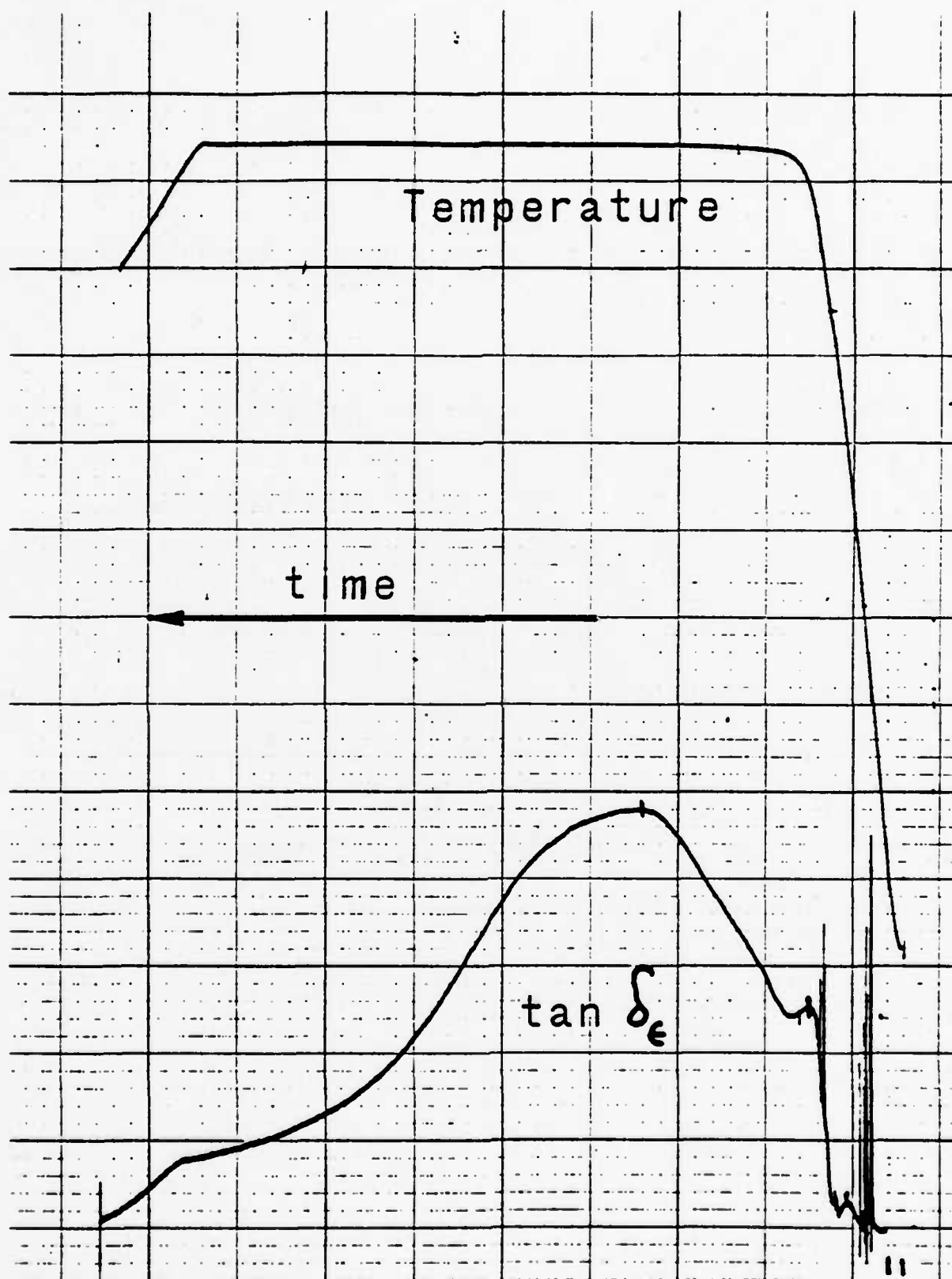


Fig. 3 - Dynamic dielectric analysis of the isothermal cure of a C-10/T-300 prepreg sample.

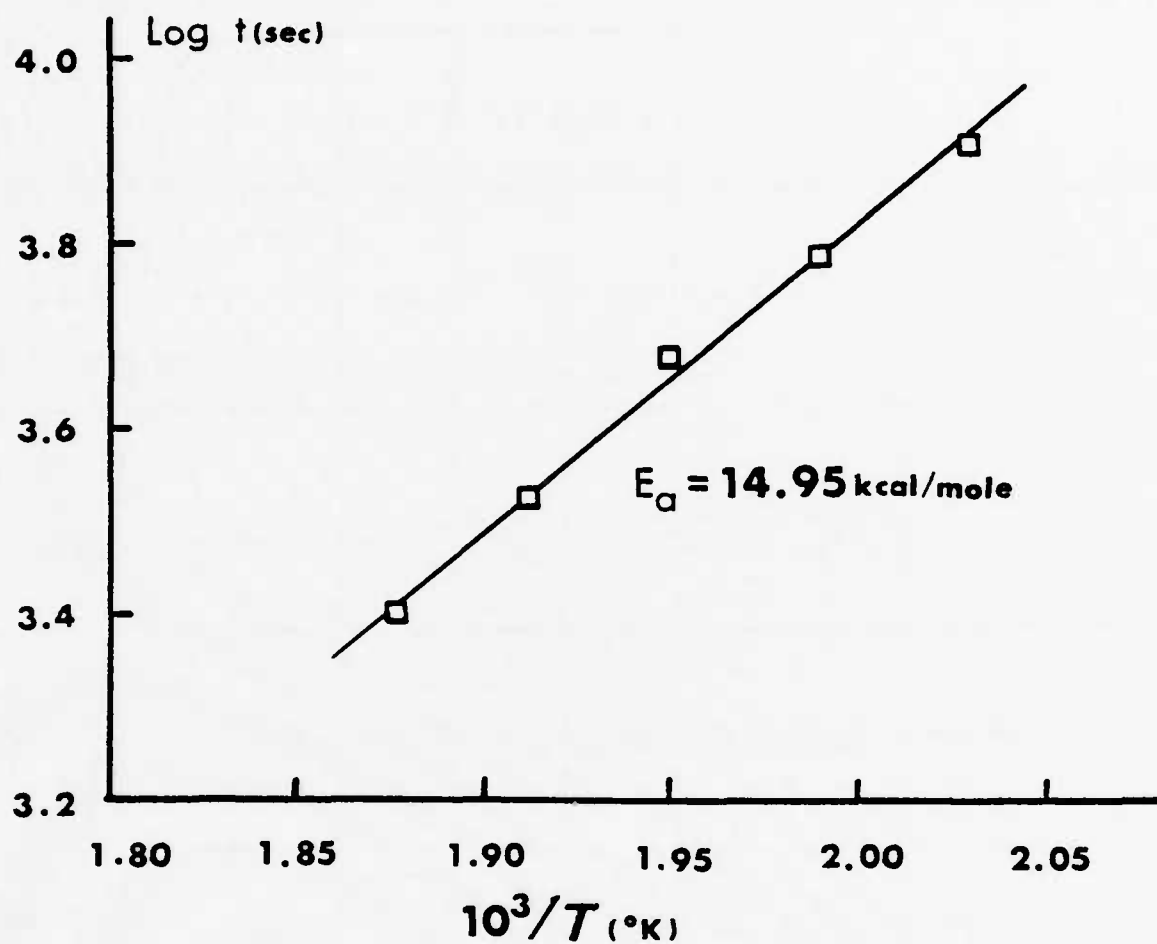


Fig. 4 - Arrhenius plot of gelation time vs. cure temperature for C-10/T-300 prepreg.

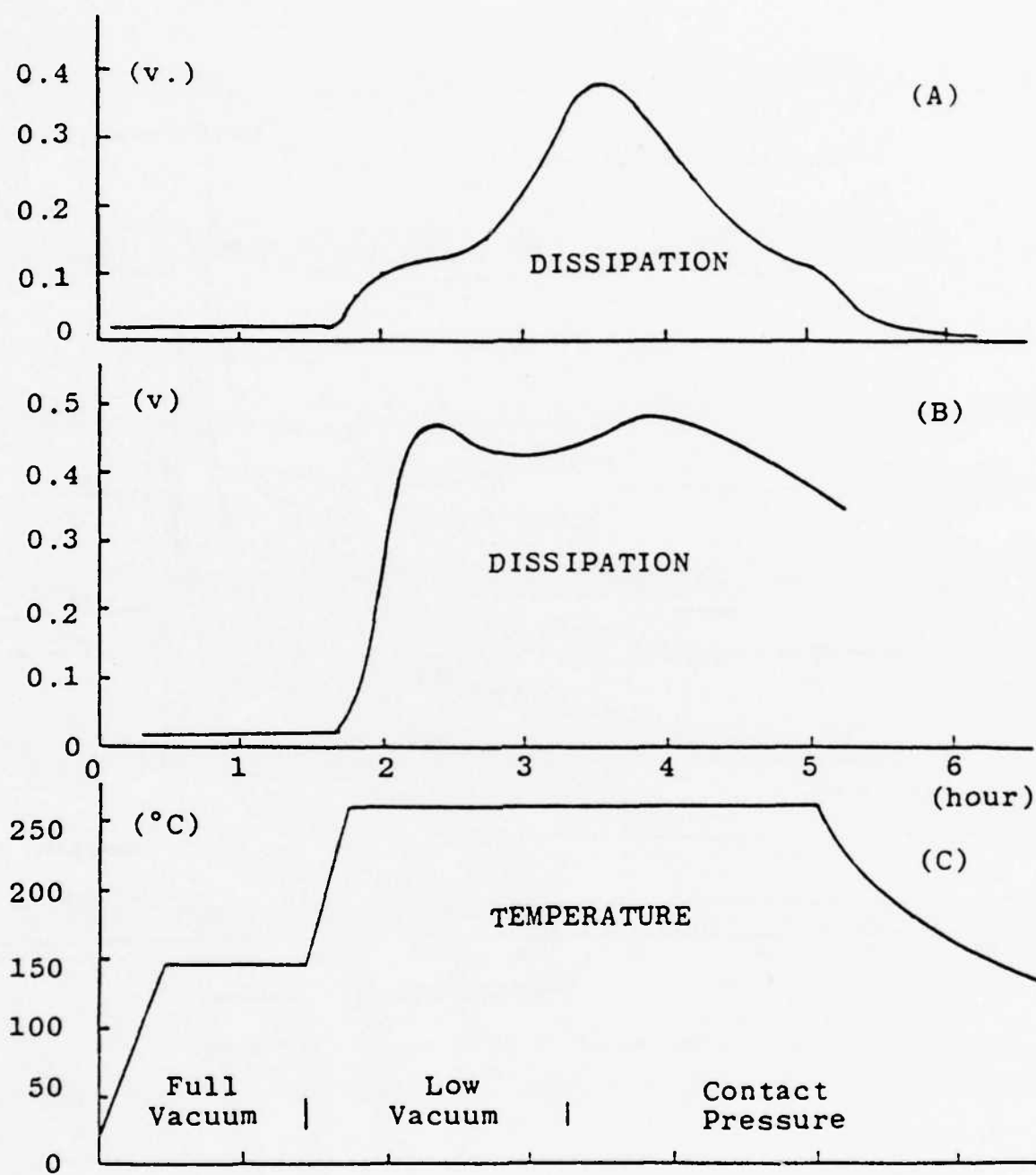


Fig. 5 - Dielectric dissipation of C-10/T-300 laminate sample during press cure.

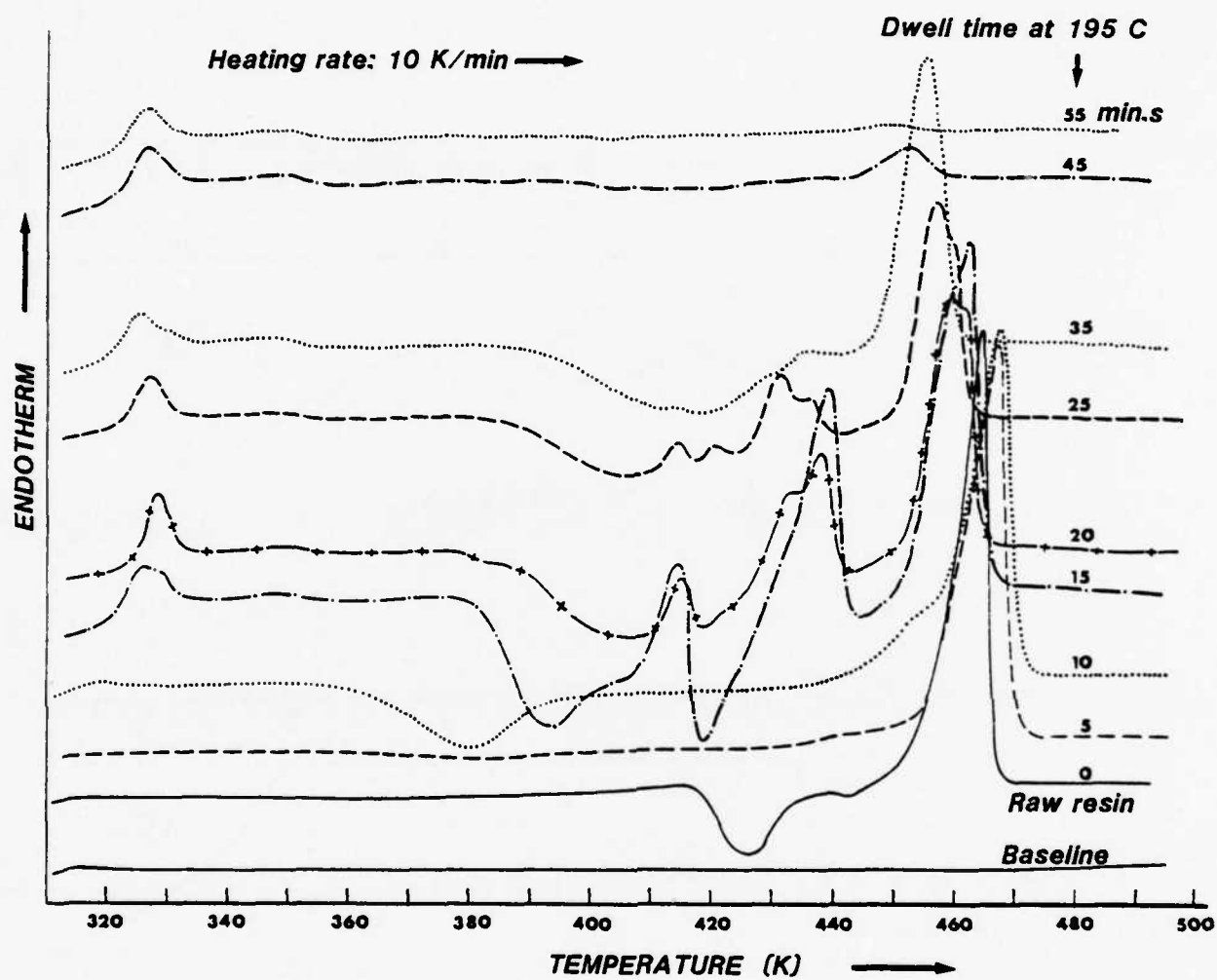


Fig. 6 - DSC scans of "B"-staged C-10 resins.

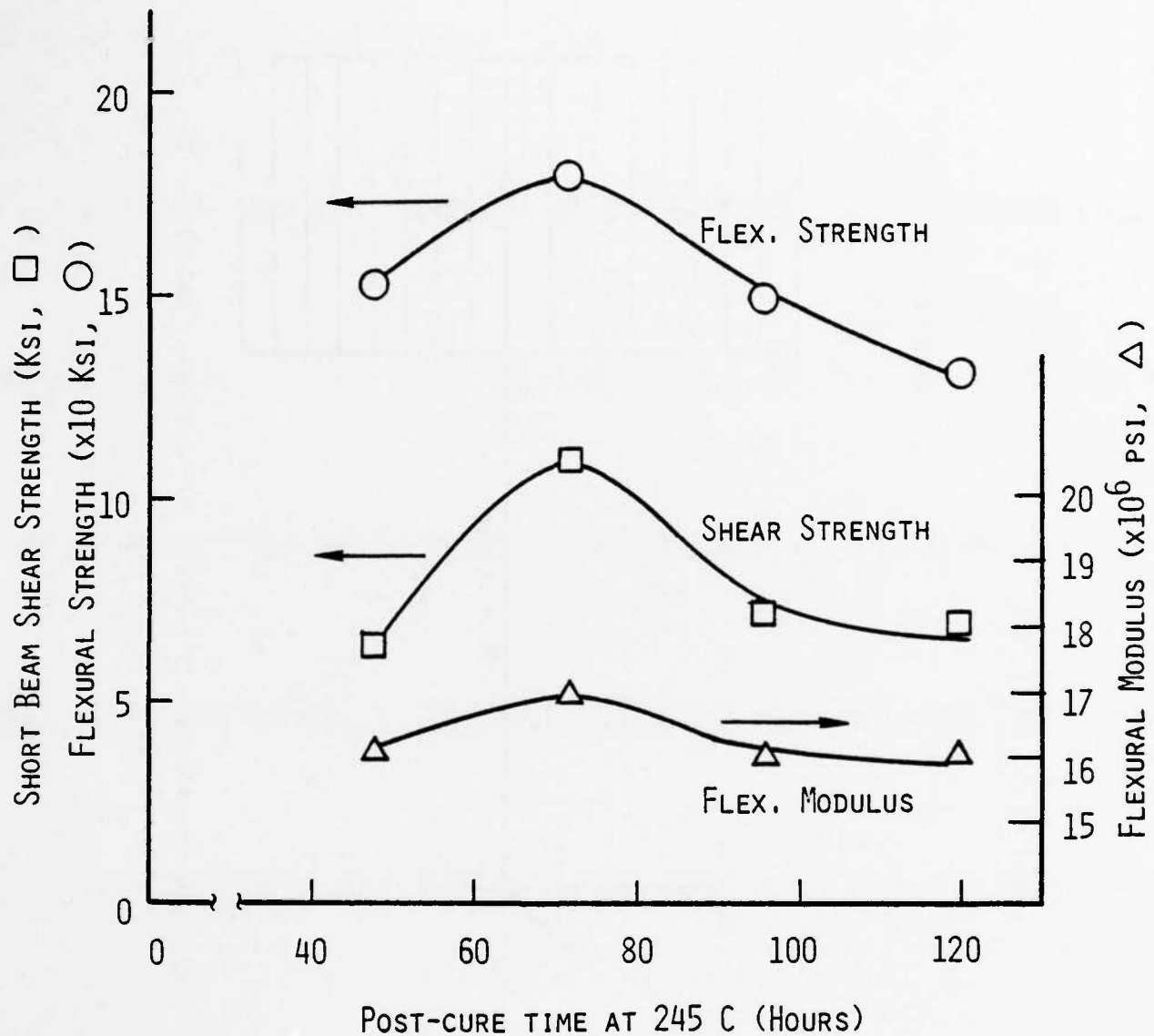
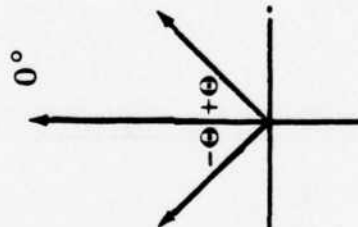
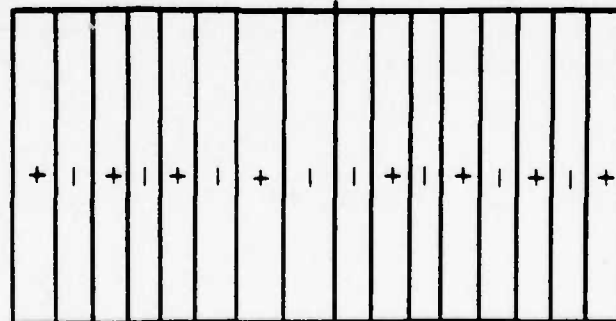


Fig. 7 - Effect of post-cure on the mechanical properties of unidirectional C-10/T-300 laminates.

LAMINATE DESIGNS

1. Angle Plies (16-ply)



Midplane

2. Quasi-isotropic

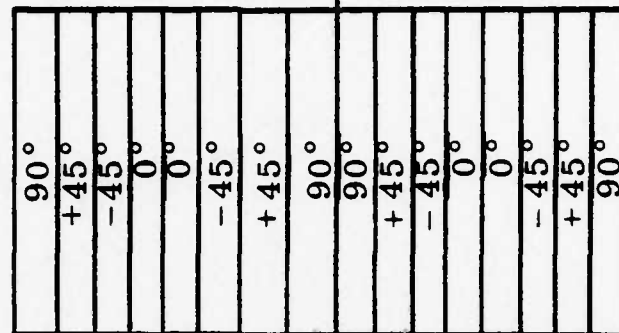


Fig. 8 - Stacking sequence of angle-ply and quasi-isotropic laminates.

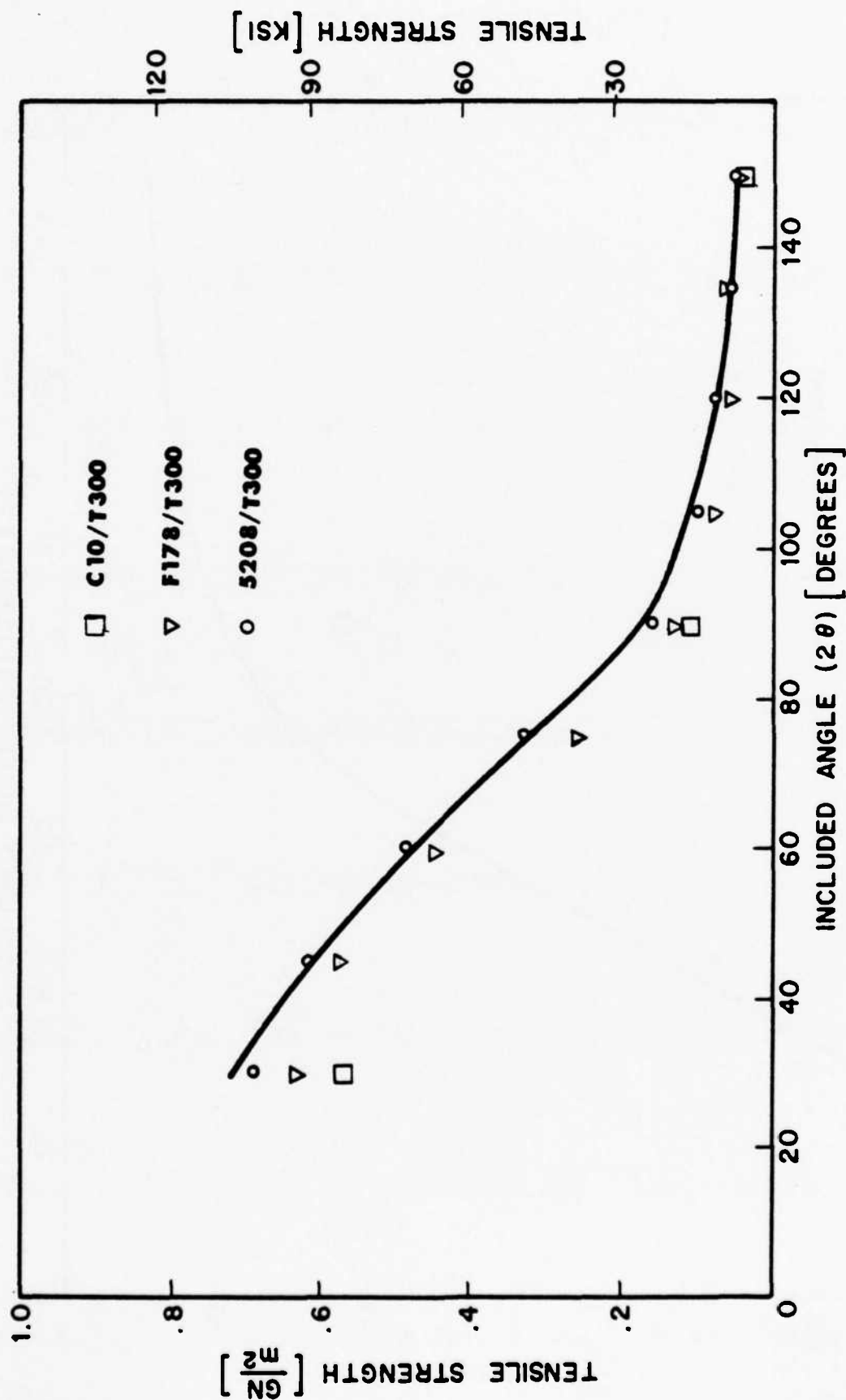


Fig. 9 - Laminate tensile strength as a function of fiber included angle.

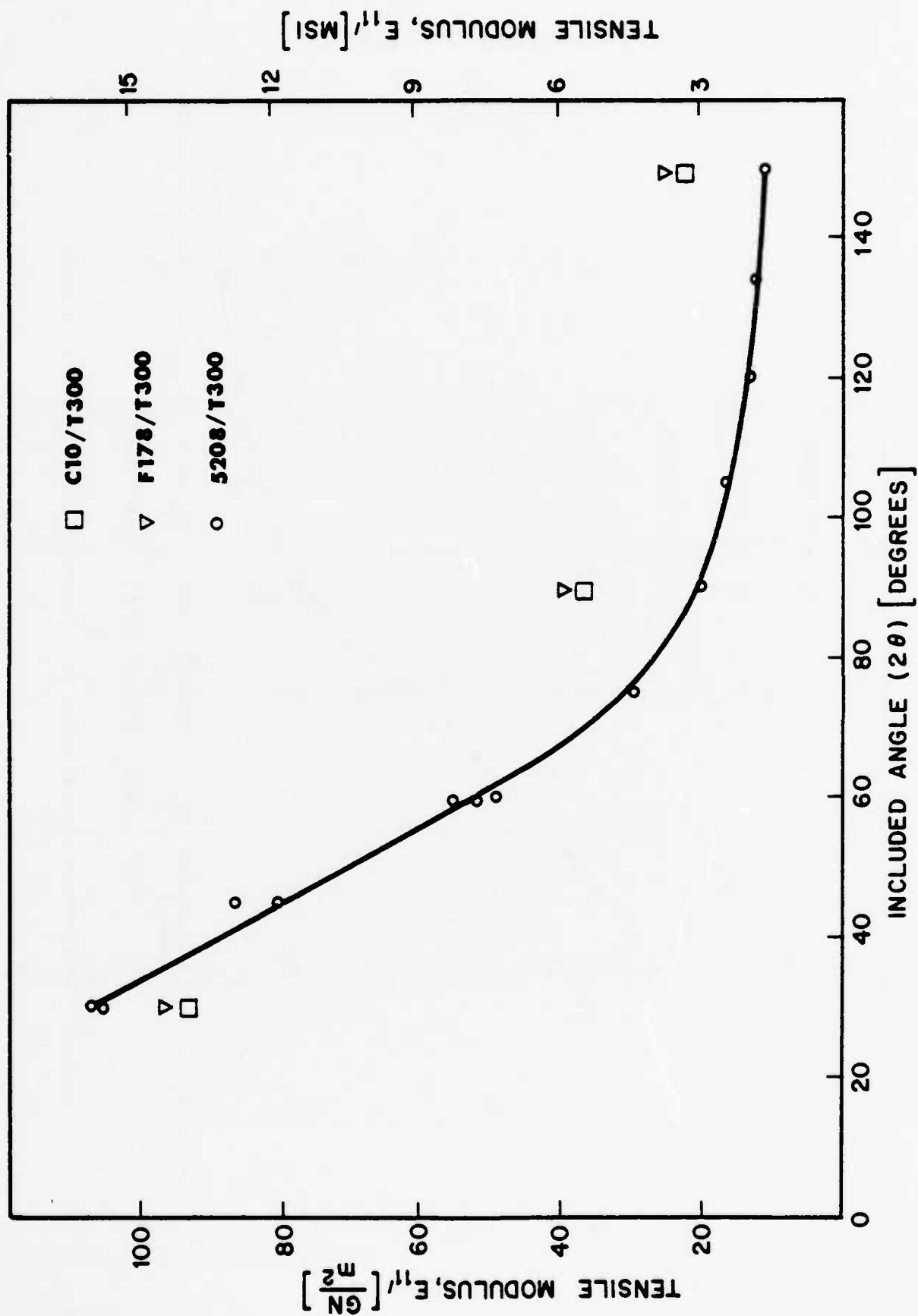


Fig. 10 - Laminate tensile modulus as a function of fiber included angle.

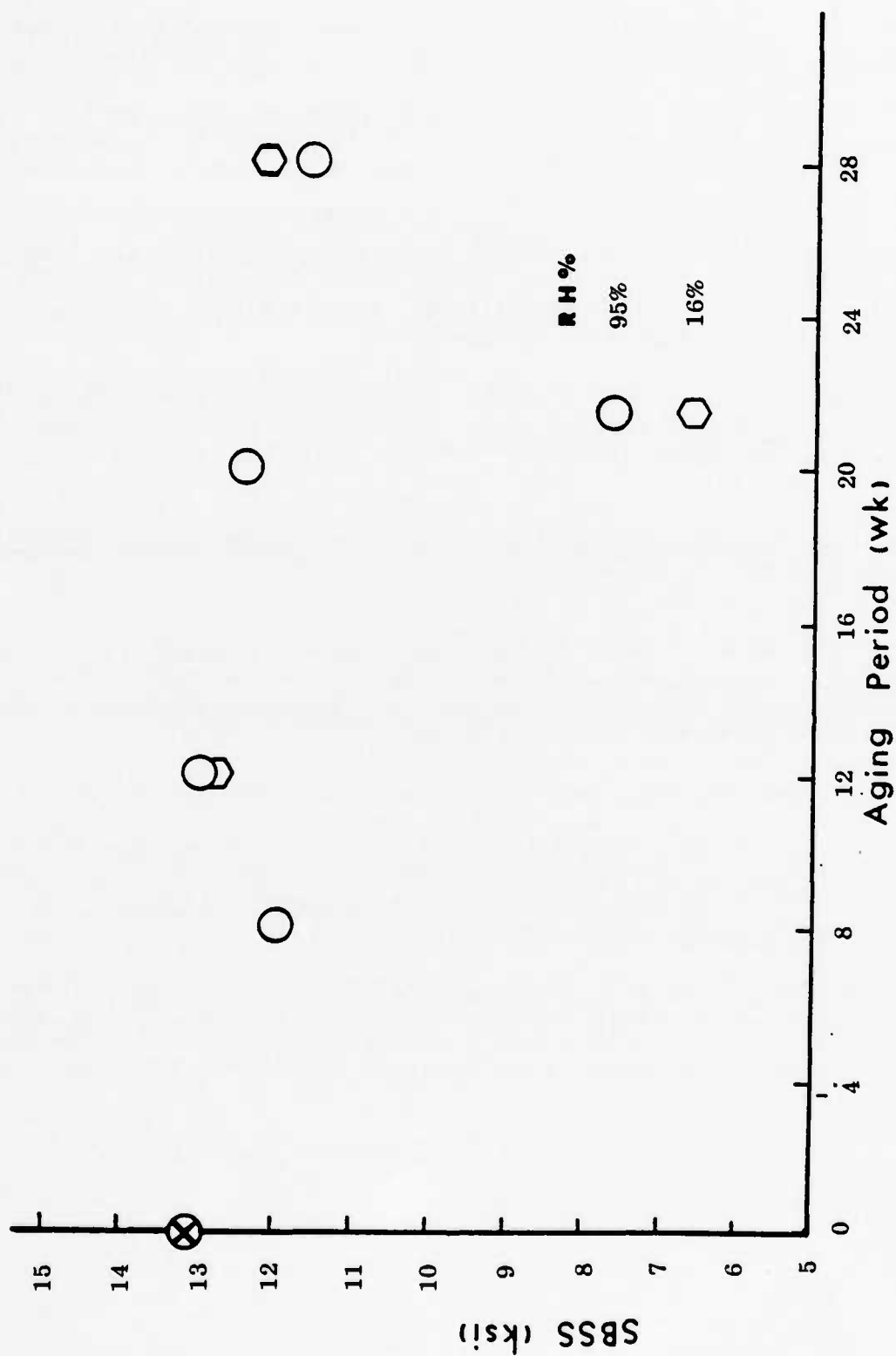


Fig. 11 - Effect of prepreg aging on the interlaminar shear strength of the C-10/T-300 composites.

REFERENCES

1. T. R. Walton, J. R. Griffith and J. G. O'Rear, ACS Org. Coat. Plast. Chem. Preprint, 34, 446 (1974).
2. J. V. Gauchel and H. C. Nash, in High Performance Composites and Adhesives For V/STOL Aircraft, eds. W. D. Bascom and L. B. Lockhart, Jr., NRL Memorandum Report 3433, December 1976. Article Title: "Composites Fabrication" pg. 79 AD/A035928
3. R. Y. Ting and H. C. Nash, in High Performance Composites and Adhesives For V/STOL Aircraft, eds. W. D. Bascom and L. B. Lockhart, Jr., NRL Memorandum Report 3721, February 1978. Article Title: "Fabrication of Composites" p. 93 thru 103 AD/A054 637
4. J. R. Griffith and J. G. O'Rear, in High Performance Composites and Adhesives For V/STOL Aircraft, eds. W. D. Bascom and L. B. Lockhart, Jr., NRL Memorandum Report 3433, Dec. 1976. AD/A035 928 Article Title: "Task A. Resin Synthesis" p. 7.
5. T. R. Walton, J. R. Griffith and J. G. O'Rear, in Copolymers, Polyblends and Composites, ed. N.A.J. Platzner, Adv. in Chem. Ser. of ACS, 142, 458 (1975).
6. R. Y. Ting and H. C. Nash, in High Performance Composites and Adhesives For V/STOL Aircraft, ed. L. B. Lockhart, Jr., NRL Memorandum Report 4005, May 1979. p. 95, Article Title: "Cure Analysis and Fabrication Technique For Advanced Composite Materials" AD/A 069 611.
7. J. K. Gillham, ACS Org. Coat. Plast. Chem. Preprint, 40, 866 (1979).
8. C. A. May, D. K. Whearty and J. S. Fritzen, SAMPE Series, 21, 803 (1976).
9. N. E. McCrum, B. E. Read and G. Williams, Anelastic and Dielectric Effects in Polymeric Solids, John Wiley, NY, 1967.
10. Z. N. Sanjana, in Science and Technology of Polymer Processing, eds. N. P. Suh and N.-H. Sung, The MIT Press, Cambridge, MA, 1979, p. 827.
11. J. K. Gillham, J. A. Benci, and A. Noshey , J. Polym. Sci.-Symposium, 46, 279 (1974).
12. W. D. Bascom, J. L. Bitner and R. L. Cottingham, ACS Org. Coat. Plast. Chem. Preprint, 38, 477 (1978).

FAILURE CRITERIA FOR COMPOSITE STRUCTURES

P. W. Mast, L. A. Beaubien, D. R. Mulville,
S. A. Sutton, R. W. Thomas, J. Tirosh and I. Wolock

Mechanics of Materials Branch
Material Science and Technology Division

INTRODUCTION

This task deals with the development of failure criteria for structural composites, using resin matrices discussed in the prior tasks, and the demonstration of the applicability of these criteria in structural components. Previous aspects of this task were reported in prior publications (1, 2, 3). Fracture tests are being conducted on small test coupons in a unique in-plane loader developed at NRL. A large base of experimental data is obtained under complex loads to simulate service conditions. A concept of similar strain fields was developed for predicting failure in structures, based on data obtained on test coupons in the in-plane loader, as described in the second annual report (2). This concept states that if the strain field in the region of interest in the structure is similar to that previously observed in a test coupon, the loads that caused failure initiation in the test coupon will also cause failure in the structure. Several tests were reported which demonstrated the validity of this prediction technique. Results reported in this section include extensive fracture tests on graphite fiber composites of varying reinforcement angles and under a broad range of in-plane loads. Three resin systems were used as matrices - an epoxy, a bismaleimide, and an experimental phthalocyanine resin. Fracture tests were conducted at room temperature and at 450°F (232°C).

TEST DETAILS

In-Plane Loader

The tests were conducted on an in-plane loader developed at the Naval Research Laboratory (Figure 1). Three independent computer-controlled hydraulic actuators are connected to a movable head. By programming predetermined displacements to each actuator, combinations of horizontal displacements (in-plane shear), vertical displacements (tension or compression) and rotational displacements (in-plane bending) can be applied to a test specimen through the movable head (Figure 2). A single-edge-notch specimen is used, 1 in. x 1.5 in. x 0.1 in. (25 mm x 38 mm x 2 mm) with a notch 0.6 in. (15 mm) long parallel to the 1-inch dimension. The specimen is held by a pair of hydraulically-controlled grips in which the clamping pressure is programmed. One grip is attached to the movable head, and the other to a fixed head. The specimens are removed from a

loading magazine and inserted in the grips by a mechanical feeding device. Initial data regarding specimen geometry, such as notch location, is obtained via a digitized video picture of the specimen in the grips and the data is then stored in a computer. A computer system is interfaced with these components and controls the tests, gathering the specimen geometry data, controlling the pressure in the grips, loading the specimen in a prescribed proportional loading path and gathering and storing data on force and displacement. Force and displacement are measured 50 times during each 15-second test.

From the load and displacement data, one can calculate the energy absorbed by the specimen. Initially there is a linear relation between load and displacement. Then non-linear behavior is observed. If one subtracts the linearly recoverable energy from the energy supplied to the specimen, one obtains a measure of the non-linear energy absorption or the dissipative energy (Figure 3). The point at which non-linearity is first exhibited is defined as the point of fracture initiation.

Plots of the displacement, load and dissipated energy versus time are presented in Figure 4. From the time at which non-linearity is first observed, one can determine the corresponding load and displacement, which are called the critical load and displacement or that necessary to initiate failure. One can also determine the maximum load the specimen supports during the test. All three of these parameters can be presented as measures of "fracture toughness".

A plot of critical displacement is shown in Figure 5, in spherical coordinates mapped onto a cartesian reference frame for one octant of load space. This figure also shows the relation between the components of shear, tension and bending applied to the specimen, d_0 , d_1 and d_2 , respectively, and the spherical coordinates, θ_1 , θ_2 and r used to represent the fracture surface. The results represent the conditions for failure initiation for a broad range of complex loading conditions and reflect the complexity of the failure process in composites.

The data needed to define the conditions for failure initiation are the horizontal, vertical, and rotational displacements or loads, and a measure of the toughness. In order to present the data pictorially as a graph, only three variables can be used. Therefore, the horizontal and vertical displacements are combined as a ratio θ_1 . Thus the positive X-axis represents the ratio of tension to shear, while the negative X-axis represents the ratio of compression to shear. The data is presented for four octants of load space (Figure 6), in which the shear is positive. In the other four octants, the shear would be negative, but this is the same as positive shear for the specimen used. Each vertical line in Figure 6 represents the results of a single test. The reproducibility of the data is obvious. If one joins the data points, a surface is formed as shown in Figure 7. If one varies the reinforcement included angle, a series of surfaces is obtained, as shown in Figure 8. If instead of using critical displacement as the toughness parameter, one uses maximum load, a failure surface is obtained which is somewhat similar in shape to that for critical displacement (Figure 9).

Materials

Tests were conducted to compare the fracture behavior of graphite fiber composites made with three different resins - Narmco 5208 epoxy resin, Hexcel Fl78 bismaleimide resin, and a phthalocyanine resin (C-10) developed at NRL. These resins and the laminate fabrication procedures are described in a prior section and in the previous reports (1, 2, 3).

The crossply laminates were made using Union Carbide Thornel T300 graphite fibers. Tests were conducted at room temperature on T300/5208 laminates having reinforcement included angles of 30° , 60° , 75° , 90° , 105° , 120° , 135° , and quasi-isotropic (0° , $+45^\circ$, 90°); T300/Fl78 laminates having reinforcement included angles of 30° , 45° , 60° , 75° , and quasi-isotropic (0° , $+45^\circ$, 90°); and T300/C-10 laminates having reinforcement included angles of 30° , 90° , and quasi-isotropic (0° , $+45^\circ$, 90°).

Tests were also conducted at 450°F (232°C) on T300/5208 laminates having reinforcement included angles of 45° , 60° , 75° , 90° , and quasi-isotropic (0° , $+45^\circ$, 90°); T300/Fl78 laminates having reinforcement included angles of 30° , 45° , 60° , 75° , 90° , and quasi-isotropic (0° , $+45^\circ$, 90°); and T300/C-10 laminates having reinforcement included angles of 30° , 90° , and quasi-isotropic (0° , $+45^\circ$, 90°).

The 450°F tests were conducted by heating the specimens for 1 hour in an oven at 450°F , placing them in the loading magazine over which a heating unit is placed which maintains the temperature at 450°F , and then placing each specimen in the hydraulic grips using a heated pair of forceps which remain in place just above and below the specimen during the test to reduce cooling by the specimen during the test. The testing cycle takes 15 seconds. Tests were also conducted on T300/5208 composites after 24 hours heating in the oven at 450°F .

RESULTS

General

The complexity of the fracture process in fiber-reinforced composites is apparent from the complex failure surfaces previously presented. The "fracture toughness" depends on the loading, the reinforcement angle, and the failure criterion used. Thus comparing the toughness of two composites is extremely complex. It becomes a matter of comparing several surfaces or a large number of points. It is difficult to express such a comparison in a simple manner. The more detailed the comparison, the more complex is the expression. The simpler the comparison, the less detailed it is. The data obtained during the course of each test is stored in a computer. It is not necessary to present the data as graphs or failure surfaces to use it in predicting the fracture behavior of a structural component. Such figures are useful for visualization but not necessary for utilization. In order to compare the data obtained in this study, it will be necessary to simplify the representation.

For each of the composites, a series of plots were prepared expressing the data as shown in Figure 6. However, it is difficult to compare several such sets of data. Therefore, the first simplification was made by taking a slice

through each failure surface such as Figure 9 at a single value of θ_2 , and then plotting these slices as a function of the reinforcement included angle, as shown in Figure 10 for $\theta_2 = 0$ (no in-plane rotation). This is for the T300/5208 laminate with a reinforcement included angle of 60° . Obviously, any conclusions drawn apply to the conditions shown only. The same procedure could be followed for other values of θ_2 . This is part of the complexity of the process of comparing the failure behavior of different composites.

T300/5208 Laminates

The room temperature tests (Figure 10) were first compared with those conducted at 450°F after 1 hour heating at the elevated temperature (H1) (Figure 11). The comparisons could be made for reinforcement included angles (α) of 60° , 75° , 90° , and quasi-isotropic (0° , $+45^\circ$, 90°). Comparisons were made using as criteria the load at which failure initiated and the maximum load the specimen supported. A simplified comparison plot is shown in Figure 12. The specimens tested at 450°F exhibited toughness values that were close to those obtained at room temperature. In some cases, there was no significant difference between the two. In most cases, however, the specimens tested at 450°F exhibited slightly reduced toughness values, usually no more than about 25 percent less than the room temperature values. In a few cases, the values were as much as 50 percent less. Overall, the specimens exhibited significant fracture toughness at 450°F . The results are somewhat surprising since 5208 resin composites are generally considered as not being useable over 300°F (149°C). To further evaluate the behavior of the 5208 epoxy at elevated temperature, specimens were heated for 24 hours at 450°F before testing at that temperature (Figure 13). The results duplicated those obtained after one hour heating. There was no significant difference between the two elevated temperature tests (Figure 14). The reproducibility of the testing process is apparent from this data.

T300/F178 Laminates

The results of the room temperature tests (Figure 15) were compared with those obtained at 450°F after one hour exposure at that temperature (Figure 16). Comparisons were made for reinforcement included angles of 30° , 45° , 60° , 75° and quasi-isotropic (0° , $+45^\circ$, 90°). Again the comparisons were made using as criteria the load at which failure initiated and the maximum load the specimen supported. For most of the panels tested, the data obtained at the elevated temperature was slightly less than that obtained at room temperature (Figure 17).

T300/C-10 Laminates

The C-10 material was tested in panels having reinforcement included angles of 30° and 90° (Figures 18 and 19), along with quasi-isotropic (0° , $+45^\circ$, 90°). The material tested at 450°F had a slightly lower toughness than the material tested at room temperature in most cases (Figure 20), but slightly higher in some others, mainly for the quasi-isotropic material under tensile loading.

Comparison of Materials

As pointed out previously, to express the relative fracture toughness of two composites in relatively simple terms, it is necessary to simplify the data, because of the complex nature of the failure process. The first simplification in comparison of the data obtained in this investigation involved taking slices of failure surfaces at $\theta_2 = 0$, meaning no in-plane rotation, and plotting these slices as a function of reinforcement included angle. This is done for the three materials at room temperature for several included angles (Figure 21). The data shows that there is little difference in the in-plane fracture toughness of the three materials at room temperature. Similar data for tests conducted at 450°F (Figure 22) also shows little difference in composites made from these three resins.

A second simplification can be made by taking only one reinforcement included angle and plotting this data for the three materials. The room temperature data is shown in Figure 23 for an included angle of 90°. Unfortunately, there was no data at room temperature for all three materials for a single reinforcement angle. This data again shows little difference at room temperature between 5208 and C-10 composites having the reinforcement included angle of 90°. The data obtained at 450°F is shown in Figure 24 and again shows little difference between the three materials. Comparison of Figures 23 and 24 shows little difference between room temperature and 450°F for the 90° laminates, with no in-plane rotation ($\theta_2 = 0$).

The quasi-isotropic material did not lend itself to the data representation shown in Figures 10 to 22 for various reinforcement included angles. The room temperature data for the quasi materials at $\theta_2 = 0$ is shown in Figure 25. There is some difference exhibited by the three materials. The elevated temperature data is shown in Figure 26. There is little difference between the materials under tensile loading, but under compression loading the C-10 laminates again showed slightly lower properties. Comparing these two figures, there is little difference between room temperature and elevated temperature behavior, except that the C-10 material exhibited improved properties at the elevated temperature under tensile loading. One must always keep in mind that these comparisons represent a simplification of the data.

SUMMARY AND CONCLUSIONS

1. Comprehensive data characterizing the failure behavior of fiber-reinforced composites is quite complex. It cannot be represented by the usual methods — a simple equation or simple graph. Automated techniques are needed to analyze and utilize the data properly. As was apparent in this report, it is necessary to simplify the data to discuss it or compare it using conventional methods.
2. For the range of resins studied in this investigation — a standard epoxy, a bismaleimide, and a phthalocyanine — there is little difference in the in-plane fracture toughness of composites made with these resins at room temperature and at elevated temperature. Composites exhibit significant in-plane fracture toughness at temperatures significantly higher than what

is considered to be the maximum use temperature of the resin matrix. These observations indicate that the in-plane fracture toughness of fiber-reinforced composites is dominated by the fiber and that significant variations in matrix properties have little effect.

REFERENCES

1. W. D. Bascom and L. B. Lockhart, Jr., High Performance Composites and Adhesives for V/STOL Aircraft, NRL Memo Report 3433, Washington, DC, December 1976 AD/A035 928
2. W. D. Bascom and L. B. Lockhart, Jr., High Performance Composites and Adhesives for V/STOL Aircraft, NRL Memo Report 3721, Washington, DC, February 1978 AD/A054 637
3. L. B. Lockhart, Jr., High Performance Composites and Adhesives for V/STOL Aircraft, NRL Memo Report 4005, Washington, DC, May 23, 1979 AD/A069 611

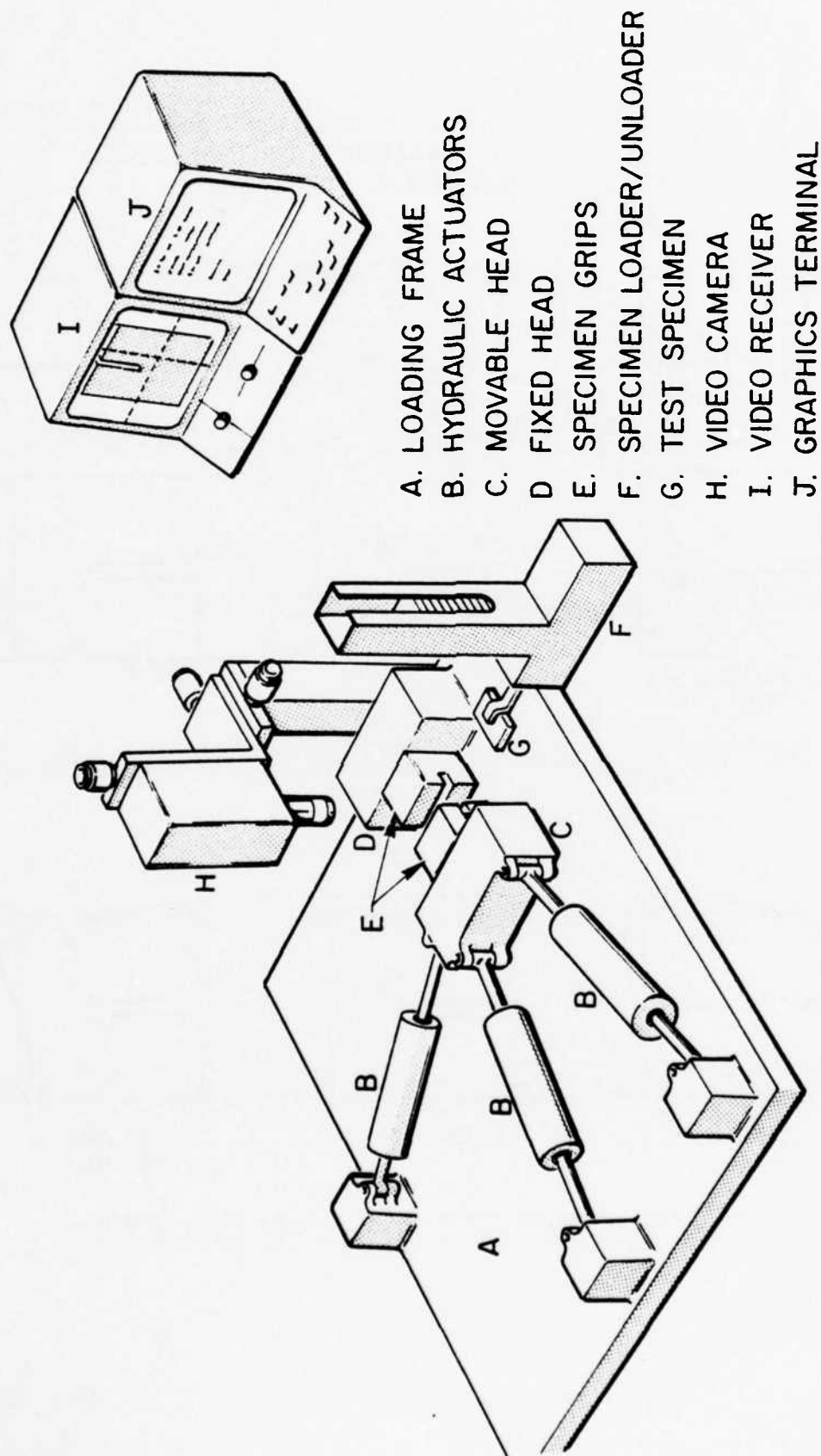


Figure 1 Schematic diagram of the in-plane loader

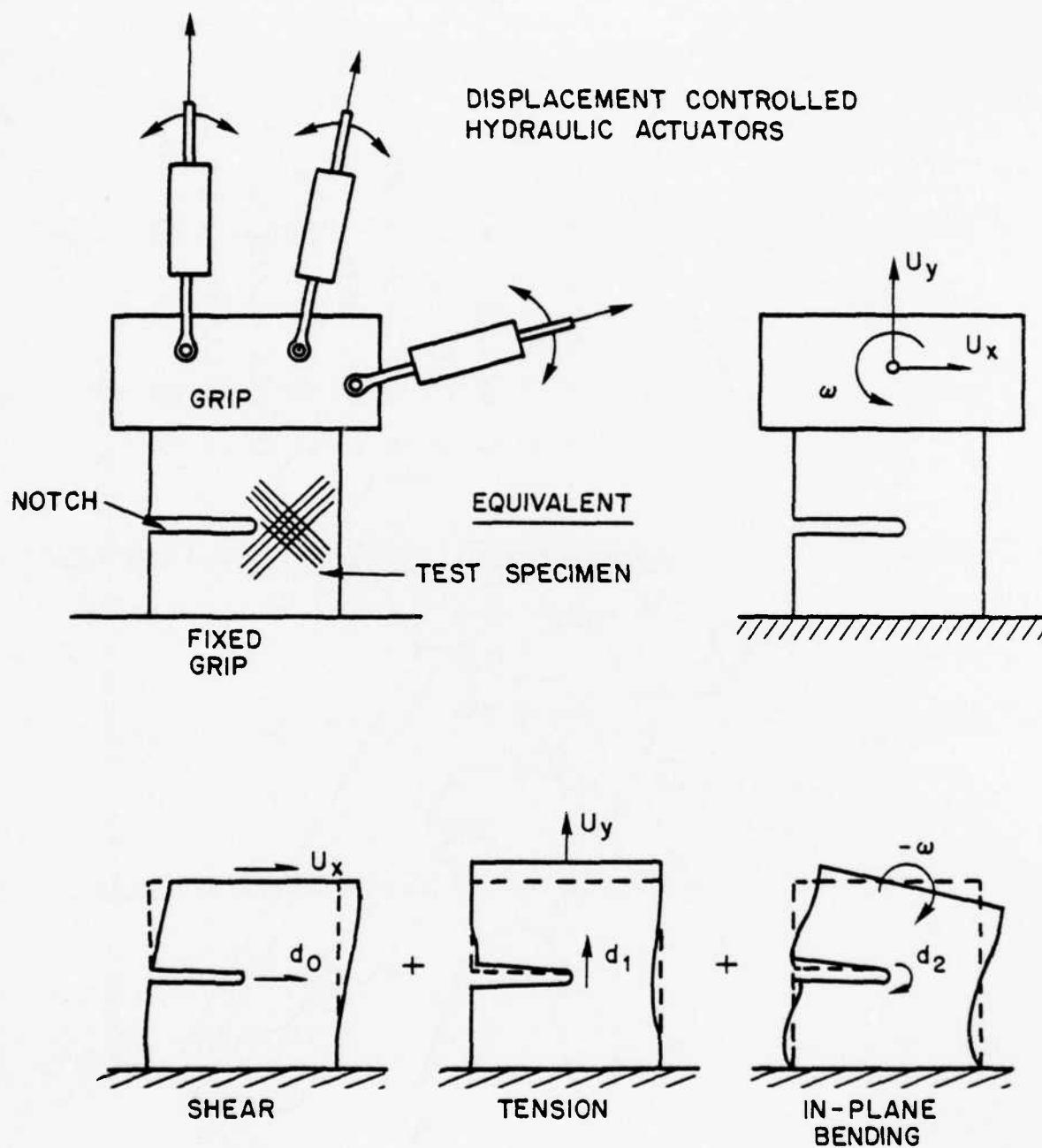
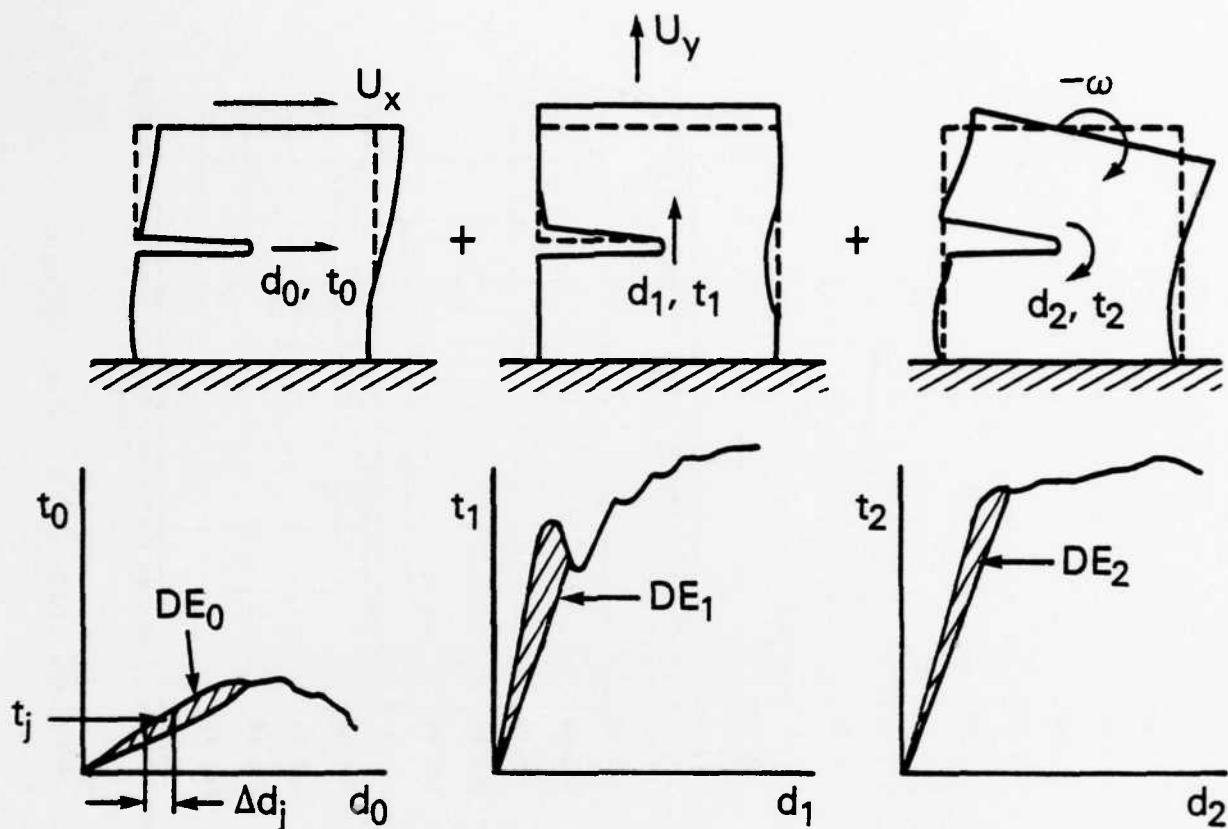


Figure 2 Displacements produced by the in-plane loader



$$DE_i = \frac{1}{2} \left\{ \left[\sum_{j=0}^n t_j \Delta d_j \right] - [d_j t_j] \right\} \quad i = 0, 1, 2$$

$$DE = DE_0 + DE_1 + DE_2 \quad j = 1, 2 \dots n$$

$$R = \sqrt{d_0^2 + d_1^2 + d_2^2}$$

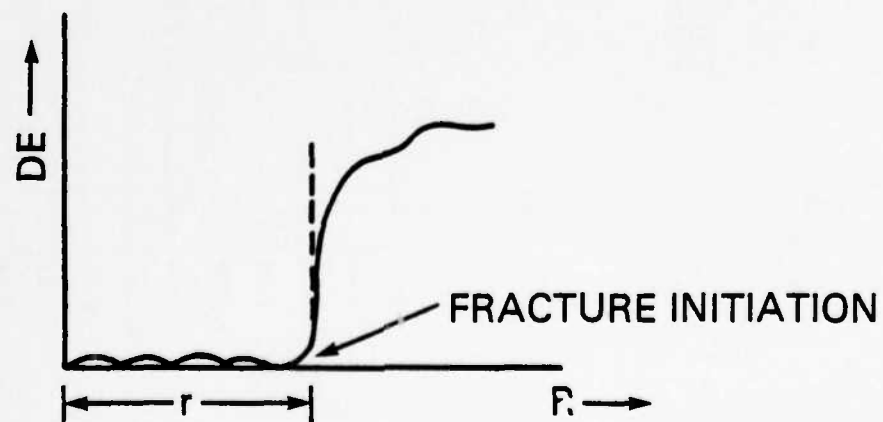


Figure 3 Dissipative energy of composites under in-plane loads

DATE 11/28/77
 TIME 15154124
 EXPR: PAST
 FILE: IPL>T300-5208>L-15
 MATERIAL GR193

SPEC. NU: 35
 HUMIDITY: 46.4773(X)
 THICK: 0.0735(INS)

GRIP OPEN: 0.000(INS)
 WIDTH: 0.4257(INS)
 X-TRANS: 0.0846(INS)
 Y-TRANS: -0.2674(INS)

THETA-1: 90.0000(DEG)
 THETA-2: 0.0000(DEG)
 MAG: 0.0500(INS)

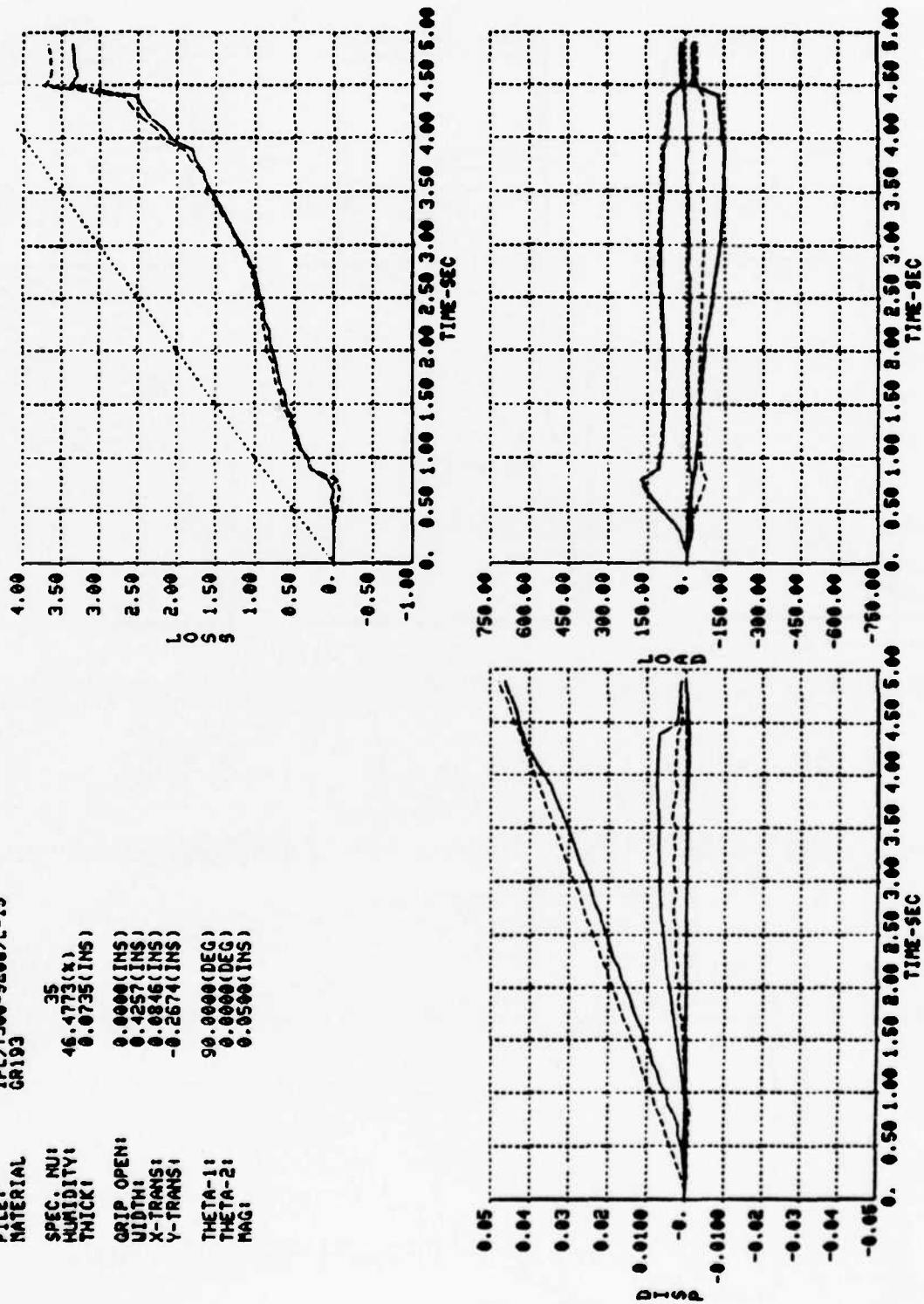


Figure 4 Plots of data obtained during in-plane loader test - displacement, load, and energy loss versus time

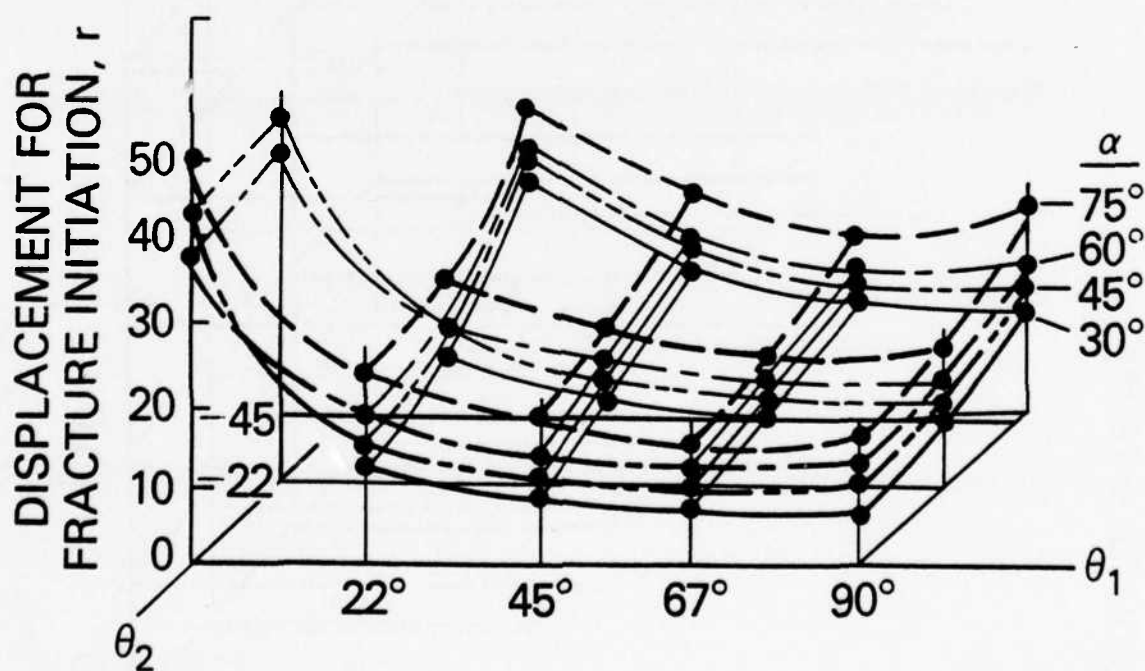
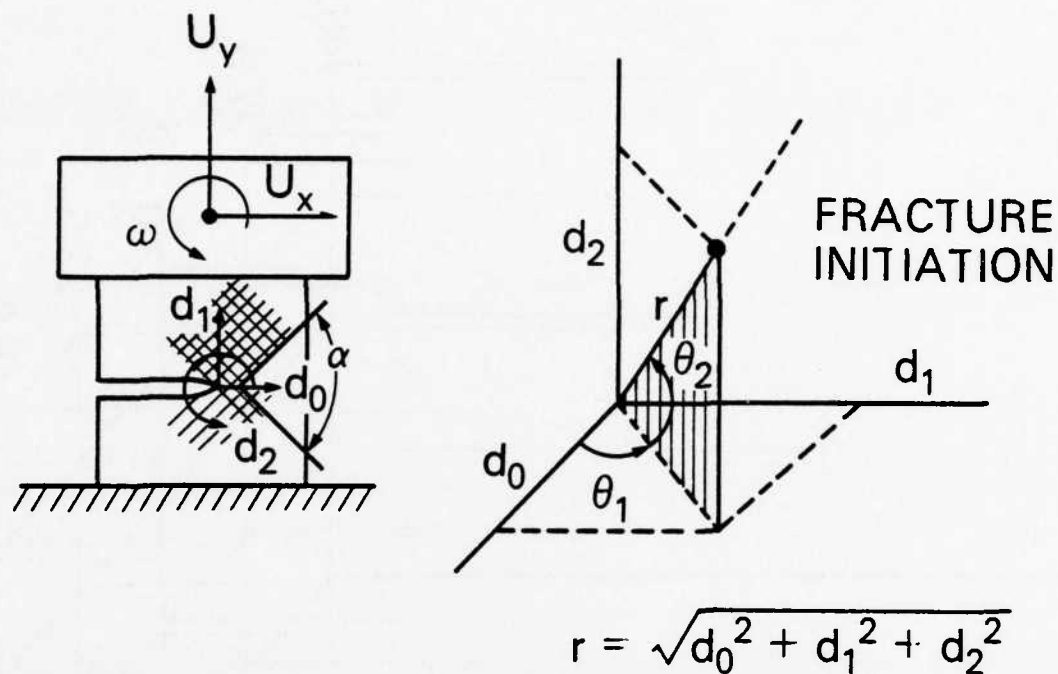


Figure 5 Failure surfaces for Thornel 300/5208 composite for several angles of lay-up (α) in one octant of load space

T300/5208 (60°)

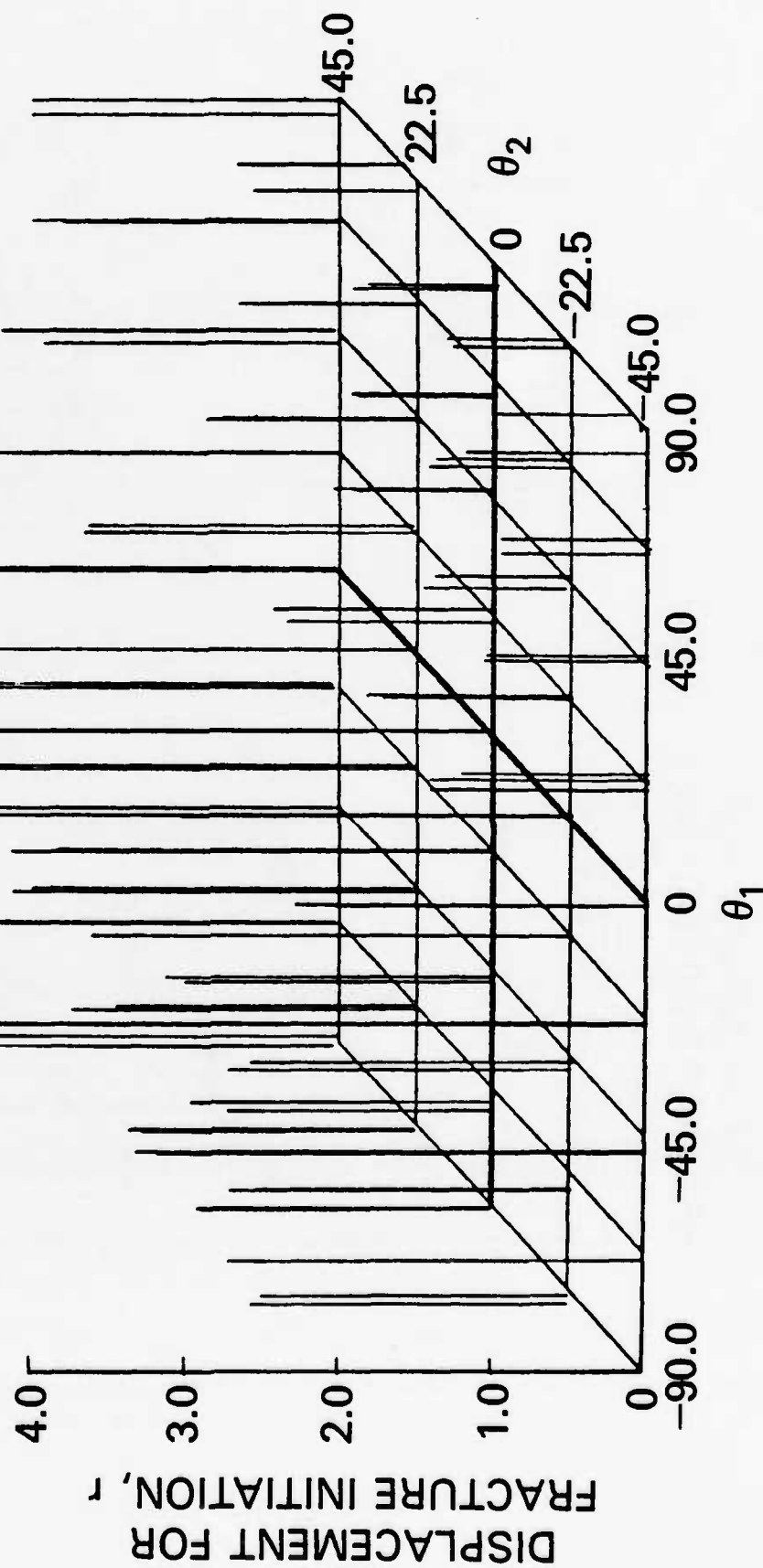


Figure 6 Typical plot of critical displacement data for four octants of load space

T300/5208 (60°)

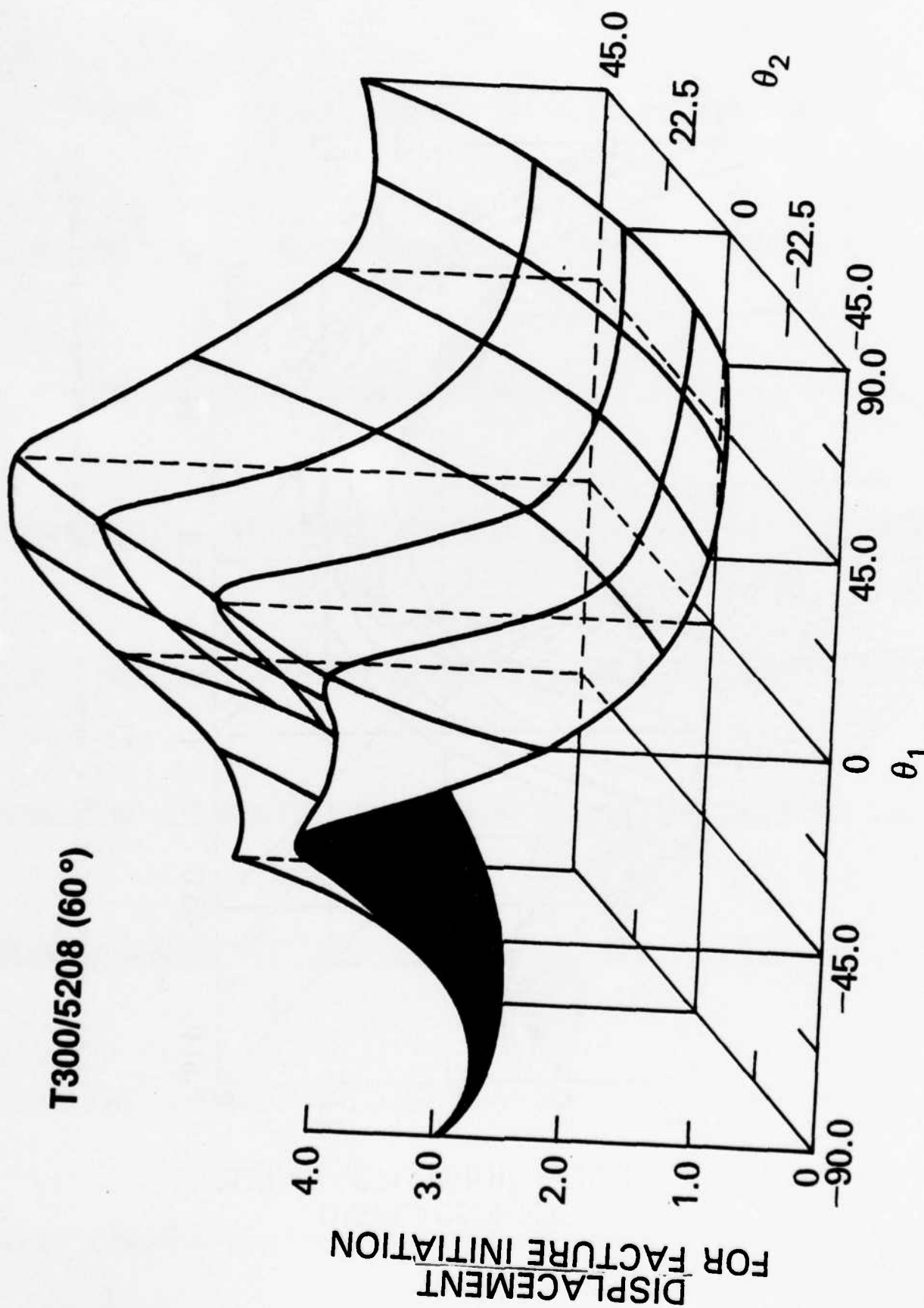


Figure 7 Failure surface for composite based on critical displacement

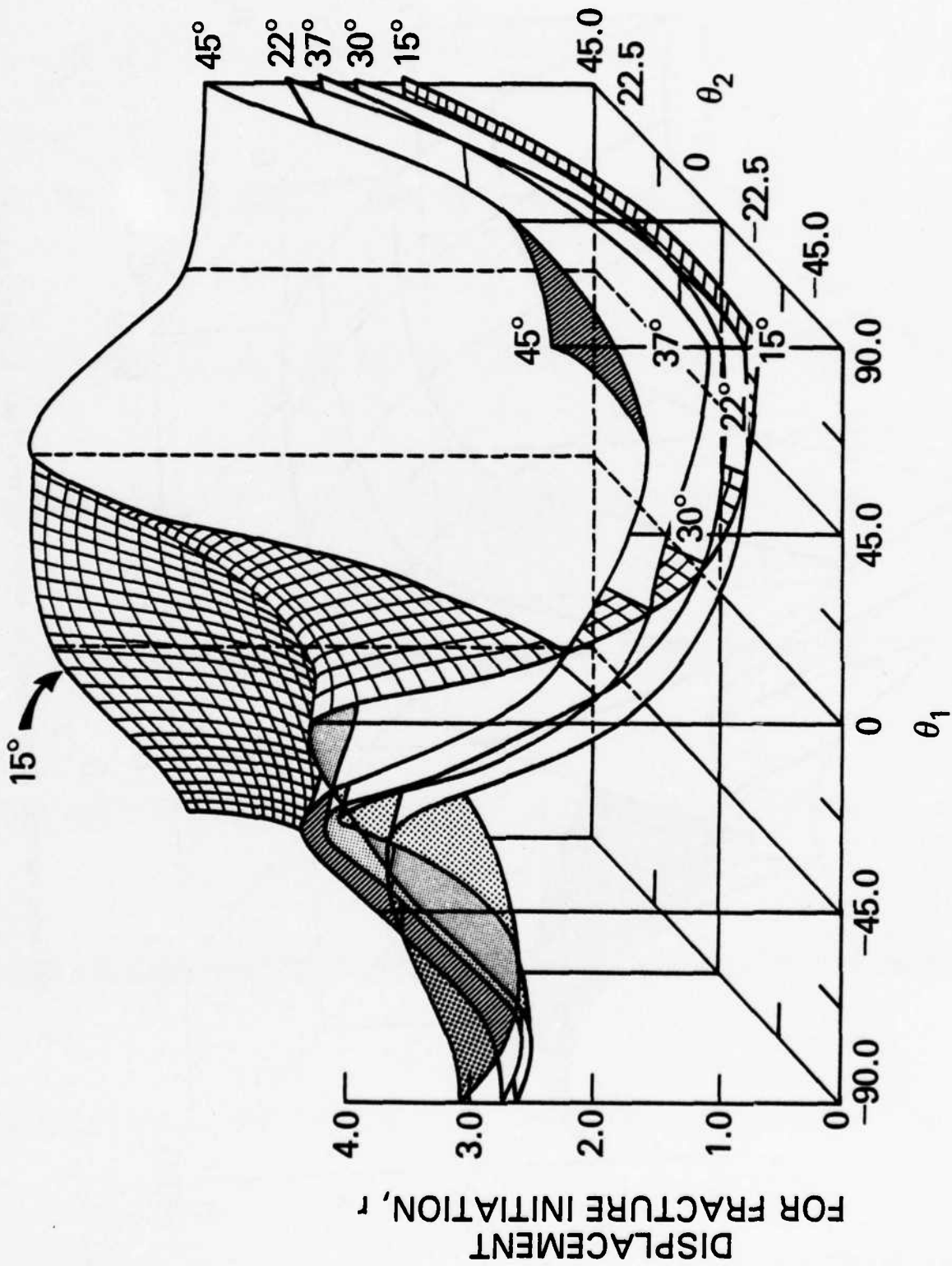


Figure 8 Series of failure surfaces for different reinforcement included angles

T300/5208 (60°)

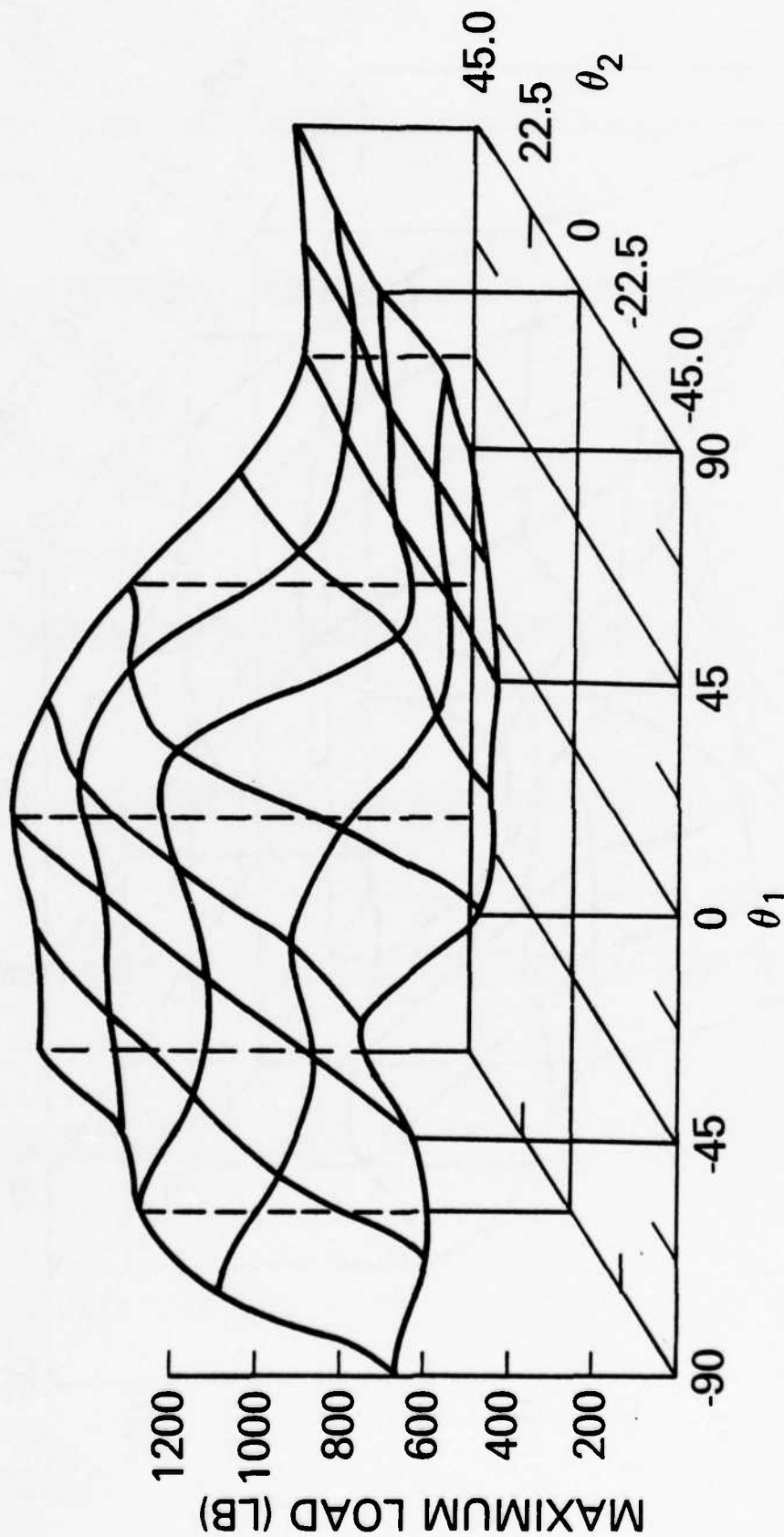


Figure 9 Failure surface for composite based on maximum load

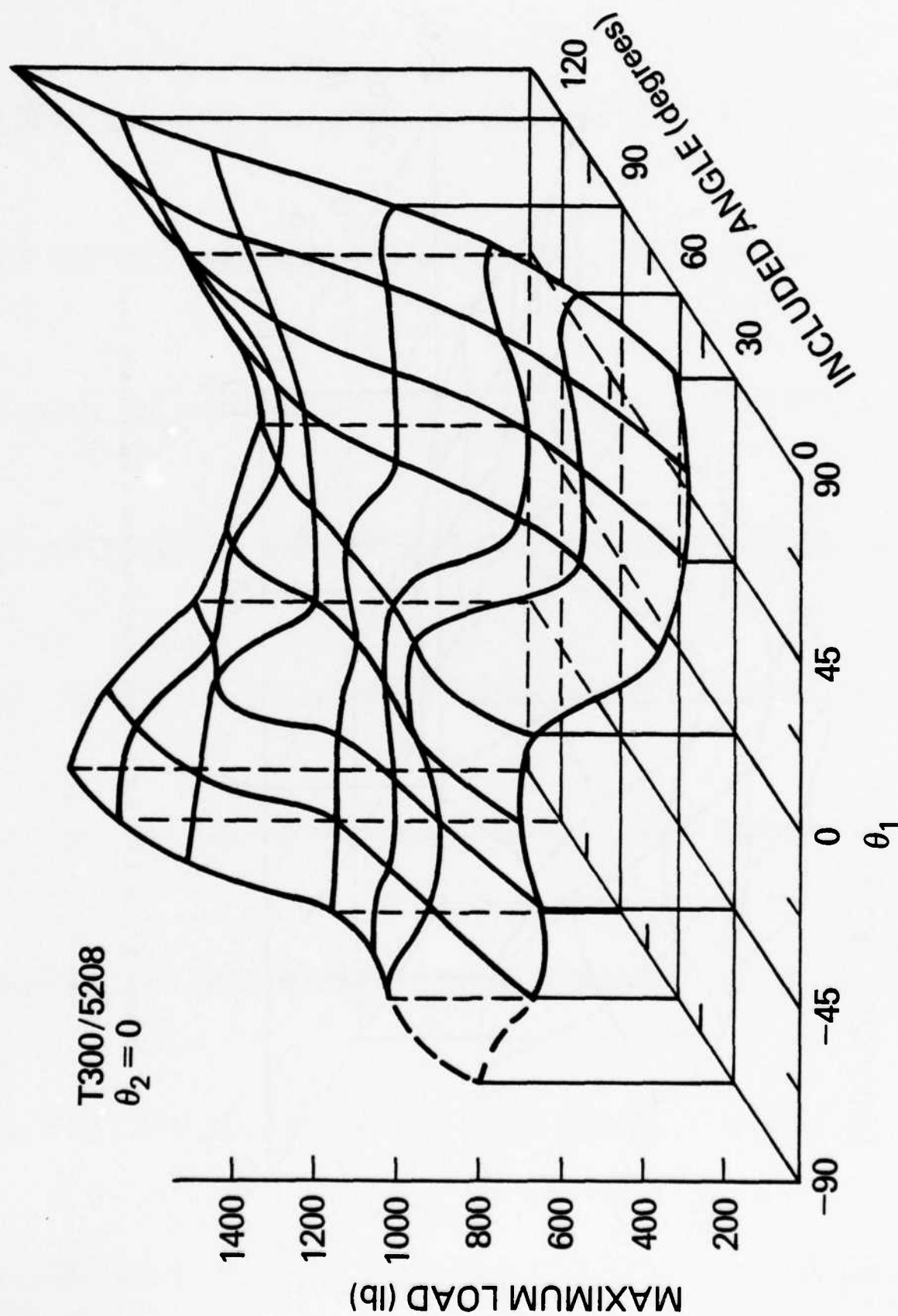


Figure 10 Failure surface for T300/5208 at room temperature for different reinforcement included angles, $\theta_2 = 0$

T300/5208 (H1)
 $\theta_2 = 0$

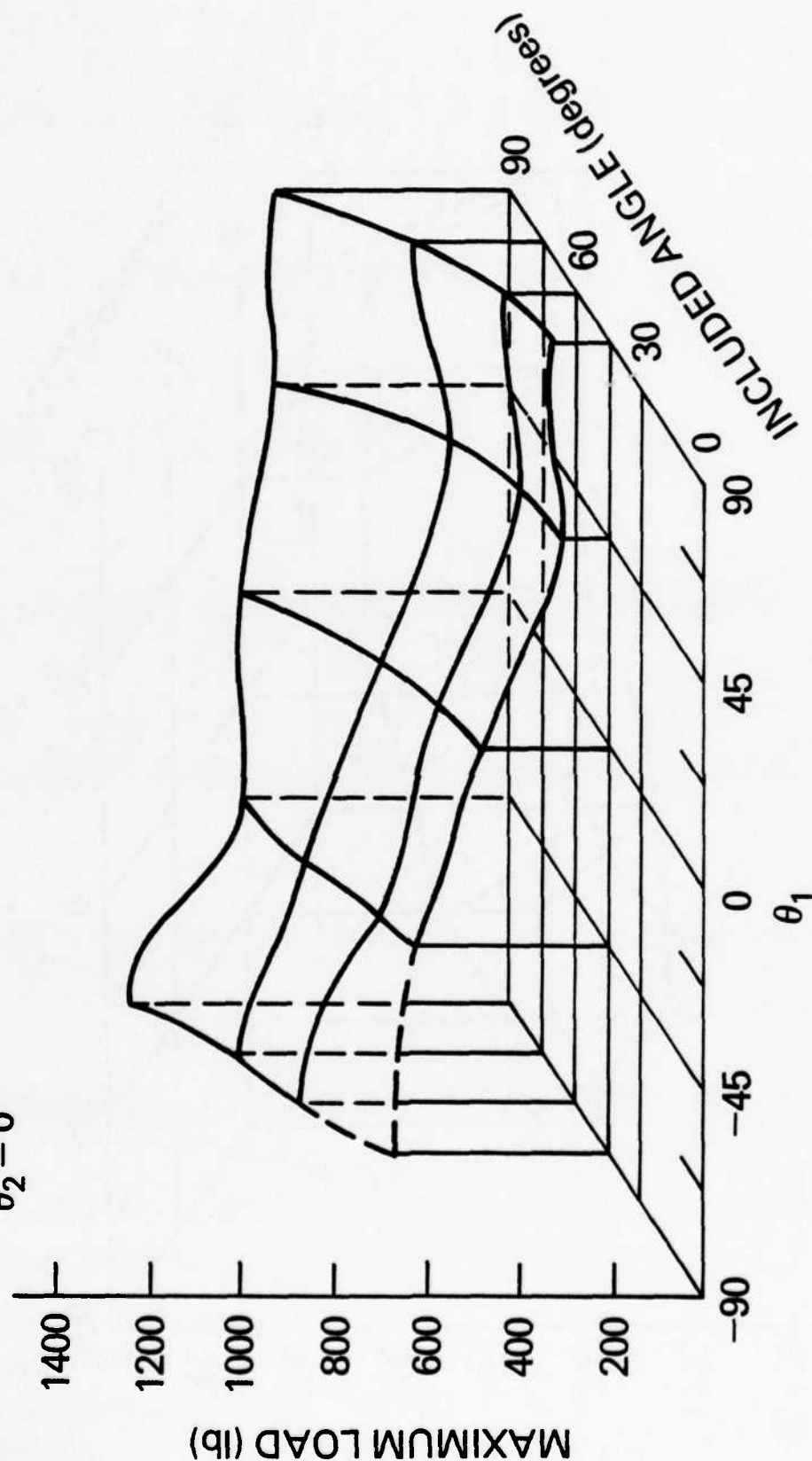


Figure 11 Failure surface for T300/5208 at 450°F (232°C) for different re-inforcement included angles, $\theta_2 = 0$

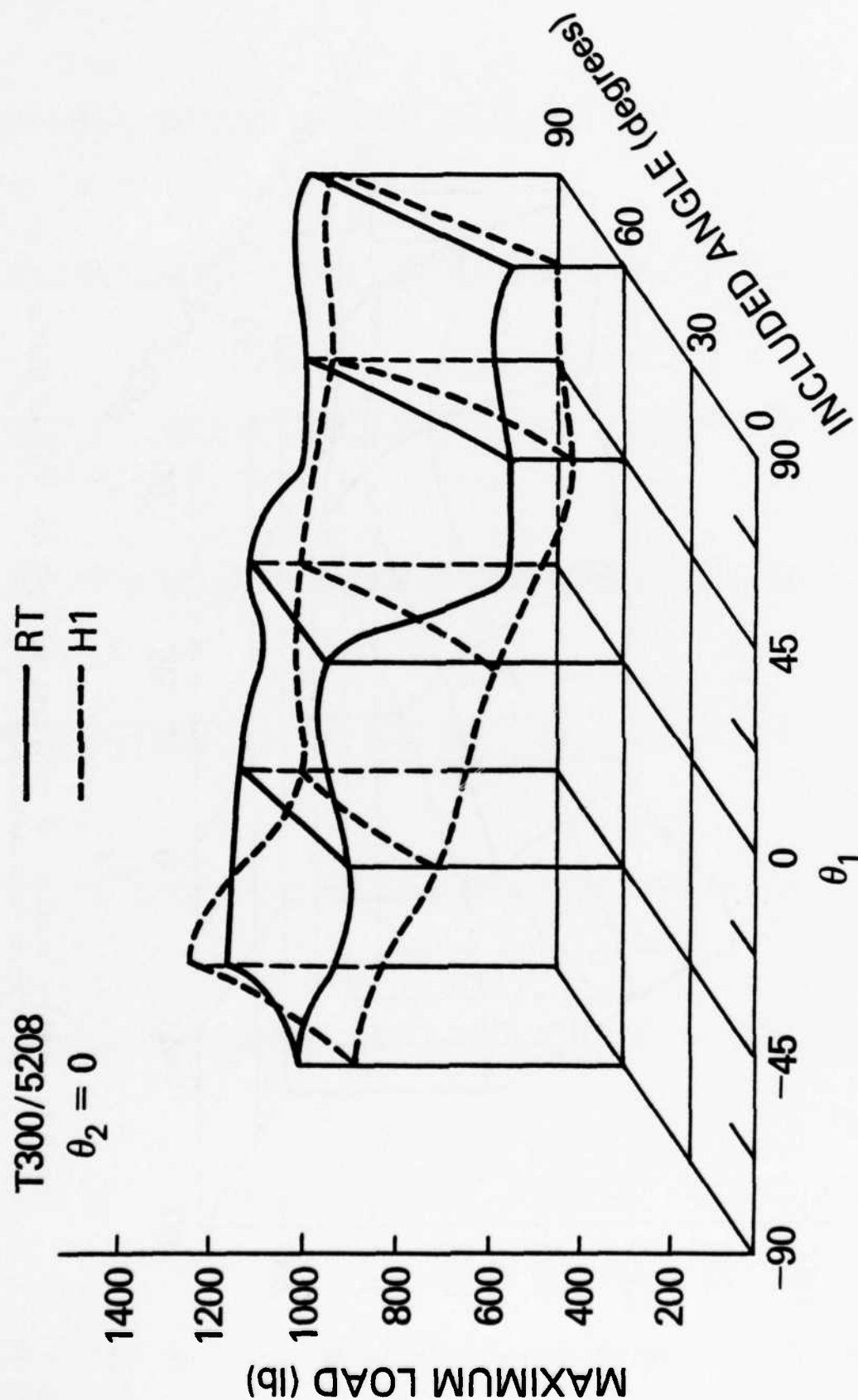


Figure 12 Comparison of room temperature (RT) and 450°F (232°C) (H1) data for T300/5208

T300/5208 (H24)
 $\theta_2 = 0$

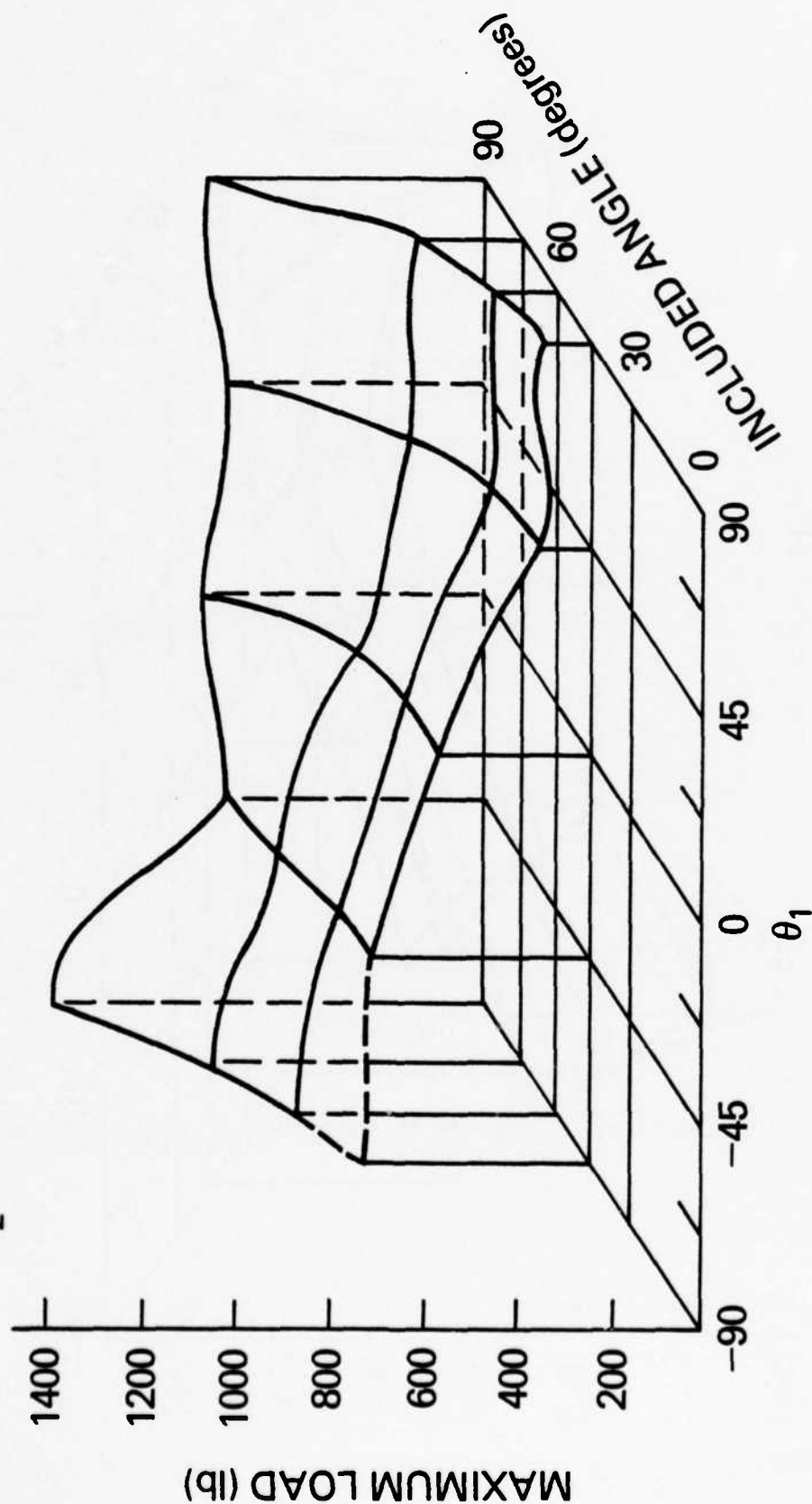


Figure 13 Failure surface for T300/5208 at 450°F (232°C) after heating for 24 hours

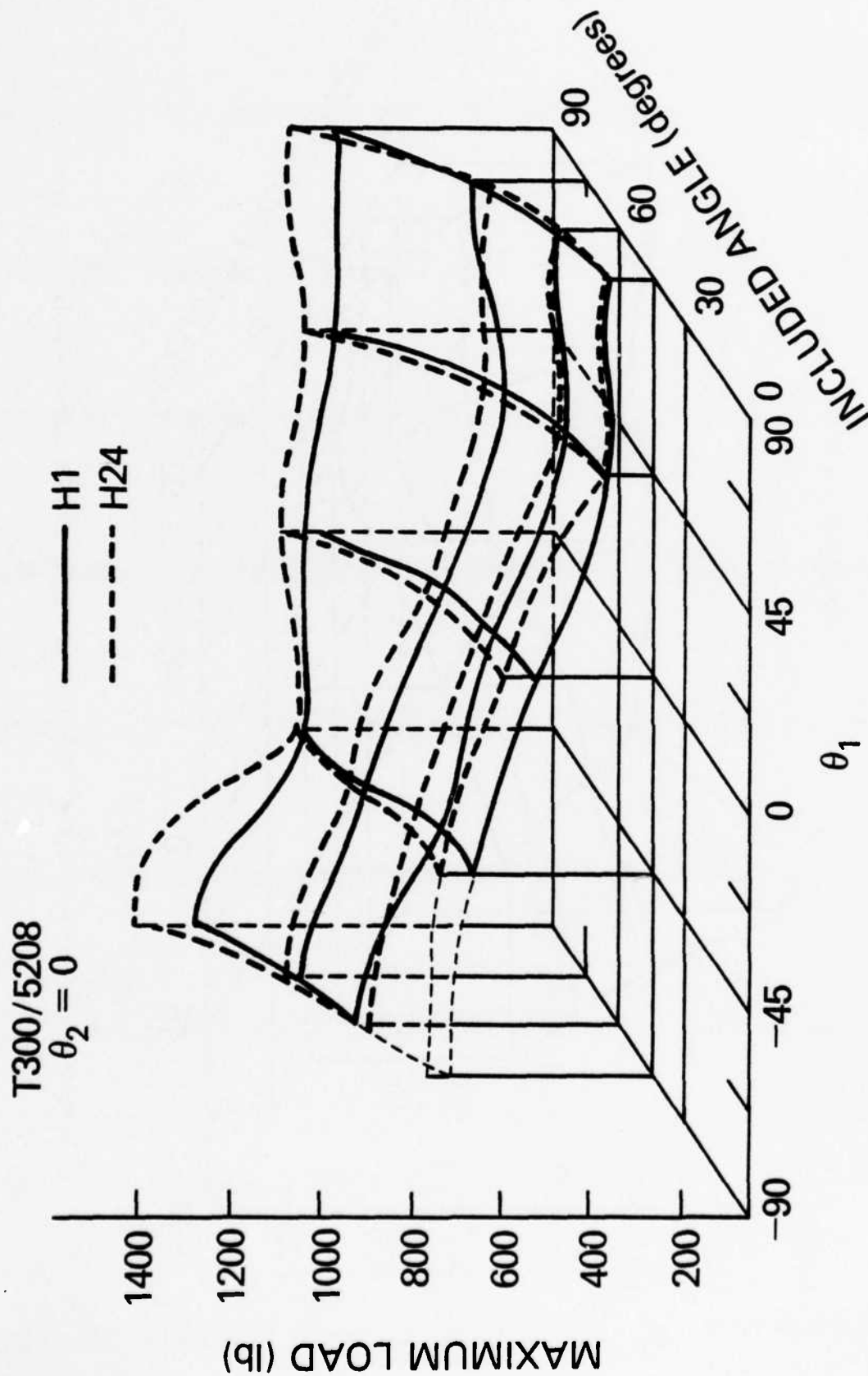


Figure 14 Comparison of failure surfaces of T300/5208 at 450°F (232°C); H1, after heating 1 hour; H24, after heating 24 hours

T300/F178
 $\theta_2 = 0$

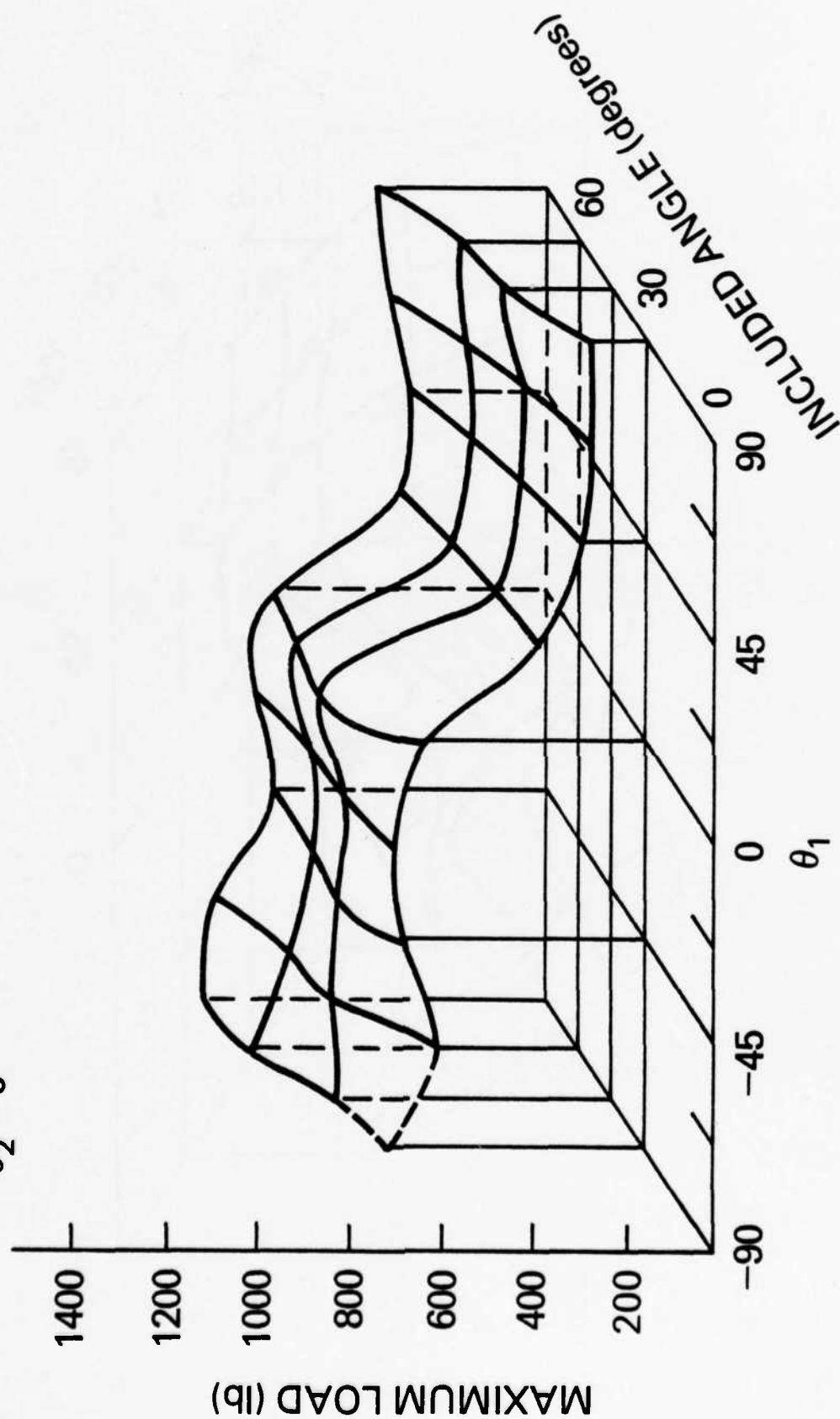


Figure 15 Failure surface for T300/F178 at room temperature for different reinforcement included angles, $\theta_2 = 0$

T300/F178 (H1)
 $\theta_2 = 0$

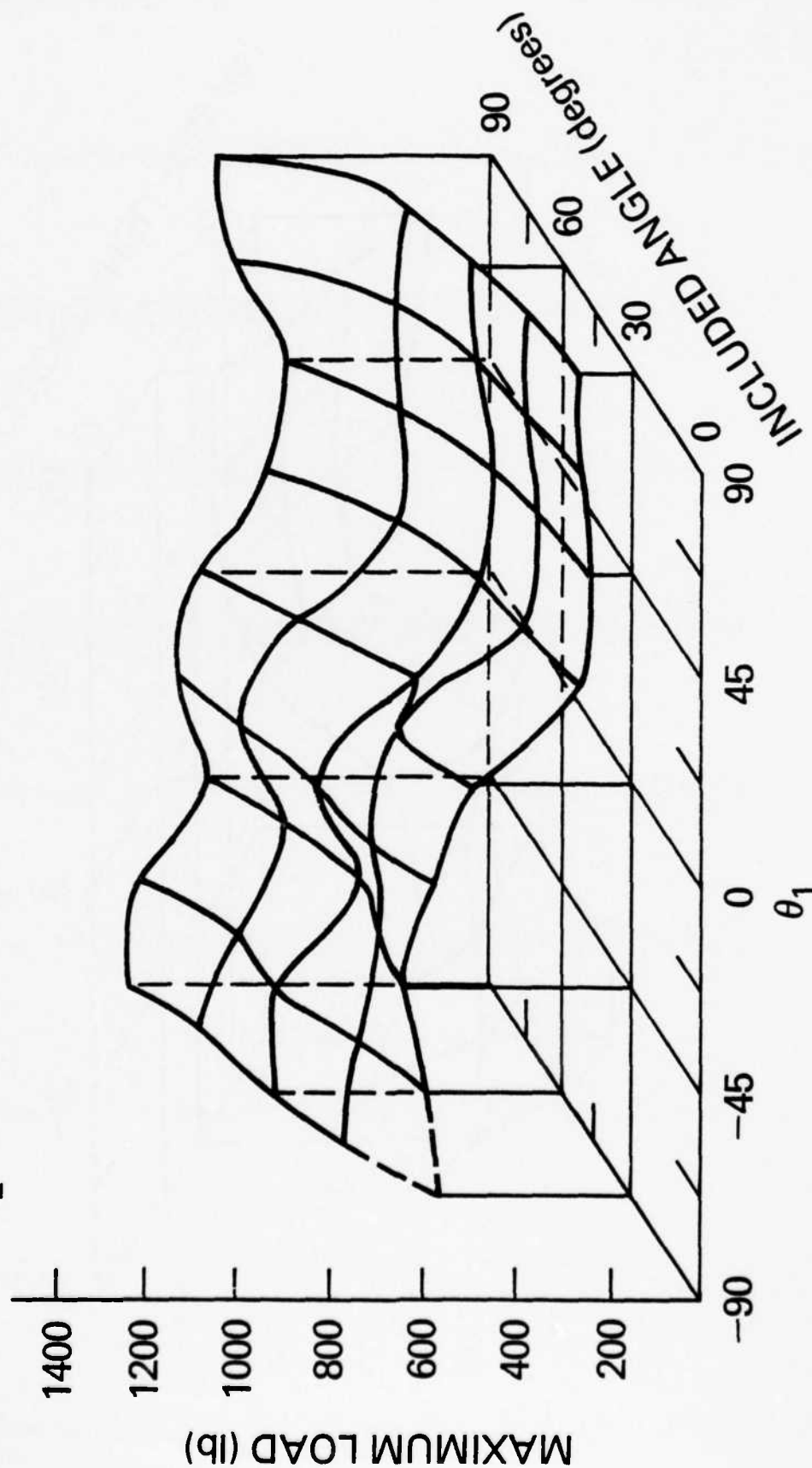


Figure 16 Failure surface for T300/F178 at 450°F (232°C) for different re-inforcement included angles, $\theta_2 = 0$

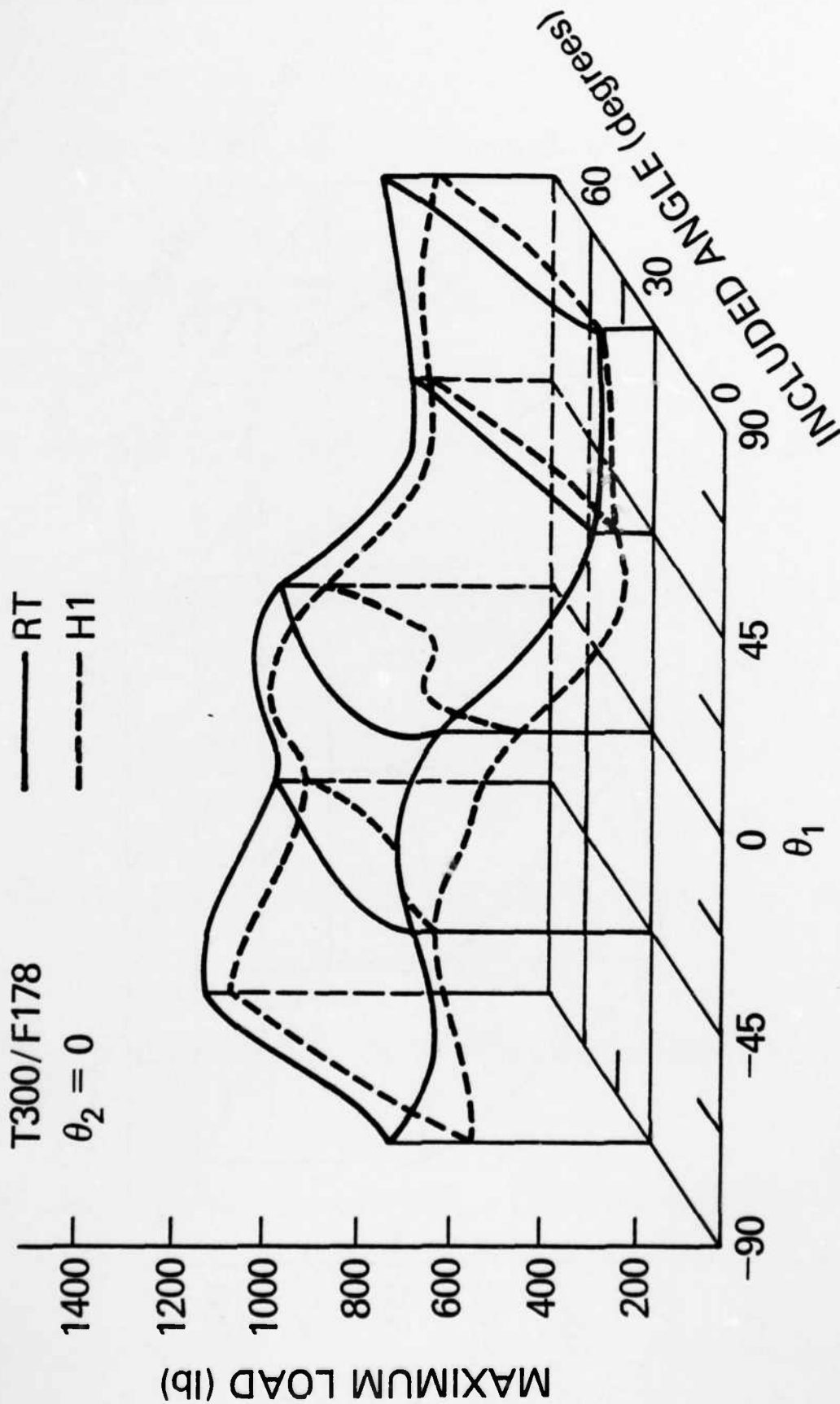


Figure 17 Comparison of room temperature (RT) and 450°F (232°C) (H1) failure surfaces for T300/F178

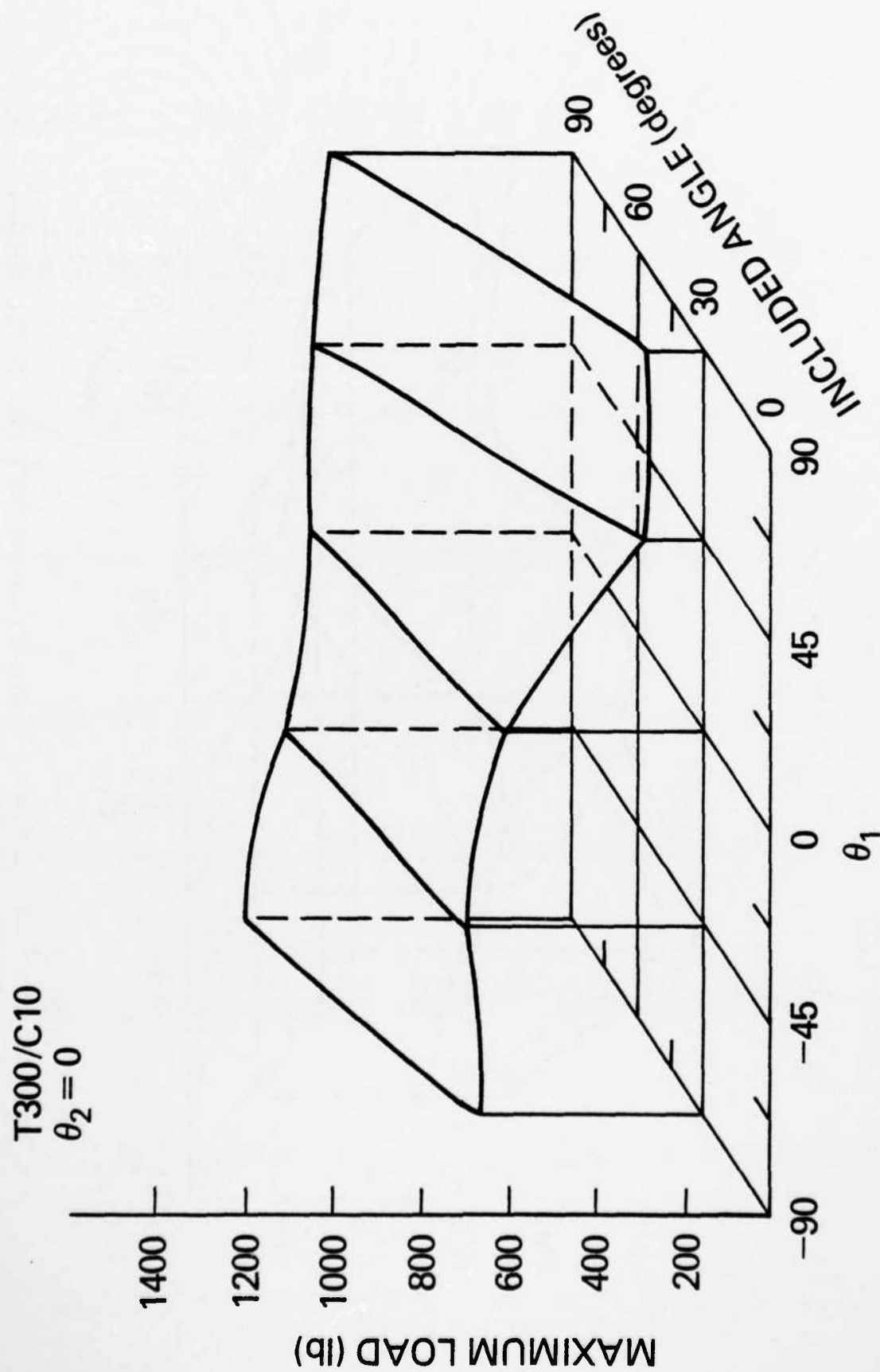


Figure 18 Failure surface for T300/C10 at room temperature for different reinforcement included angles, $\theta_2 = 0$

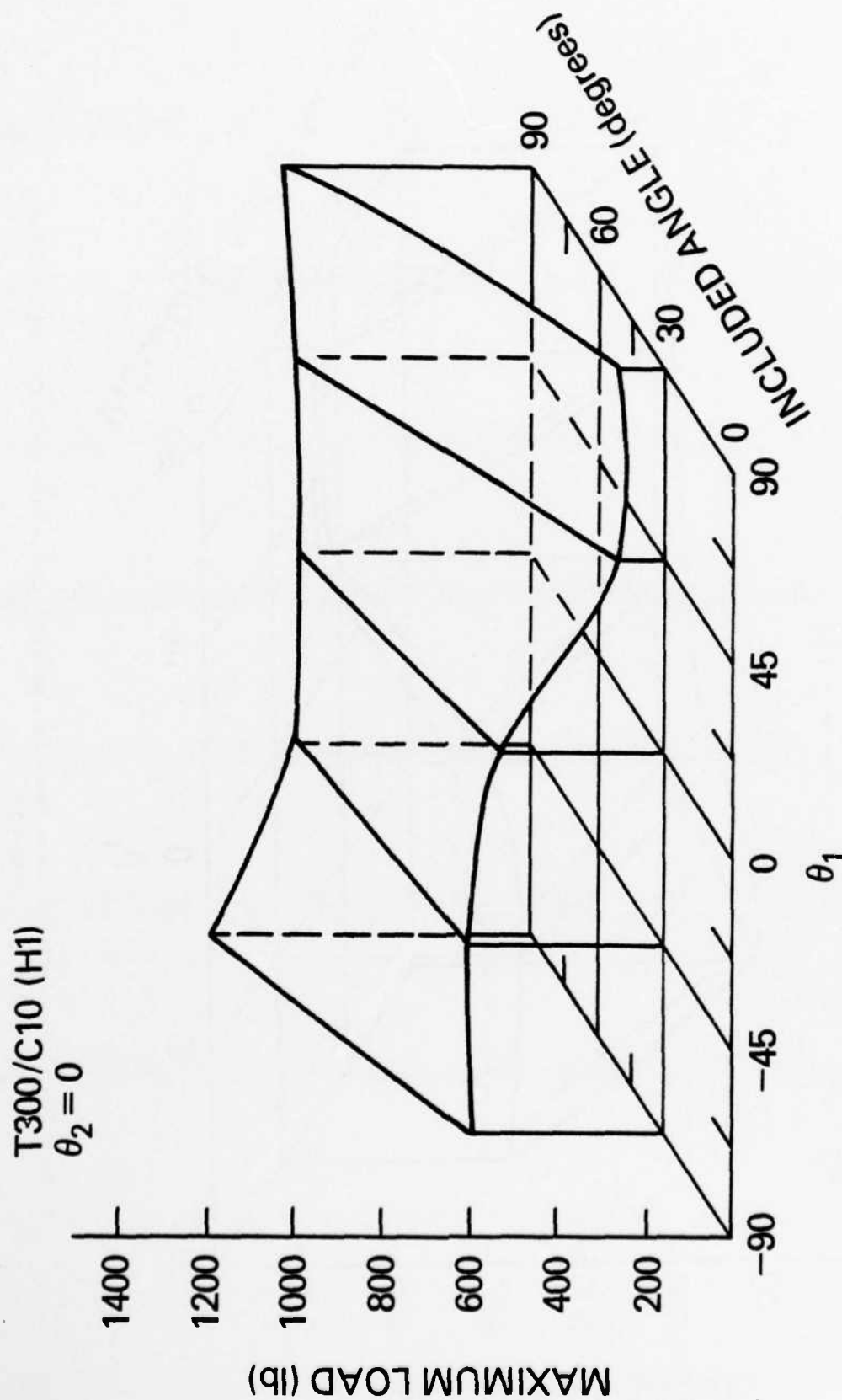


Figure 19 Failure surface for T300/C10 at 450° (232°C) for different reinforcement included angles, $\theta_2 = 0$

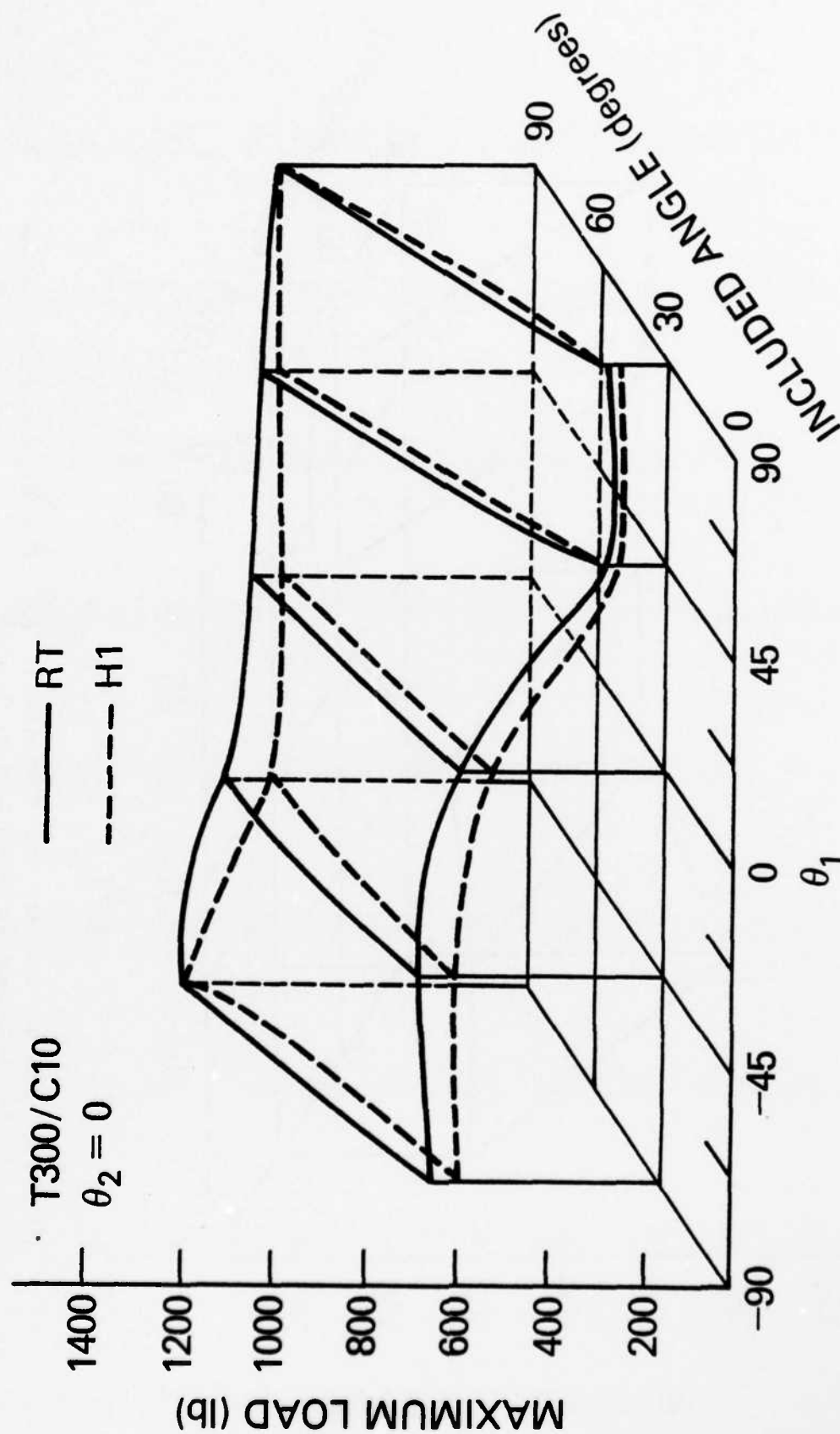


Figure 20 Comparison of room temperature (RT) and 450°F (232°C) (H1) failure surfaces for T300/C10

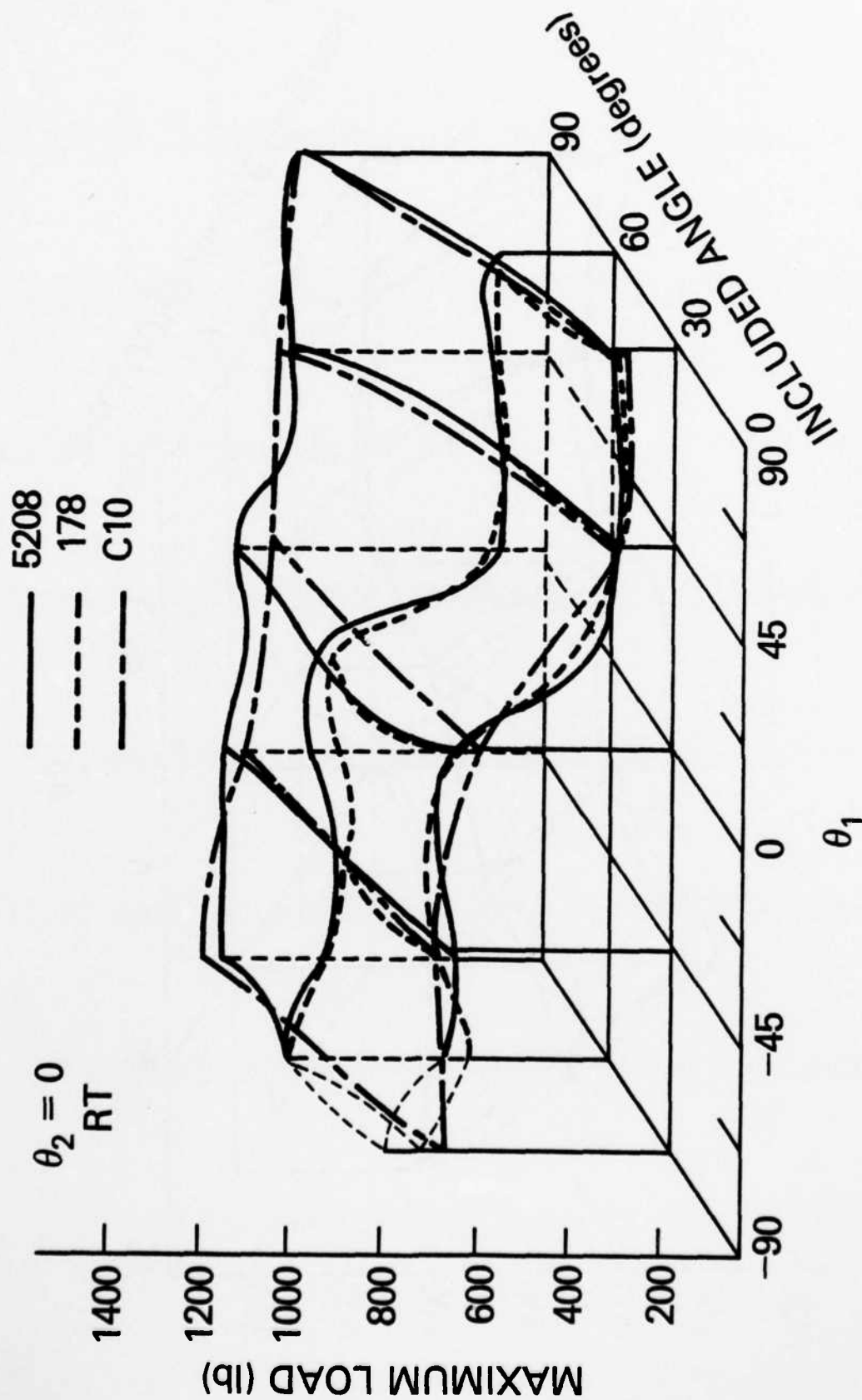


Figure 21 Comparison of room temperature failure surfaces for T300/5208, T300/F178, and T300/C10

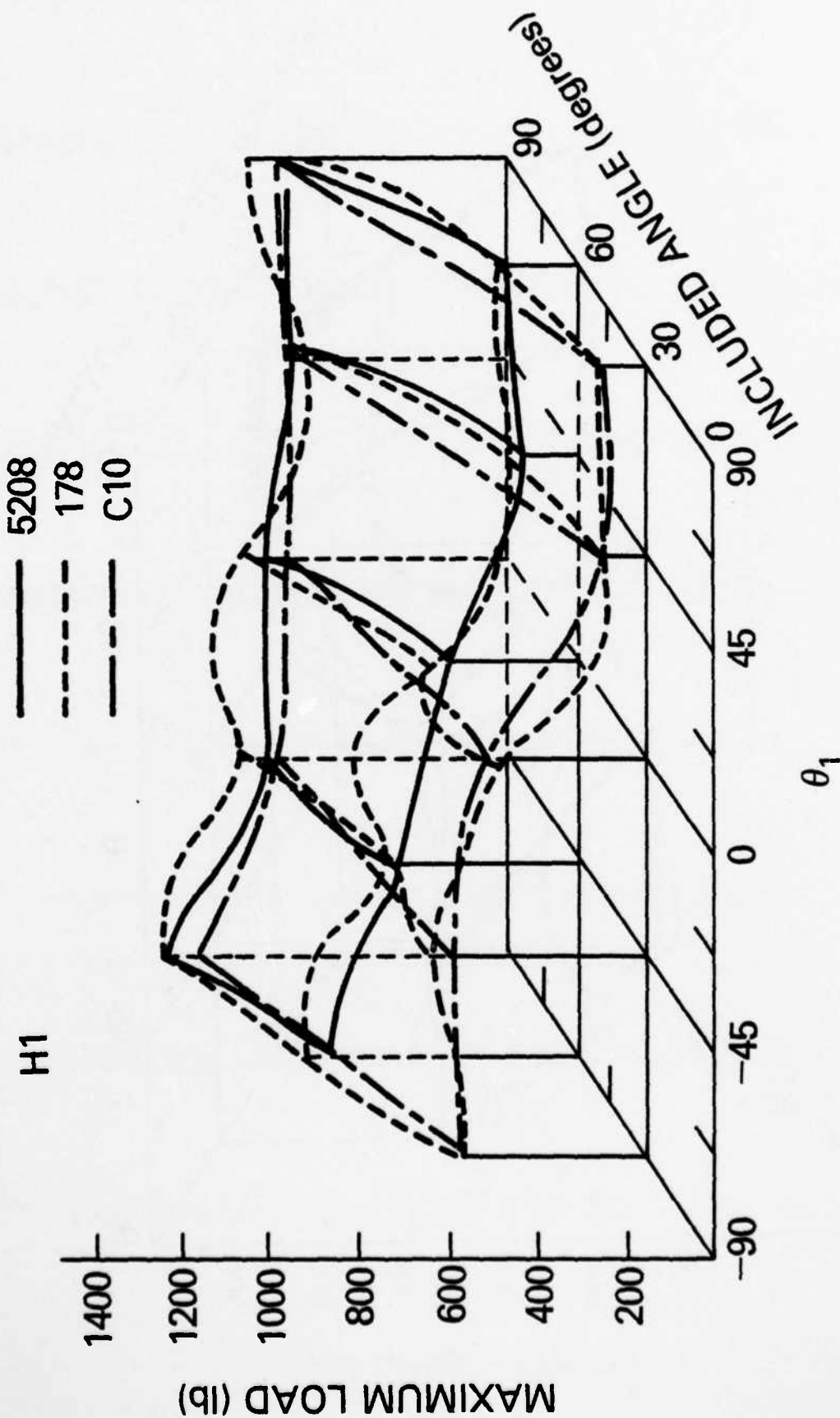


Figure 22 Comparison of 450°F (232°C) failure surfaces for T300/5208, T300/F178, and T300/C10

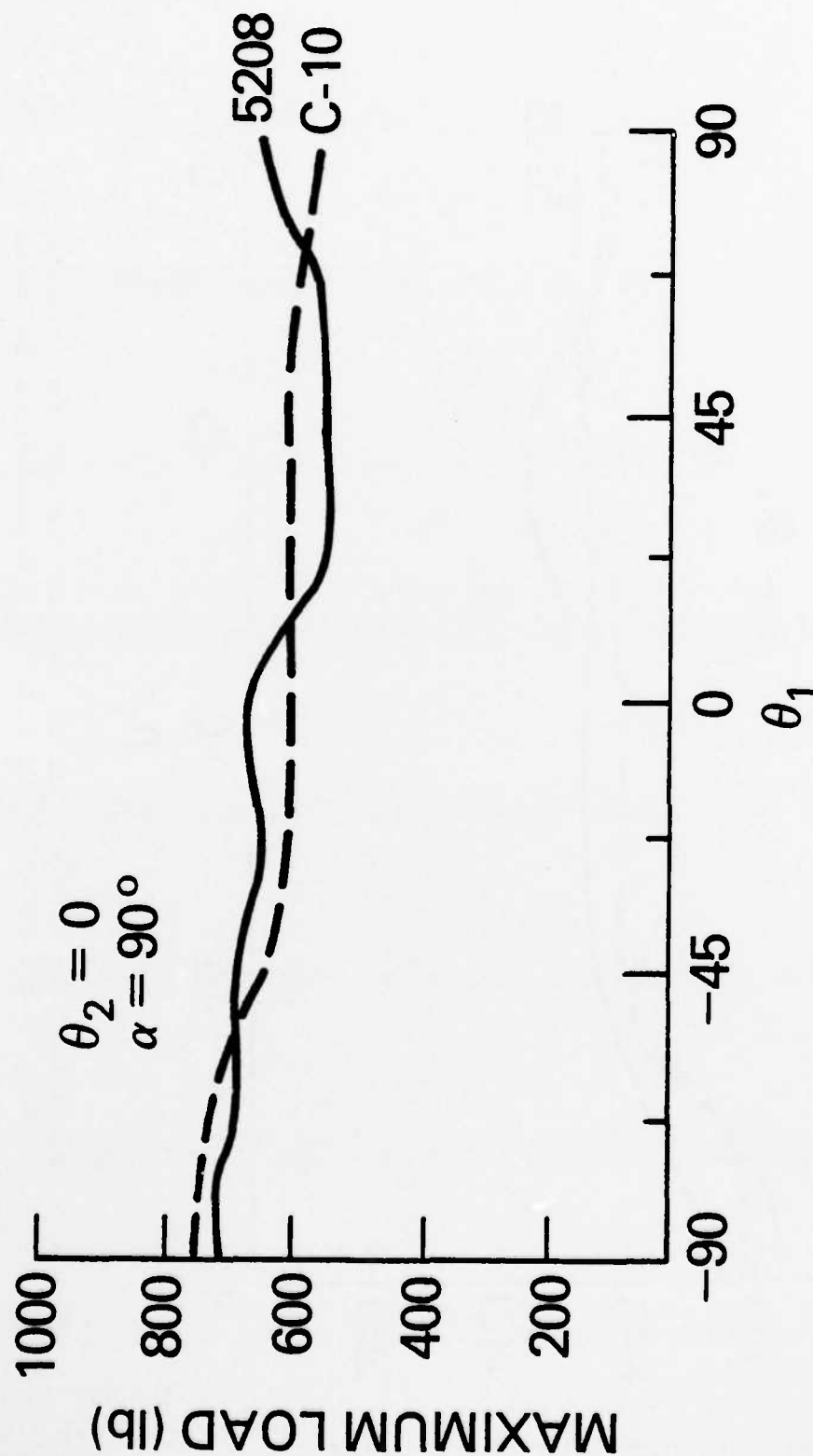


Figure 23 Comparison of room temperature failure curves for T300/5208 and T300/C10, $\theta_2 = 0$, reinforcement included angle $\approx 90^\circ$

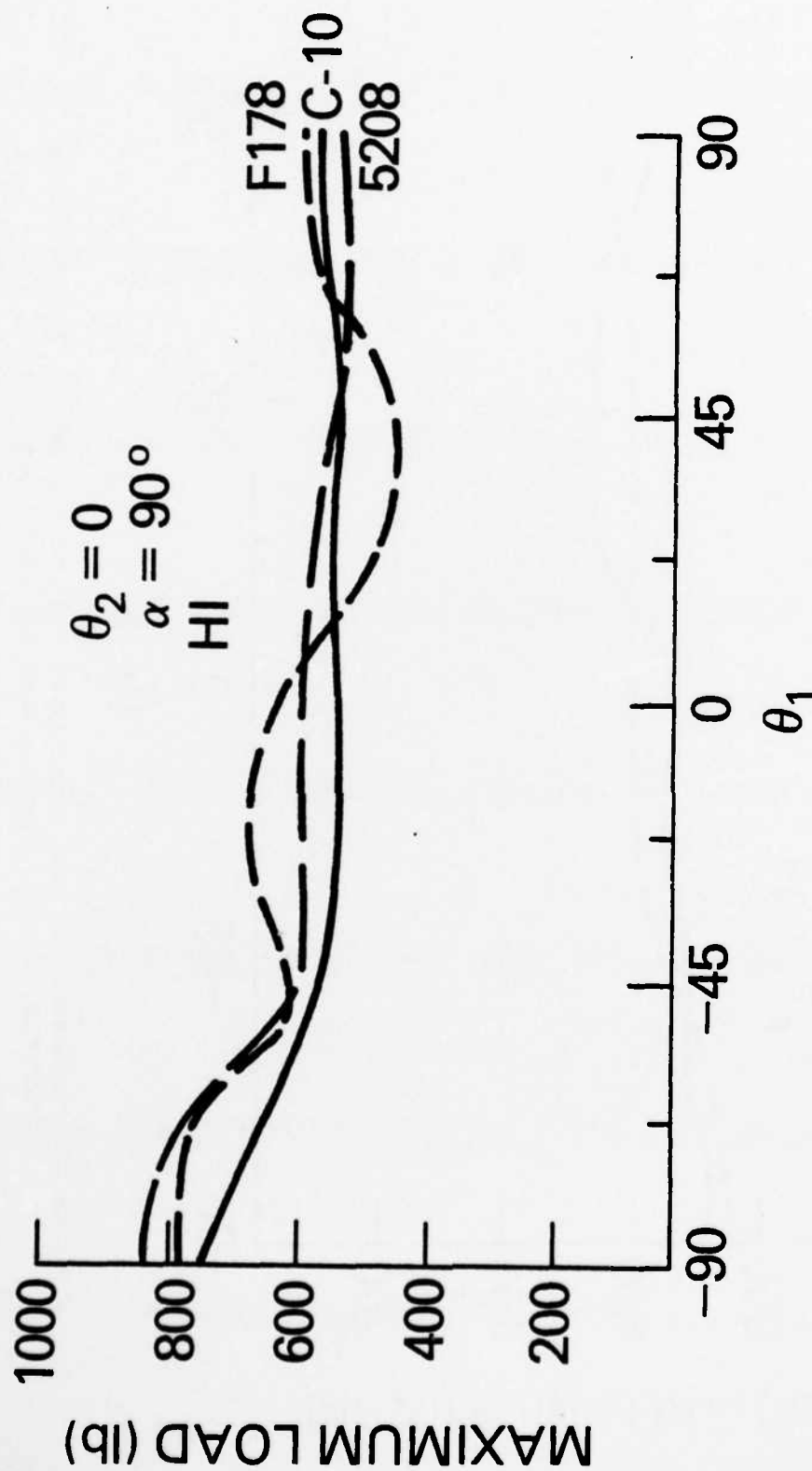


Figure 24 Comparison of 450°F (232°C) failure curves for T300/5208, T300/F178, and T300/C10, $\theta_2 = 0$, reinforcement included angle = 90°

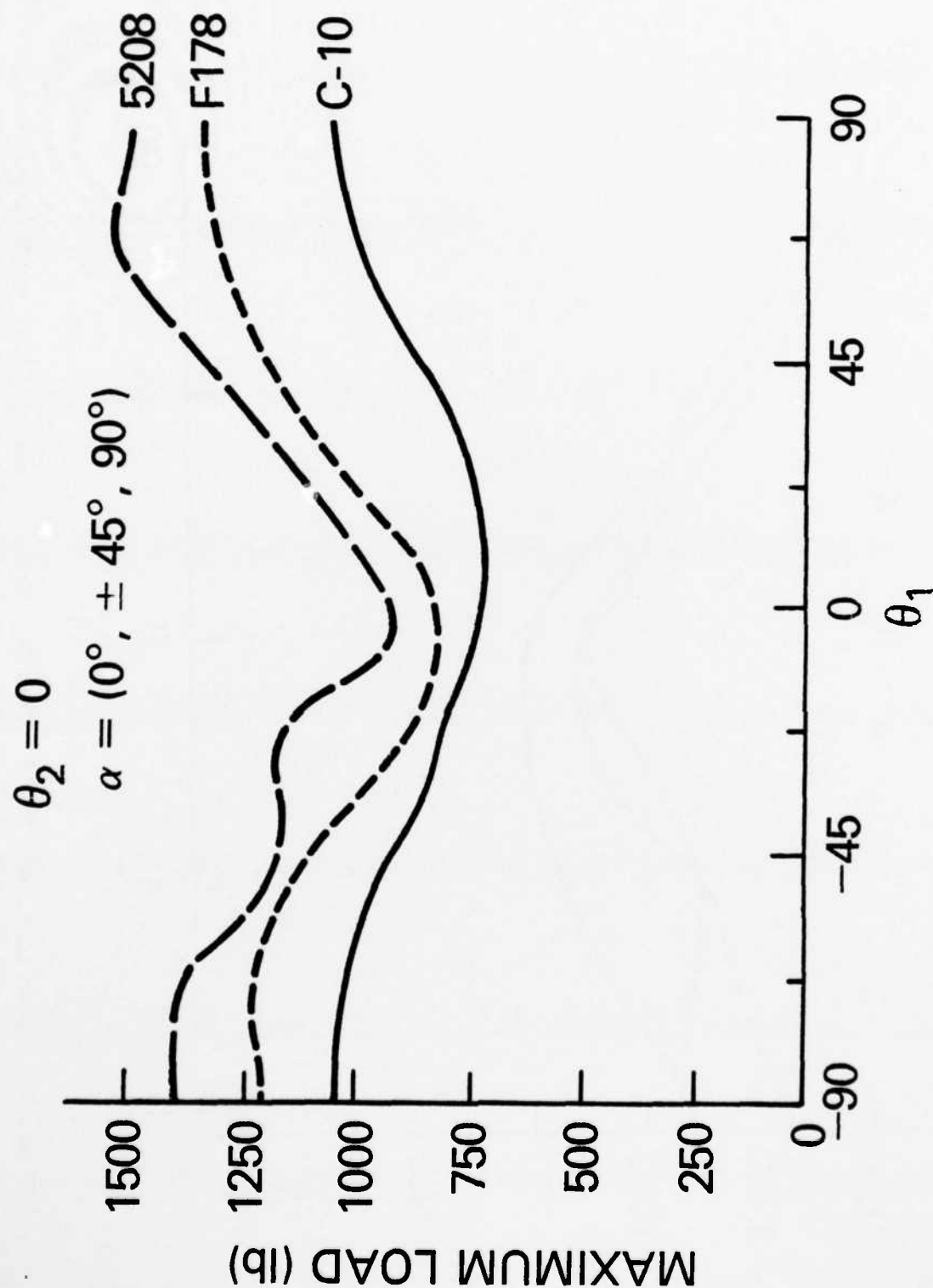


Figure 25 Comparison of room temperature failure curves for T300/5208, T300/F178, and T300/C10, $\theta_2 = 0$, reinforcement angle = $(0^\circ, \pm 45^\circ, 90^\circ)$

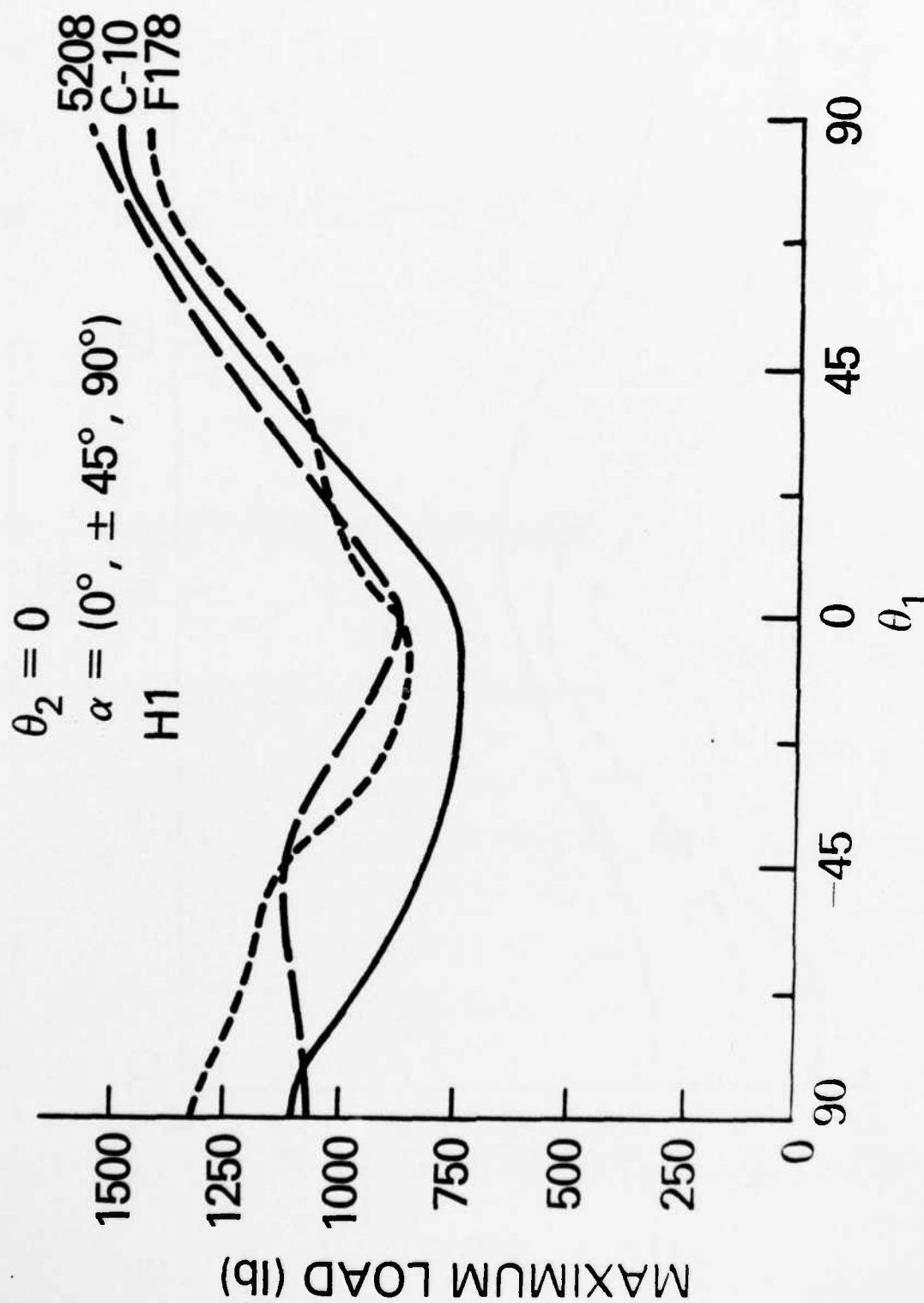


Figure 26 Comparison of 450°F (232°C) failure curves for T300/5208, T300/F178, and T300/C10, $\theta_2 = 0$, reinforcement angles = $(0^\circ, \pm 45^\circ, 90^\circ)$

RADIATION CURING STUDIES CONDUCTED AS FOLLOW-ON TO THE V/STOL PROGRAM INITIATIVE

F. J. Campbell, L. M. Johnson and J. S. Burr
Radiation-Matter Interactions Branch
Condensed Matter and Radiation Sciences Division

Introduction

Two of the studies on radiation cured adhesives that were initiated during the V/STOL Program were expanded in a follow-on program in the Radiation Sciences Subelement, Task Area on Radiation Applications. This program is providing more detailed thermal characterization of cured materials and greater insight on processing variables which could be applied to further improve material properties. One study has utilized a dynamic thermal analysis method for characterizing and defining the high temperature limits of cured adhesive and composite polymer formulations. The other study has illustrated how temperature control during the irradiation process can affect the fracture toughness of the cured adhesive material.

Characterization of Adhesives by Dynamic Mechanical Thermal Analysis

The relative temperature stabilities of three adhesive formulations were presented in an early V/STOL report (1). Each adhesive was prepared by the addition of a vinyl-reactive monomer to the base resin, Epocryl 12, a commercial acrylic-modified epoxy. The monomers, listed in increasing number of functional vinyl groups per molecule, are: styrene (STY), diallyl phthalate (DAP) and triallyl cyanurate (TAC). The formulations were applied as adhesives in aluminum single lap-shear strength specimens which were cured by irradiating with a high energy electron beam. The specimens were pulled at a series of elevated temperatures to obtain data of strength vs. temperature at discrete points of 115°, 150°, 200°, and 260°. Curves plotted through these points gave a visual comparison of the temperature stabilities of these adhesives (1).

Using a DuPont Dynamic Mechanical Analyzer (DMA), it is possible to obtain a continuous scan of Young's modulus vs. temperature for the radiation cured resins. The instrument utilizes a thin rectangular specimen for the analysis, hence specimens can be cut from blocks or from molded sheets. In this case the specimens were molded sheets of resin with graphite supporting fibers imbedded in the resin, simulating a graphite/polyester composite. The same three formulations used in the lap-shear strength study were prepared as composites with a woven cloth of T300-3000 graphite fiber and cured with the same dose of electron-beam radiation, 100 kilograys. Modulus vs. temperature scans were performed over the temperature range of -100° to +400°C by the DMA method. The three scans are plotted on the same graph of Young's modulus vs. temperature in Figure 1. Superimposing

the lap-shear strength data over the Young's modulus curves on the same temperature scale shows that the same order of temperature stability was obtained by the DMA method on composite specimens as was determined on the adhesive specimens. That is, in order of temperature stability, the monomers to be used for maximum temperature service are: DVB, TAC and STY. In addition, the DMA method of analysis provides more information since it shows the temperature at which the cured adhesive or composite material begins to lose strength and, thus, gives an actual value for the limiting service temperature.

Effect of Internal Temperature Reached During Irradiation on Fracture Toughness of a Commercial Adhesive

In the other follow-on study initiated during the V/STOL Program, the fracture toughness of an electron-beam cured modified polyimide adhesive was determined as a function of the internal temperature reached during the radiation cure. This material, Loctite LO-559, is a formulation containing a bismalimide, a urethane methacrylate, an inert filler and a peroxide (2). It is an experimental adhesive product intended for heat curing in normal adhesive-bonding applications. The initial study demonstrated that electron-beam curing to the optimum dose would produce higher values of lap-shear strength and fracture energy than could be obtained by heat curing at the recommended cycle of 60 min. at 150°C (3).

The temperature rise occurring in a material or a system of materials during irradiation is a result of the transformation of a major portion of the absorbed radiation energy into thermal energy within the material. The actual temperature reached is then a function of the integral absorbed dose, the dose-rate, specific heat of the irradiated materials, and the thermo-physical characteristics of the materials and the surrounding media. Under completely adiabatic conditions the temperature rise in a uniform material is expressed as:

$$\Delta T = \frac{0.24D}{c}$$

where T is in degrees Celsius, D is in kilograys (kGy), and c is the specific heat.

Thus, a uniformly absorbed dose of 10 kGy (1 Mrad) would raise the temperature of water by 2.4°C, or of polyethylene (c = 0.5) by 4.8°C. The internal temperature rise, ΔT , of other materials would likewise be in proportion to their specific heats. Introduction of mineral-type fillers would somewhat increase the temperature rise of a compound due to the relatively low values of specific heat of these materials. Additional specimen heating may also occur as a result of the chemical crosslinking reaction if it is an exothermic process. Application of cooling methods and surface interface characteristics controlling the heat dissipation from the specimen make the thermal balance calculations rather complex. Therefore, direct measurements of temperatures by a thermocouple implanted into a representative specimen are normally more accurate than can be determined by calculation.

During the irradiation of experimental specimens it was observed that each system reached an equilibrium temperature which was a function of the

dose-rate and the heat dissipation rate. In these experiments the specimen rested on a large aluminum block which removed heat by conduction, and a nearby blower forced air across the top to remove heat by convection. The fracture energy specimens were formed as plachets, 5-cm in diameter by approximately 0.4-cm thick, by pouring the fluid adhesive material into aluminum cylindrical bowls prior to curing. The electron-beam radiation cured specimens were machined into compact tension specimens for measurement of fracture energy by the method described by Bascom, et al. (4). Temperature during the cure was controlled on three different sets of specimens by varying the heat dissipation procedure to obtain a maximum temperature-during-cure of 38°C, 90° and 110°C. Data of fracture energy versus dose were then plotted (Figure 2) for each set of specimens (the mean of five specimens was used for each point). The one data point at zero dose was obtained by oven curing the specimens for 60 min. at 110°C.

These plots of isothermal cures show clearly that fracture energy decreased markedly for this material with increasing temperature reached during irradiation. Thus, keeping the material cooled to limit the temperature to 38°C during irradiation resulted in values of fracture energy in the range of 1120 J/m². When the temperature was increased to 110°C by removing the cooling air and warming the aluminum block, the fracture energy deteriorated to approximately 100 J/m². For this adhesive, at least, it appears advisable to apply cooling to the area of a bonded joint during the radiation curing to obtain the maximum strength characteristics.

Conclusions

These results demonstrate the progress that can be made by continuing research efforts in radiation-curing. It is a well-known maxim in materials development efforts that variables in both composition and processing must be studied in order to improve the final product. Of the three reactive diluents selected in this study for modifying a high molecular weight polymer, one has produced an adhesive with appreciably higher temperature stability as well as greater bond strength. In the other study of temperature effects on the radiation curing process of a particular adhesive, it was demonstrated that temperature control was necessary to develop maximum fracture toughness. Other materials may not be as sensitive to temperature, but the factor should be evaluated in future studies.

Future Work .

The on-going program will investigate other high temperature polymer materials having unsaturated terminal and pendent groups in the structure. These will be tailored in compositions with various reactive diluents and toughness modifiers to facilitate radiation processing procedures and improve fracture energy. Another study will soon begin which will investigate the feasibility of applying various radiation methods to modify surfaces of fillers, fibers and metals to enhance bonding interface characteristics of radiation cured adhesives and composites. The DMA and other thermal analysis methods will be more fully utilized to characterize the materials in these studies.

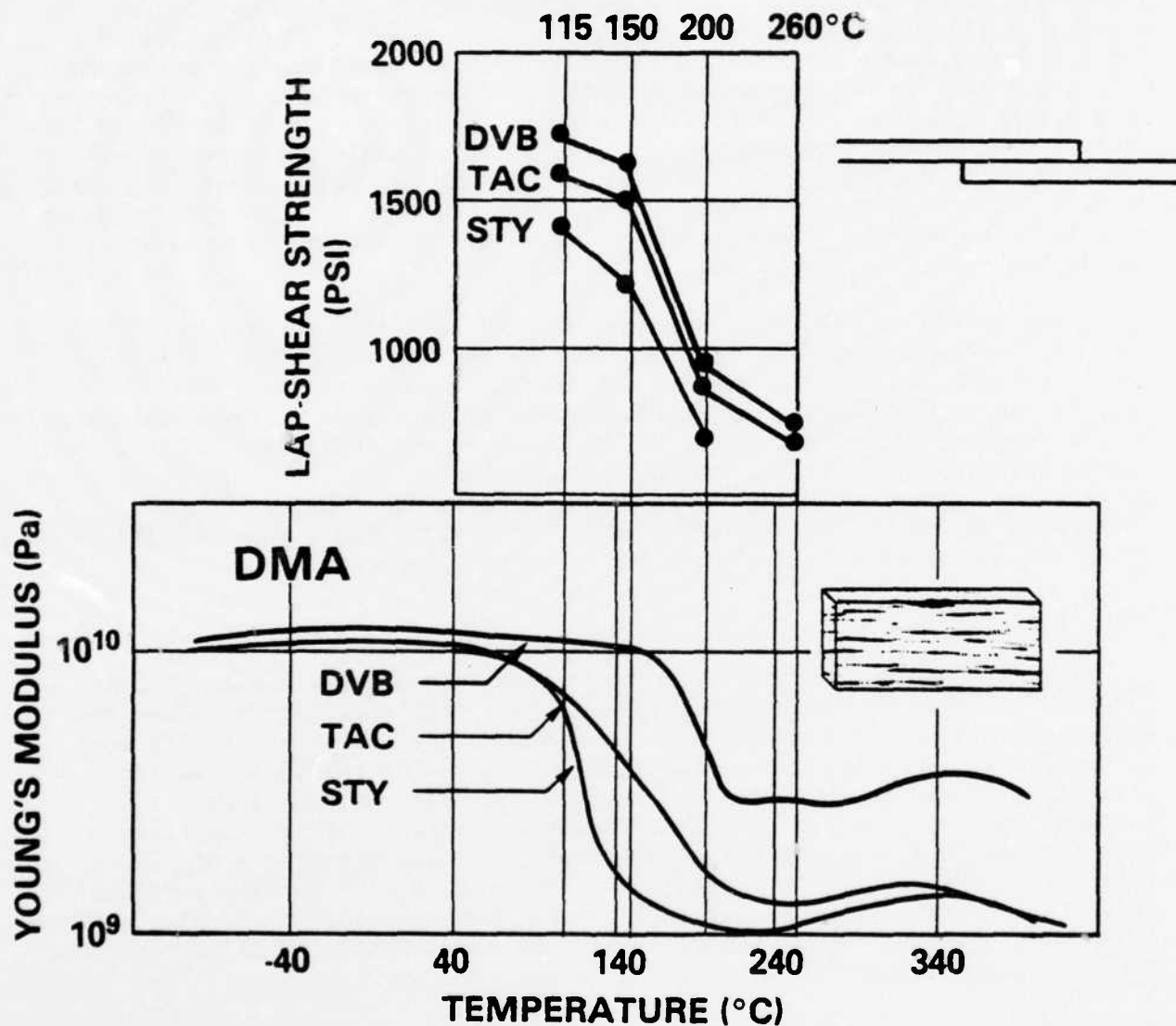


Fig. 1 - Correlation of temperature stability determinations by lap-shear strength and dynamic mechanical analysis (DMA) of electron-beam cured formulations of Epocryl-12/vinyl-reactive monomers.

AD-A139 168

HIGH PERFORMANCE COMPOSITES AND ADHESIVES FOR V/STOL
AIRCRAFT(U) NAVAL RESEARCH LAB WASHINGTON DC
C F PORANSKI 22 FEB 84 NRL-MR-5231

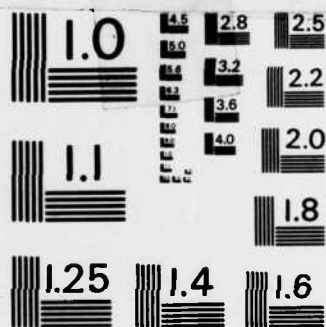
2/2

UNCLASSIFIED

F/G 11/4

NL





MICROCOPY RESOLUTION TEST CHART
NATIONAL BUREAU OF STANDARDS-1963-A

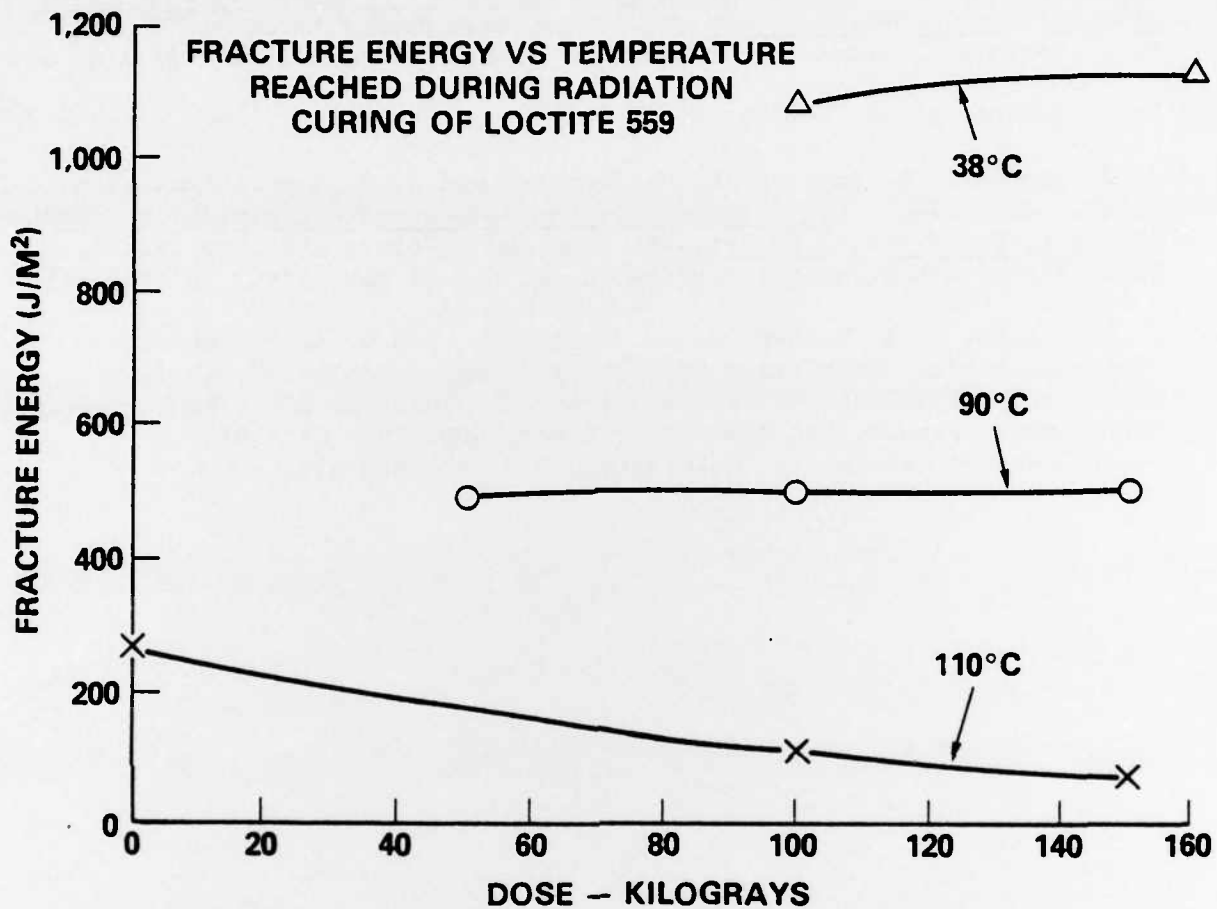


Fig. 2 - Fracture energy vs temperature reached during radiation curing of Loctite LO-559.

References

1. F. J. Campbell, W. Brenner, L. M. Johnson, and M. E. White, "Task D. Radiation Curing", High Performance Composites and Adhesives for V/STOL Aircraft, First Annual Report, NRL Memorandum Report 3433, pp. 55-77, Naval Research Laboratory, Washington, D. C., December 1976. AD/A035 928
2. Loctite Corporation, Newington, CT 06111.
3. F. J. Campbell, W. Brenner, L. M. Johnson, and J. S. Burr, "Radiation Curable Adhesives", High Performance Composites and Adhesives for V/STOL Aircraft, Third Annual Report, NRL Memorandum Report 4005, pp. 81-93, Naval Research Laboratory, Washington, D. C., 23 May 1979. AD/A069 611
4. W. D. Bascom, J. L. Bitner, R. L. Cottingham, and C. M. Henderson, "Thermomechanical Properties of High-Performance Polymers", *ibid.*, pp. 13-38. High Performance Composites and Adhesives for V/STOL Aircraft, Third Annual Report, NRL Memorandum Report 4005, May 23, 1979 Naval Research Laboratory, Washington, D.C. AD/A069 611,

APPENDIX 1

Bibliography of major publications resulting from this program

"High Performance Composites and Adhesives for V/STOL Aircraft: First Annual Report," W. D. Bascom and L. B. Lockhart, Jr., Eds., NRL Memorandum Report 3433, December 1976.

"High Performance Composites and Adhesives for V/STOL Aircraft: Second Annual Report," W. D. Bascom and L. B. Lockhart, Jr., Eds., NRL Memorandum Report 3721, February 1978.

"High Performance Composites and Adhesives for V/STOL Aircraft: Third Annual Report," L. B. Lockhart, Jr., Ed., NRL Memorandum Report 4005, May 1979.

"Effect of Temperature on the Adhesive Fracture Behavior of an Elastomer Epoxy Resin," W. D. Bascom and R. L. Cottingham, J. Adhesion, 7, 333 (1976).

"Fracture Design Criteria for Structural Adhesive Bonding-Promise and Problems," W. D. Bascom, R. L. Cottingham and C. O. Timmons, Naval Engineers Journal, August (1976).

"The Effect of Long-Term Water Immersion on the Fracture Toughness, Strength and Modulus of Graphite-Epoxy Composites," J. V. Gauchel and H. C. Nash, Bicentennial of Materials Progress, Science of Advanced Materials and Process Engineering Series, 21, 948 (1976).

"Carbon-13 Fourier Transform NMR for Characterization and Quality Control," C. F. Poranski Jr., S. A. Sojka, and W. B. Moniz, Bicentennial of Materials Progress, Science of Advanced Materials and Process Engineering Series, 21, 755 (1976).

"A Fracture Approach to Thick Film Adhesion Measurements," W. D. Bascom and J. L. Bitner, J. Materials Sci., 12, 1401 (1977).

"Fracture Markings on Stress-Corroded Epoxy/Aluminum Butt Joints," W. D. Bascom, S. T. Gadoski, C. M. Henderson and R. L. Jones, J. Adhesion, 8, 213 (1977).

"Electron Beam Curing Improved High Temperature Strength of Vinyl Ester Adhesives," F. J. Campbell, B. A. Rugg, and W. Brenner, Science of Advanced Materials and Process Engineering Series, 22, 59 (1977).

"Characterization of Epoxy Resin Systems Using Carbon-13 Fourier Transform NMR," C. F. Poranski and W. B. Moniz, J. Coatings Tech., 49, (No. 632), 59 (1977).

"Carbon-13 and Proton NMR Spectra for Characterizing Thermosetting Polymer Systems 1: Epoxy Resins and Curing Agents," C. F. Poranski, W. B. Moniz, D. L. Birkle, J. T. Kopfle and S. A. Sojka, NRL Report No. 8092, 1977.

"Fracture Behavior of Elastomer Modified Epoxy Adhesives," W. D. Bascom, D. L. Hunston and C. O. Timmons, Org. Coatings and Plastics Preprints, 38, 179 (1978).

"Adhesive Fatigue Failure of an Elastomer-Modified Epoxy," W. D. Bascom and S. Mostovoy, Org. Coatings and Plastics Preprints, 38, 156 (1978).

"The Fracture Behavior of an Epoxy Polymer Having a Bimodel Distribution of Elastomeric Inclusions," W. D. Bascom, R. J. Moulten, E. H. Rowe and A. R. Siebert, Org. Coatings and Plastics Preprints, 39, 164 (1978).

"Adhesive Fracture Behavior of CTBN-Modified Epoxy Polymers," W. D. Bascom and D. L. Hunston, Toughening of Plastics: International Congress. The Rubber and Plastics Institute, London, 1978. pp. 22.1-22.

"Use of Fracture Mechanics Concepts in Testing of Film Adhesion," W. D. Bascom, P. R. Becher, J. L. Bitner, and J. S. Murday, in Adhesion Measurement of Thin Films, Thick Films and Bulk Coatings, ASTM STP 640, 63 1978.

"Effect of Bond Angle on Mixed-Mode Adhesive Fracture," W. D. Bascom and J. Oroshnik, F. Materials Sci., 13, 1411 (1978).

"Electron Beam Curing of Vinyl Ester Adhesives," F. J. Campbell, B. A. Rugg and W. Brenner, Adhesives Age, 21, No.5, 41 (May 1978).

"Electron Beam Curing Studies of Selected Thermosetting Adhesives," F. J. Campbell, B. A. Rugg, R. P. Kumar, J. Arnon and W. Brenner, Science of Advanced Materials and Process Engineering Series, 23, (1978).

"Developing Failure Criteria For Adhesive Joints Under Complex Loading," D. R. Mulville, D. L. Hunston and P. W. Mast, Journal of Engineering Materials and Technology, 100, 25 (1978).

"Carbon-13 NMR Spectroscopy of Thermosetting Polymers: Structural Analysis of an Acetylene-Terminated Polyimide Oligomer," C. F. Poranski, W. B. Moniz and T. W. Giants, Org. Coatings and Plastics Preprints, 38, 605 (1978).

"Environmental Aging Studies of Electron-Beam-Cured Adhesives," F. J. Campbell, B. A. Rugg, R. P. Kumar, J. Arnon and W. Brenner, Adhesives Age, 22, No. 1,40 (January 1979).

"Radiation Curing of Selected Structural Adhesives," F. J. Campbell, B. A. Rugg, R. P. Kumar, J. Arnon and W. Brenner, Radiat. Phys. Chem., 14, 699 (1979).

"Automated Torsion Pendulum Analysis of the Formation and Properties of a Phthalocyanine," J. K. Gillham, Poly. Eng. and Sci., 19 (4), 319 (1979).

"Mechanical Characterization of Structural Adhesives," D. L. Hunston, W. D. Bascom, E. E. Wells, J. D. Fahey and J. L. Bitner, Org. Coatings and Plastics Preprints, 40, 266 (1979).

"Epoxy Equivalent Weight Determination by Carbon-13 Nuclear Magnetic Resonance," W. B. Moniz and C. F. Poranski, Jr., ACS Symposium Series No. 114, "Epoxy Resin Chemistry", R. S. Bauer, Ed., American Chemical Society, Wash., D. C. 1979, Chapter 7.

"Effects of Room Temperature Aging on Composite Prepregs," H. C. Nash, C. F. Poranski, Jr. and R. Y. Ting, Proceedings of the Symposium on Advanced Composites: Design and Application, NBS Special Publication 563, 17 (Oct 1979).

"Effects of Prepreg Out-time and Humidity on the Composition and Processing of Polyimide/Graphite Prepregs," H. C. Nash, C. F. Poranski, Jr. and R. Y. Ting, Composites Tech. Rev., 1, (No. 4) 16 (1979).

"Carbon-13 and Proton NMR Spectroscopy of Thermosetting Polymers; Analysis of Tetraglycidyl Methylenedianiline/Diaminodiphenylsulfone Formulations," C. F. Poranski, Jr. and W. B. Moniz, Proceedings of the 5th Symposium on Composite Materials: Testing and Design, S. W. Tsai, Ed., American Society for Testing and Materials, 1979, pp. 553.

"Rate and Temperature Effects in the Failure of Adhesive Joints," J. R. Rushford, J. L. Bitner and D. L. Hunston, Org. Coatings and Plastics Preprints, 41, 379 (1979).

"Application of Instrumental Techniques to the Study of the Cure of Phthalocyanine/Graphite Composites," R. Y. Ting, Proceedings of the Symposium on Advanced Composites: Design and Applications, NBS Special Publication 563, pp. 25-31 (1979).

"The Interlaminar Fracture of Organic-Matrix Woven Reinforcement Composites," W. D. Bascom, J. L. Bitner, R. J. Moulton and A. R. Siebert, Composites, Jan. 1980, p. 9.

"The Use of the Width-Tapered Double-Cantilever Specimen for Assessing the Interlaminar Toughness of Woven Reinforcement Laminates," W. D. Bascom, J. L. Bitner, R. J. Moulton and A. R. Siebert, Composites, July 1980, p.132.

"The Dynamic Mechanical Properties and Fracture Behavior of Phthalocyanine Polymers," W. D. Bascom, R. L. Cottingham and R. Y. Ting, J. Materials Sci., 15, 2097 (1980).

"Viscoelastic Characterization of Structural Adhesives Via Forced Oscillation Experiments," D. L. Hunston, W. D. Bascom, E. E. Wells, J. D. Fahey and J. L. Bitner, Adhesion and Adsorption of Polymers, Part A (1980), L-H. Lee, Ed., Plenum, New York, p. 321.

"Failure in Elastomer-Toughened Epoxies: Viscoelastic Effects," D. L. Hunston, J. L. Rushford, J. L. Bitner, J. Oroshnik and R. S. Rose, J. Elast. Plas., 12, 133 (1980).

"Effect of Room Temperature Aging on Graphite/Polyimide Prepreg Materials," H. C. Nash, C. F. Poranski, Jr., and R. Y. Ting, ACS Symposium Series No. 132, "Resins for Aerospace", C. A. May, Ed., American Chemical Society, Wash., D. C., 1980, Chapter 25.

"NMR Characterization of Some Polyphthalocyanine Precursors," C. F. Poranski, Jr. and W. B. Moniz, ACS Symposium Series No. 132, "Resins for Aerospace," C. A. May, Ed., American Chemical Society, Wash., D. C., 1980, Chapter 25.

"The Loading-Rate Dependent Fracture Property of a Toughened Epoxy polymer," R. Y. Ting and R. L. Cottingham, Polymer Bulletin, 2, 211 (1980).

"Comparison of Laboratory Techniques for Evaluating the Fracture Toughness of Glassy Polymers," R. Y. Ting and R. L. Cottingham, J. Appl. Poly. Sci., 25, 1813 (1980).

"Effects of Molecular structure on the Mechanical Properties of Phthalocyanines," R. Y. Ting and R. L. Cottingham, Org. Coatings and Plastics Preprints, 42 496 (1980).

"The Anomalous Lowering of the Glass transition of an Epoxy Resin By Plasticization with Water," P. Peyser and W. D. Bascom, J. Materials Sci., 16, 75 (1981).

"Fracture Energy and Surface Topology in the Cracking of High Performance Sulphone Polymers," R. Y. Ting, J. Materials Sci., 16, 3059.

"The Development of C-10 Phthalocyanine for Composite Matrix Applications," R. Y. Ting and H. C. Nash, Polymer Eng. and Sci., 21, 441 (1981).

"Adhesive Fracture Energies of Some High Performance Polymers," R. Y. Ting and R. L. Cottingham, J. Adhesion, 12, (4), 243 (1981).

"Curing High Performance Structural Adhesives By Electron-Beam Radiation," F. J. Campbell and W. Brenner, Naval Engineers Journal, 4, No. 3, 160 (1982).

END

FILMED

5-84

DTIC